

2016

Comparison of SASW Systems for Coastal and Offshore Applications

Finn Groenewold
University of Rhode Island, finn_groenewold@my.uri.edu

Follow this and additional works at: <https://digitalcommons.uri.edu/theses>

Recommended Citation

Groenewold, Finn, "Comparison of SASW Systems for Coastal and Offshore Applications" (2016). *Open Access Master's Theses*. Paper 869.
<https://digitalcommons.uri.edu/theses/869>

This Thesis is brought to you for free and open access by DigitalCommons@URI. It has been accepted for inclusion in Open Access Master's Theses by an authorized administrator of DigitalCommons@URI. For more information, please contact digitalcommons@etal.uri.edu.

COMPARISON OF SASW SYSTEMS FOR COASTAL AND
OFFSHORE APPLICATIONS

By

FINN GROENEWOLD

A THESIS SUBMITTED IN PARTIAL FULFILLMENT OF THE
REQUIREMENTS FOR THE DEGREE OF

MASTER OF SCIENCE

IN

CIVIL AND ENVIRONMENTAL ENGINEERING

UNIVERSITY OF RHODE ISLAND

2016

MASTER OF SCIENCE THESIS
OF
FINN GROENEWOLD

APPROVED:

Thesis Committee:

Major Professor

Christopher Baxter

Aaron Bradshaw

Gopu Potty

James Kaklamanos

Nasser H. Zawia

DEAN OF THE GRADUATE SCHOOL

UNIVERSITY OF RHODE ISLAND
2016

Abstract

Spectral analysis of surface wave (SASW) systems are an increasingly popular tool for the estimation of shear wave velocity profiles of geotechnical sites as a reasonable alternative to expensive and difficult downhole and crosshole tests. However, there are relatively few commercial systems using this new approach. The prime-objective of this study is to understand the application of a commercial SASW system manufactured by Olson Instruments, Inc. and to compare the results obtained with it to a Multi-Channel Analysis of Surface Wave system developed at the University of Rhode Island. For the field testing program, different sized sledgehammers and weights were used to impact the soil while measuring the passing Rayleigh surface waves with pairs of 4.5 Hz and 2 Hz geophones that were connected to a dynamic signal analyzer for different spacings. This data was processed in the programs WinTFS and WinSASW to develop site-specific dispersion curves, which were then inverted to estimate shear wave velocity profiles. After preliminary testing, the system was used to conduct tests at different sites where investigations of shear wave velocity with different systems have already been performed. Additionally, tests were performed at two different beach sites to collect data that might be useful to explore the relationship between soil stiffness and coastal erosion. The results showed some agreement from inversions using a different system and software package. Nevertheless, there is still a need for further investigation to examine the reliability of the measurements and analysis methods.

Acknowledgements

My sincere appreciation goes to my Major Professor, Dr. Chris Baxter for his guidance and support throughout my whole academic career, including the research and writing of this thesis, here at the University of Rhode Island. Your great enthusiasm for the geotechnical field of study inspired me in a way that increased my motivation and effort for my studies.

I would also like to truly thank Dr. Aaron Bradshaw, Dr. Gopu Potty and Dr. James Miller for their constant help, support and ideas throughout my research.

A special thanks goes to Dr. James Kaklamanos for his genuine help and support and for providing the Spectral Analysis of Surface Waves system, without which this work would not have been possible.

In addition I would like to thank Dr. Sung-Ho Joh for his aid with the SASW method and especially the WinSASW software.

Another thanks goes to my student colleagues and friends Shane Taylor, Marius Wenck and Friederike Wulff who were a source of motivation and comedy but also never hesitated to help regardless of the circumstances. Thanks also to Dr. Harry Cooke and Ryan Lozinski for their assistance and support during field testing.

Thanks to Robin Freeland, Fred Pease and Kevin Broccolo for their help and provision of needed equipment, sometimes with their knowledge and sometimes without.

Table of Contents

Abstract	ii
Acknowledgements	iii
List of Figures	vii
List of Tables.....	xiv
1 Introduction	1
1.1 Overview	1
1.2 Justification for and Significance of the Study	4
1.3 Objectives.....	5
1.4 Organization of the Thesis	5
2 Literature Review/Background	7
2.1 Seismic Waves	7
2.1.2 Rayleigh Surface Waves	9
2.2 Spectral Analysis of Surface Waves (SASW)	11
2.2.1 Producing and Measuring Rayleigh Surface Waves	12
2.2.2 Dispersion Curve.....	14
2.2.3 Forward Modelling	17
2.2.4 Multi-Channel Analysis of Surface Waves (MASW).....	20
2.3 Challenges Associated with SASW testing.....	21

3. Details of Olson Instruments, Inc. SASW System.....	23
3.1 Hardware/Set Up.....	24
3.2 NDE 360 Non-Destructive Testing Platform.....	25
3.3 Post Processing	28
3.3.1 WinTFS	29
3.3.2 WinSASW.....	30
3.3.2.1 Masking.....	31
3.3.2.2 Generation of the Dispersion Curve.....	34
3.3.2.3 Inversion Analysis.....	37
4. SASW Testing and Results	42
4.1 Gainer Memorial Dam, Scituate, RI	43
4.1.1 Results for Gainer Dam.....	49
4.2 Old Farmer’s Market, Providence, RI.....	54
4.2.2 Results of Farmer’s Market.....	58
4.3 Middleton Building, URI Bay Campus.....	61
4.3.2 Results for Middleton Building Site	65
4.4 Quonochontaug Beach, Weekapaug, RI	68
4.4.1 Results for Quonochontaug Beach.....	71
4.5 Misquamicut Beach, Westerly, RI	74
4.5.2 Results for Misquamicut Beach	77

5 Analysis and Discussion	81
5.1 Gainer Dam site.....	81
5.2 Old Farmer's Market Site	85
5.3 Middleton Building Site.....	89
5.4 Comparison of Beach Sites	92
6. Conclusion	94
Appendix	98
Bibliography.....	108

List of Figures

Figure 1. Test setup with geophones (red) connected to a dynamic signal analyzer (inside box) and the location for the source impact which is underlain by a rubber and a steel plate.....	1
Figure 2. URI SASW system with geophones (yellow) and several hydrophone receive units (SHRUs) on a sled (Giard 2013).	3
Figure 3. Illustration of the direction of particle motion in P-Waves (left) and S-Waves (right) (Pei 2007).....	8
Figure 4. Illustration of particle motions produced by (a) Rayleigh waves; and (b) Love waves. (Kramer 1996).....	9
Figure 5. 2D radiation pattern of Rayleigh surface waves generated by a vertical point source (Foti et al. 2015).	10
Figure 6. Illustration of dispersion of Rayleigh waves. The depth of particle motion is directly related to the frequency of the surface wave and in turn the velocity is a function of the stiffness of the underlying layers (Foti et al. 2015).	11
Figure 7. An impact source generates surface waves that are measured by two geophones at certain distances (SASW; Greene 2011).....	12
Figure 8. Basic setup for SASW testing.	13
Figure 9. (a) A generic non-periodic signal can be decomposed in (b) the sum of simple cyclic functions. The amplitude and phase of the elementary cyclic signal are the frequency-domain representation of the signal, or its spectrum, consisting of the (c) amplitude and (d) phase (Foti et al. 2015).	15

Figure 10. Example for dispersion curve plotted with phase velocity vs. wavelength. Phase velocity is in m/s and wavelength is in m.....	16
Figure 11. Example for dispersion curves plotted with phase velocity vs. frequency. Phase velocity is in m/s and frequency is in Hz.....	17
Figure 12. Schematic representation of SASW measurement process: (a) Linear array is placed in field; (b) Time records are collected at various spacings; (c) Phase difference and signal coherence are calculated in frequency domain; (d) Experimental dispersion curve (“signature” of site) is generated from measurements at four to six spacings x ; (e) Inverse theory is applied to develop (f) Shear wave velocity profile (Luke and Stokoe, 1998).....	19
Figure 13. Basic setup for a MASW system (McCaskill 2014).....	20
Figure 14. Geophones used for the testing of this study: (a.) 4.5 Hz Geophones, (b.) 2 Hz Geophones.	23
Figure 15. SASW test setup with NDE 360 acquisition system.	24
Figure 16. Photograph of the front screen of the NDE 360 platform showing the Mode and gain settings.	25
Figure 17: NDE 360 platform parameter settings.	27
Figure 18. Overview of WinTFS.	30
Figure 19. Example of masking procedure in WinSASW. The unshaded area on the left side in the upper figure is the only portion of the signal to be saved for calculation of the dispersion curve (i.e. that part of the signal is “unmasked”).	32

Figure 20. Example of phase unwrapping for a cross power spectrum. At about 140 Hz, the anomaly represents a typical example of failure of the unwrapping procedure in identifying phase jumps (Foti et al., 2015).	33
Figure 21. Example of a composite experimental dispersion curve of a test. Phase velocity is in m/s and wavelength is in m.	35
Figure 22. Example of a global representative dispersion curve (in blue) generated in WinSASW to match a composite experimental dispersion curve (in gray). Phase velocity is in m/s and wavelength is in m.	36
Figure 23. Example of an array representative dispersion curve (different colors) generated in WinSASW to match individual experimental dispersion curves (gray). Phase velocity is in m/s and wavelength is in m.	37
Figure 24. Example of a soil profile with 10 layers in WinSASW.....	38
Figure 25. Example shear wave velocity profile vs. depth. Depth is in m and shear wave velocity is in m/s.....	41
Figure 26. Locations of the different test sites. (Source: Rhode Island Base and Elevation Maps. (n.d.). Retrieved January 7, 2016, from http://www.netstate.com/states/geography/mapcom/ri_mapscom.htm)	42
Figure 27. Cross section of Gainer Memorial Dam (Reyes et al. 2016).....	43
Figure 28. Geological setting of Gainer Memorial Dam (Bradshaw and Reyes 2015).	44
Figure 29. Locations of the SASW array on the Gainer Memorial Dam (red line indicates use of 4.5 Hz geophones; blue line indicates use of 2 Hz geophones) (Google Maps).	45

Figure 30. a.) 1 kg sledge hammer; b.) Rubber pad, steel plate and 4 kg sledge hammer; and b.) Tripod with 50 kg dropping weight.	46
Figure 31. Setup with different spacing for the 2 Hz Test.	47
Figure 32. Composite dispersion curve (phase velocity vs wavelength) for the Gainer Dam site. Phase velocity is in m/s and wavelength is in m.....	49
Figure 33. Composite dispersion curve (phase velocity vs frequency) for the Gainer Dam site. Phase velocity is in m/s and frequency is in Hz.	50
Figure 34. Global representative (solid blue circles) and theoretical dispersion curve (empty red circles) for Gainer Dam. Phase velocity is in m/s and wavelength is in m.	51
Figure 35. Estimated shear wave velocity profile for the Gainer Dam site based on global array dispersion curve.	52
Figure 36. Array representative (solid blue circles) and theoretical dispersion curve (empty red circles) for Gainer Dam. Phase velocity is in m/s and wavelength is in m.	53
Figure 37. Estimated shear wave velocity profile for the Gainer Dam site based on array representative dispersion curve.....	53
Figure 38. Geological setting of the Old Farmer's Market site (Bradshaw et al. 2007).	55
Figure 39. Old Farmer's Market site in Providence, RI with the highway piers marked.	56
Figure 40. Location of the 4.5 Hz geophone array (red line) and the 2 Hz array (blue line) at the old Farmer's Market site.	56

Figure 41. Composite dispersion curve (phase velocity vs wavelength) for the old Farmer's Market site. Phase velocity is in m/s and wavelength is in m.	59
Figure 42. Composite dispersion curve (phase velocity vs frequency) for the old Farmer's Market site. Phase velocity is in m/s and frequency is in Hz.	59
Figure 43. Representative (solid blue circles) and theoretical dispersion curve (empty red circles) for the old Farmer's Market site. Phase velocity is in m/s and wavelength is in m.	60
Figure 44. Estimated shear wave velocity profile for the old Farmer's Market site. ...	61
Figure 45. Location of SASW arrays at the Middleton Building site (Red Lines - 4.5 Hz geophones; Blue Line – 2 Hz geophones) (Google Maps).....	62
Figure 46. Impact sources for the tests performed at the Middleton building: a.) Sledge hammer; and b.) Tamper.	63
Figure 47. Composite dispersion curve (phase velocity vs wavelength) for the Middleton building site. Phase velocity is in m/s and wavelength is in m.	66
Figure 48. Composite dispersion curve (phase velocity vs frequency) for the Middleton building site. Phase velocity is in m/s and frequency is in Hz.	66
Figure 49. Representative (solid blue circles) and theoretical dispersion curve (empty red circles) for the Middleton Building site. Phase velocity is in m/s and wavelength is in m.	67
Figure 50. Estimated shear wave velocity profile for the Middleton Building site.	68
Figure 51. Location of SASW test at Quonochontaug Beach; the marker shows the location of the first geophone.....	69

Figure 52. Location of test at Quonochontaug Beach with a spacing up to 6m between the geophones and the source.....	70
Figure 53. Composite dispersion curve (phase velocity vs wavelength) for the Quonochontaug Beach site. Phase velocity is in m/s and wavelength is in m.....	72
Figure 54. Composite dispersion curve (phase velocity vs frequency) for the Quonochontaug Beach site. Phase velocity is in m/s and frequency is in Hz.....	72
Figure 55. Representative (solid blue circles) and theoretical dispersion curve (empty red circles) for the Quonochontaug Beach site. Phase velocity is in m/s and wavelength is in m.	73
Figure 56. Estimated shear wave velocity profile for the Quonochontaug Beach site.	74
Figure 57. Test Location on Misquamicut Beach with the marker on the first geophone.	75
Figure 58. Location of the test (red line) with the marker on the first geophone.	76
Figure 59. Composite dispersion curve (phase velocity vs wavelength) for the Misquamicut Beach site. Phase velocity is in m/s and wavelength is in m.	78
Figure 60. Composite dispersion curve (phase velocity vs frequency) for the Misquamicut Beach site. Phase velocity is in m/s and frequency is in Hz.	78
Figure 61. Representative (solid blue circles) and theoretical dispersion curve (red empty circles) for the Misquamicut Beach site. Phase velocity is in m/s and wavelength is in m.	79
Figure 62. Estimated shear wave velocity profile for the Misquamicut Beach site.....	80
Figure 63. Composite dispersion curve for the Gainer Dam site from the ASARS system (Reyes et al. 2016).	82

Figure 64. Composite dispersion curve of this study measured with the Olson Instruments system. Phase velocity is in m/s and frequency is in Hz.....	83
Figure 65. Shear wave velocity profiles for the Gainer Dam site developed from test with (a) ASARS system (Reyes et al. 2016) and (b) the Olson Instrument system in this study.	84
Figure 66. Dispersion curve obtained from the Old Farmer's Market site in Providence, RI using the URI ASARS system (Potty, personal communication).....	86
Figure 67. Dispersion Curve obtained from the Old Farmer's Market site in Providence, RI using the Olson Instruments system. Phase velocity is in m/s and frequency is in Hz.	87
Figure 68. Shear wave velocity profile for the old Farmer's Market site developed with a) ASARS system (Potty, personal communication) and b) Olson Instruments system in this study.	88
Figure 69. Dispersion curves for the Middleton building site from Greene (2011): a.) phase velocity vs. wavelength; and b.) phase velocity vs. frequency.	90
Figure 70. Dispersion curves for the Middleton building site generated from this study: a.) phase velocity vs. wavelength; and b.) phase velocity vs. frequency. Phase velocity is in m/s, wavelength is in m and frequency is in Hz.....	90
Figure 71. Shear wave velocity profile of the Middleton Building site acquired with the Olson Instruments System.....	91
Figure 72. Shear wave velocity profiles from: a.) Quonochontaug Beach; and b.) Misquamicut Beach.....	92

List of Tables

Table 1. List of relevant parameters that need to be set in the NDE 360 platform.....	26
Table 2. Summary of testing details at the Gainer Dam site with the 4.5 Hz geophones.	48
Table 3. Summary of testing details at the Gainer Dam site with the 2 Hz geophones.	48
Table 4. Summary of testing details at the old Farmer's Market site with the 4.5 Hz geophones.....	57
Table 5. Summary of testing details at the old Farmer's Market site with the 2 Hz geophones.....	58
Table 6. Summary of testing details for Test #1 at the Middleton building site with the 4.5 Hz geophones.	63
Table 7. Summary of testing details for Test #2 at the Middleton building site with the 4.5 Hz geophones.	64
Table 8. Summary of testing details for Test #3 at the Middleton building site with the 2 Hz geophones.	64
Table 9. Summary of testing details for SASW test at Quonochontaug Beach.....	71
Table 10. Summary of testing details for SASW test at Misquamicut Beach.	77

1 Introduction

1.1 Overview

Spectral Analysis of Surface Waves (SASW) is a non-invasive site investigation technique in which a vertical profile of shear wave velocity is obtained from collection and analysis of surface wave data from an array of geophones placed on the ground. The soil is impacted by a source like a hammer or by the dropping of a weight to create non-destructive seismic waves that propagate along the surface of the soil. The ground motion caused by these waves is measured by two or more geophones which are placed in a linear array at certain known distances from the source and recorded by a dynamic signal analyzer (Figure 1).



Figure 1. Test setup with geophones (red) connected to a dynamic signal analyzer (inside box) and the location for the source impact which is underlain by a rubber and a steel plate.

The measured ground motions are transferred to the frequency domain with different phases and amplitudes, determining the surface wave characteristics and the time at which they passed the receivers. As surface waves with longer wavelengths sense deeper, an early measured arrival of these waves suggests a higher stiffness at the deeper layers. This is due to the fact that the velocities of the waves are dependent on the stiffness of the soil and therefore influence the speed of propagation.

A plot of phase difference between the frequencies of the different receivers is generated on the dynamic signal analyzer that helps in combination with a coherence function to evaluate the quality of the data. The coherence function shows the signal to noise ratio of the record to determine if the measurement was good or should be repeated. If the data is acceptable, the distance between the receivers and the source is changed and the test repeated. Smaller spacings give a better measurement of smaller wavelengths, whereas larger spacings are used to measure larger wavelengths that also determine the maximum investigation depth of the test site.

During post-processing, the measured data for the different spacings are reviewed in the aforementioned plot of phase difference vs. frequency. To remove unreasonable parts of the plot due to noise or bad measurements, certain frequencies can be masked, or removed, so that they are not used for the subsequent calculation of the dispersion curve. With the different spacings, different ranges of frequencies/wavelengths are measured. These are combined in one composite dispersion curve that represents a unique “fingerprint” of the geotechnical site in either frequency vs. phase velocity or wavelength vs. phase velocity.

To obtain the shear wave velocity profile vs. depth, an inversion process is used that calculates a dispersion curve with the use of different soil properties such as Poisson's ratio and unit weight of the soil layers. This computed theoretical dispersion curve is compared to the composite experimental dispersion curve from the field measurements. Solid parameters are iteratively changed until a valid match between the two dispersion curves is obtained.

Shear wave velocity provides important information about a soil's stiffness and is commonly used in engineering practice to evaluate site response during earthquakes. There are several commercial SASW systems available for use on land; however, there are only a few systems worldwide that have been developed for use underwater. One such system was developed in the Ocean Engineering Department at the University of Rhode Island (URI) and is shown in Figure 2 (Giard et al. 2013; Potty 2014).



Figure 2. URI SASW system with geophones (yellow) and several hydrophone receive units (SHRUs) on a sled (Giard 2013).

1.2 Justification for and Significance of the Study

The most widely accepted method for characterizing the shear wave velocity (V_s) profile of a site is through downhole or crosshole methods (Kramer 1996). These methods involve either multiple boreholes or the use of seismic cone penetrometers, which can be time-consuming and costly. In contrast, Spectral Analysis of Surface Waves (SASW) and Multichannel Analysis of Surface Waves (MASW) techniques are relatively easy and inexpensive to implement as they only require geophones and an impact source (typically ranging in size from a sledge hammer to a bulldozer) to generate and measure surface waves. However, interpretation of the results can be challenging and requires considerable experience to create accurate shear wave velocity profiles.

Recently, a commercial SASW system was lent to the geotechnical engineering group at URI by Dr. James Kaklamanos of Merrimack College. This system complements an existing system at URI developed by Drs. James Miller and Gopu Potty, and provides a unique opportunity to learn about and compare the results from the two systems. In addition to this opportunity, there is considerable interest and research at URI in the area of coastal resiliency, including understanding the potential for erosion along the southern shore of Rhode Island. It is not known whether non-destructive surface wave techniques like SASW can play a role in characterizing coastal sediment processes, and this work will provide the initial steps in addressing this issue.

1.3 Objectives

The primary objectives of this thesis are to learn how to perform SASW testing using a commercial system and to compare the performance of this system to a geophone-hydrophone system that was developed by the Department of Ocean Engineering at several terrestrial sites around Rhode Island. The URI system is called the Amphibious Seismo-Acoustic Recording System (ASARS). For the chosen sites either SASW test data or direct measurements of shear wave velocity from seismic cone penetration tests are available. A second objective is to begin collecting shear wave velocity data using SASW at two coastal beach sites in Rhode Island where coastal erosion data has been collected for decades. The hope is that stiffness data obtained at these sites may provide insight into erosion at these sites.

1.4 Organization of the Thesis

A literature review including the theory of seismic waves and the Spectral Analysis of Surface Waves technique is presented in Chapter 2. This is followed by a detailed explanation of how to use the commercial system manufactured by Olson Instruments, Inc. Chapter 3 describes the testing procedures used in the field as well as an explanation of how the software was used for the post-processing of the collected data. Chapter 4 presents details about the SASW tests conducted at the different sites, including the exact location and condition of the test sites and details of the testing procedures and the results. For the latter it will be explained which data was chosen for post processing before the dispersion curves and shear wave velocity profiles are presented. In Chapter 5 the results are analyzed and compared to earlier

tests conducted with other systems to collect shear wave velocity profiles or dispersion curves. Chapter 6 presents a summary of the results and suggestions for future studies.

2 Literature Review/Background

This chapter presents a review of the literature related to the measurement and interpretation of shear wave velocity profiles in soils using surface wave techniques. An overview of seismic waves in elastic media is presented first followed by a description of the SASW technique. Finally, challenges with using SASW techniques are discussed.

2.1 Seismic Waves

Soils and rocks have complex mechanical behavior that depends on a variety of factors. However, in many practical cases soil and rock are modeled as linear elastic materials. This is often the case for the propagation of seismic waves through a volume of soil or rock. A seismic wave is generated when there is a disturbance or rupture in an elastic material and the energy radiates away from the disturbance. (Foti et al. 2015). When strains become large enough, the linear elastic assumption may not be valid.

2.1.1 Body Waves

Seismic waves that propagate within a homogenous, unbounded linear elastic medium are called body waves. There are two different kind of body waves: primary or compressional waves (P-waves) and secondary or shear waves (S-waves). P-waves propagate in the same direction as the particle motion, whereas S-waves travel with a perpendicular particle motion to the actual direction of wave propagation, as can be seen in Figure 3.

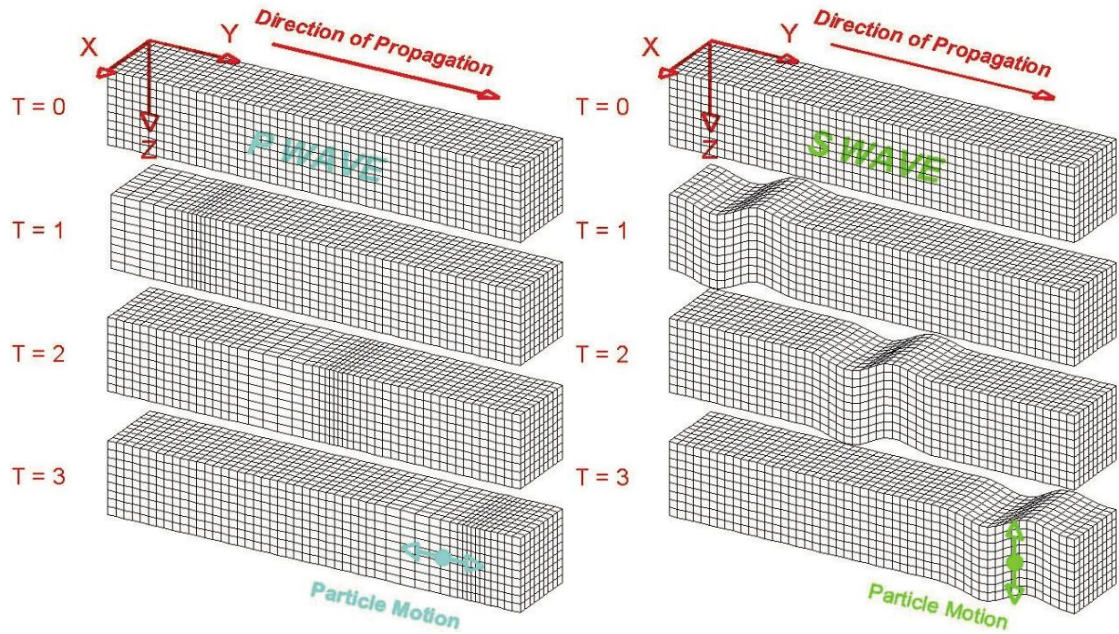


Figure 3. Illustration of the direction of particle motion in P-Waves (left) and S-Waves (right) (Pei 2007).

P-waves travel with a higher velocity than S-waves for a couple of reasons. Soils and rock are relatively incompressible in compression and there is very little energy lost with the propagation of P-waves, and thus the velocity of propagation is relatively high. In addition, P-waves travel mostly through the pore water (because of the relative incompressibility of water) and saturated soils typically have velocities comparable to the compression wave velocity of water ($\sim 1,500$ m/s). The propagation of shear waves is slower than that of compression waves because the particle motion and direction of propagation are orthogonal. Because water cannot support shear, S-waves travel through particle contacts in the soil. As a result, the shear wave velocity is heavily dependent on conditions at the particle contents and the effective stress conditions.

2.1.2 Rayleigh Surface Waves

Surface waves propagate not only within an elastic medium but also along a free surface or interface like soil and air or soil and water. There are two different kinds of surface waves between air and a solid: Rayleigh waves are surface waves that travel with vertical particle motion while Love waves are surface waves that propagate with horizontal particle motion as shown in the following figure.

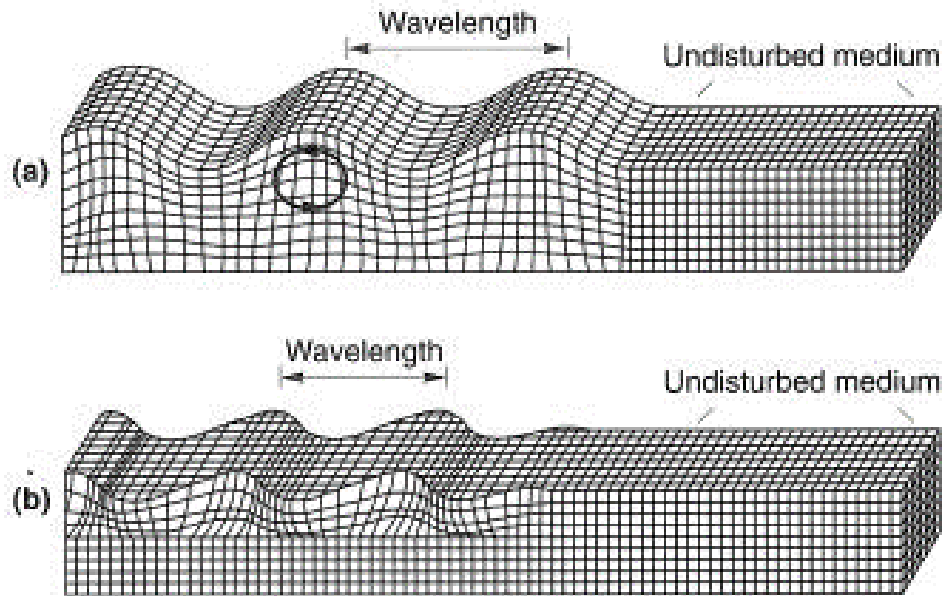


Figure 4. Illustration of particle motions produced by (a) Rayleigh waves; and (b) Love waves. (Kramer 1996)

Rayleigh waves result from the interference of P-waves and S-waves along the surface of an elastic boundary (Xia 2014). In contrast to these body waves whose energy spreads as a spherical wavefront, the radiation pattern of Rayleigh waves is mainly two-dimensional (cylindrical) as can be seen in Figure 5. This results in much lower geometric attenuation than occurs with body waves. The result of this difference in attenuation is that, at a distance of about one to two wavelengths from a source,

body waves are negligible and the wavefield is dominated by surface waves (Foti et al. 2015).

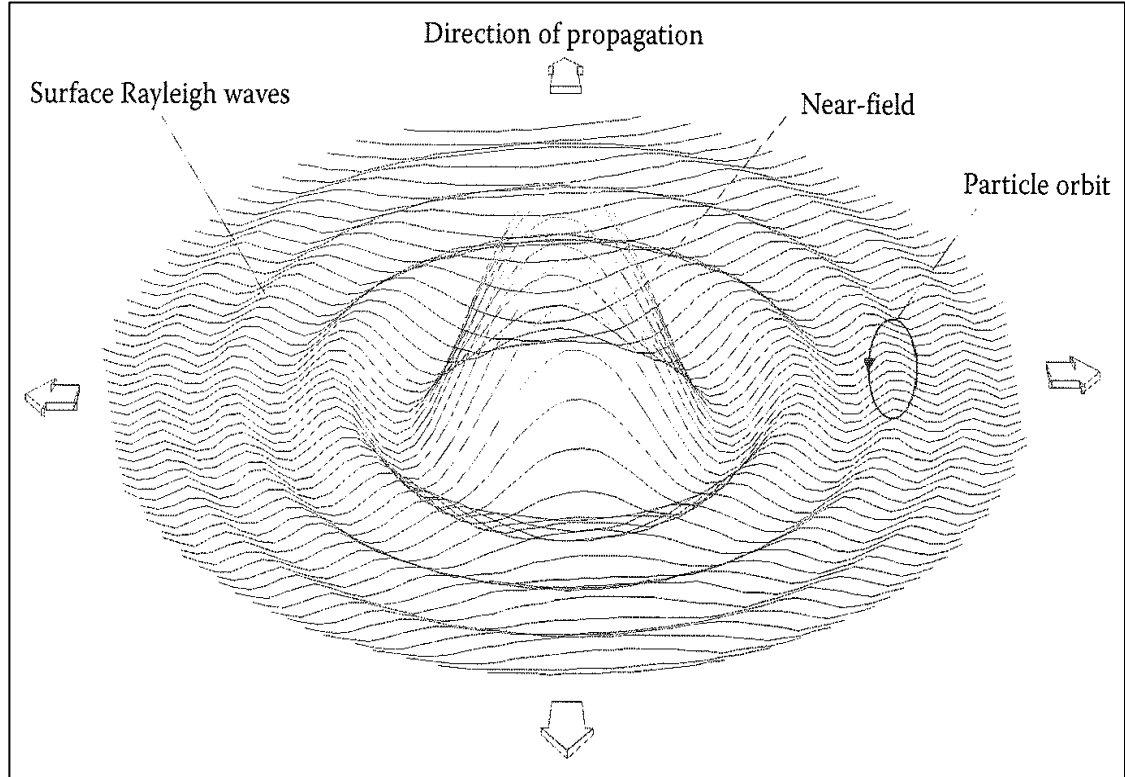


Figure 5. 2D radiation pattern of Rayleigh surface waves generated by a vertical point source (Foti et al. 2015).

The amplitude of a Rayleigh wave decreases rapidly with depth and most of the energy only propagates a depth of one wavelength into the soil (Foti et al. 2015). This means that a high-frequency wave (i.e. short wavelength) only induces particle motion at the near surface and the velocity is influenced mainly by the stiffness in this layer. On the other hand a low-frequency wave (long wavelength) also travels within deeper layers of the soil and therefore the velocity is affected additionally by soil stiffness at various depths (Figure 6). This phenomenon is called dispersion, meaning that the propagation velocities of surface waves are frequency dependent.

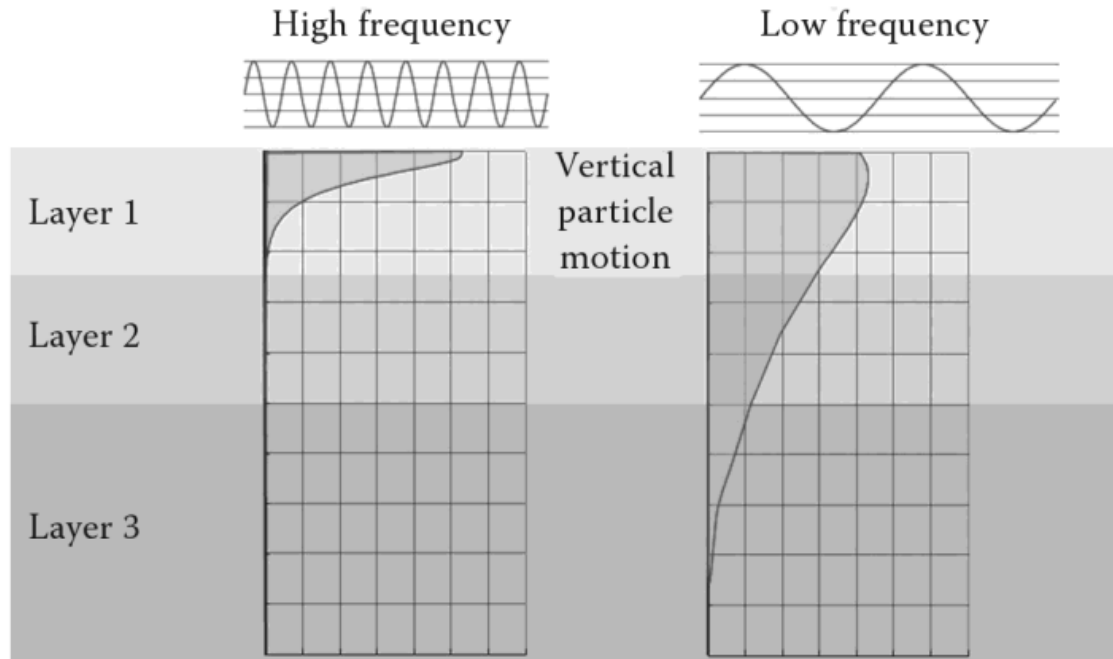


Figure 6. Illustration of dispersion of Rayleigh waves. The depth of particle motion is directly related to the frequency of the surface wave and in turn the velocity is a function of the stiffness of the underlying layers (Foti et al. 2015).

2.2 Spectral Analysis of Surface Waves (SASW)

The term SASW embraces different techniques that are used for generating and measuring surface waves and then analyzing this information to estimate the variation of shear wave velocity with depth. As Rayleigh surface waves are easier to generate and detect than Love surface waves, they are used preferably for SASW testing. In SASW techniques, the ground is impacted by a source and at least two receivers measure the passing surface waves (Figure 7). The receivers must be moved several times for a geotechnical site investigation to collect data for different source-receiver spacings so that different wavelengths can be selected to determine a shear wave velocity profile.

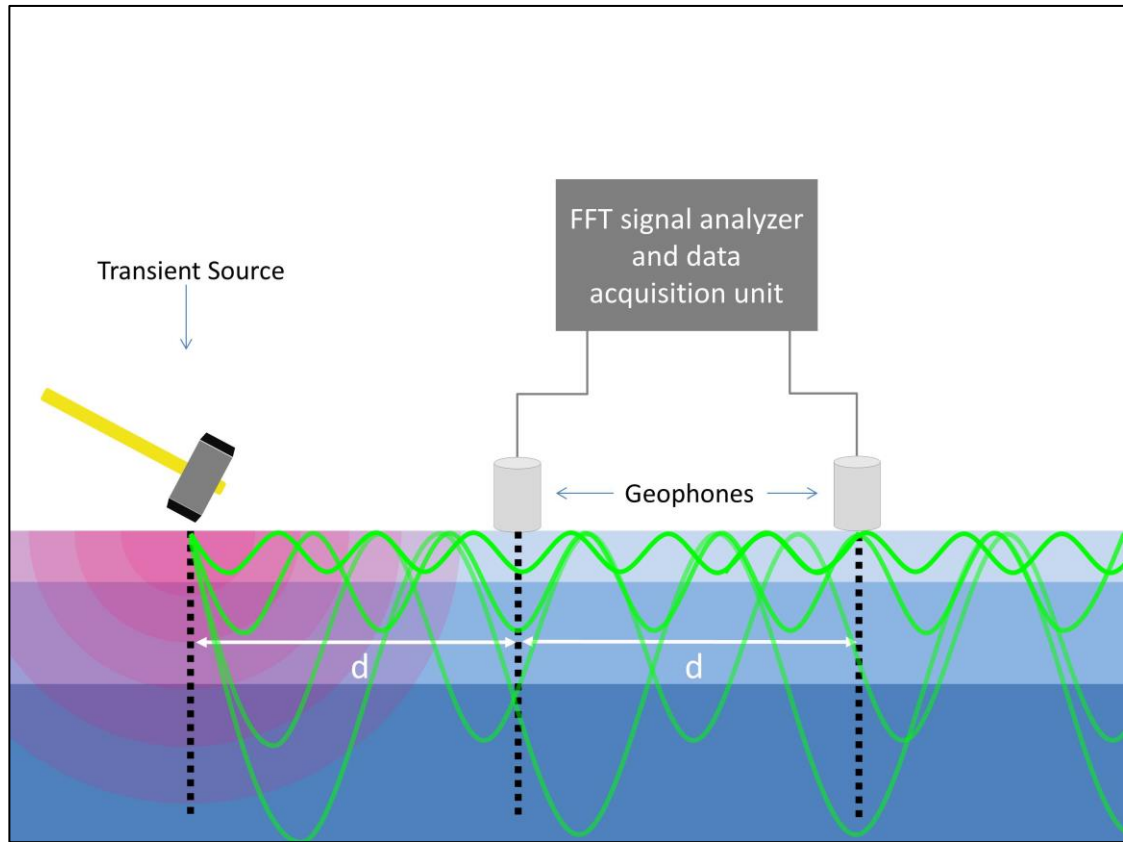


Figure 7. An impact source generates surface waves that are measured by two geophones at certain distances (SASW; Greene 2011).

2.2.1 Producing and Measuring Rayleigh Surface Waves

Rayleigh waves are generated during SASW testing by impacting the soil, and they are detected by at least two receivers placed at specific distances away from the source that pick up the motions of the surface waves. A wide variety of impact sources can be used to generate surface waves, including sledge hammers, large weights, bulldozers, and vibroseis. Different sources produce different frequency/wavelength spectra to excite different depths of the soil. For example, a heavy sledge hammer or dropped weights induce a lower frequency spectrum and therefore longer wavelengths

that propagate deeper in the soil than a light sledge hammer that would only induce higher frequency waves.

The propagating Rayleigh waves are then measured by receivers that are usually vertically orientated accelerometers or geophones. The receivers are connected to a dynamic signal analyzer to record the data as shown in Figure 8. At least two receivers are needed for a reading and are set up in a linear array at certain spacings. In SASW testing, the spacings are changed during the test procedure, as it is easier to measure longer wavelength Rayleigh waves with larger spacings. Conversely, shorter wavelength waves are measured more reliably with smaller spacings.

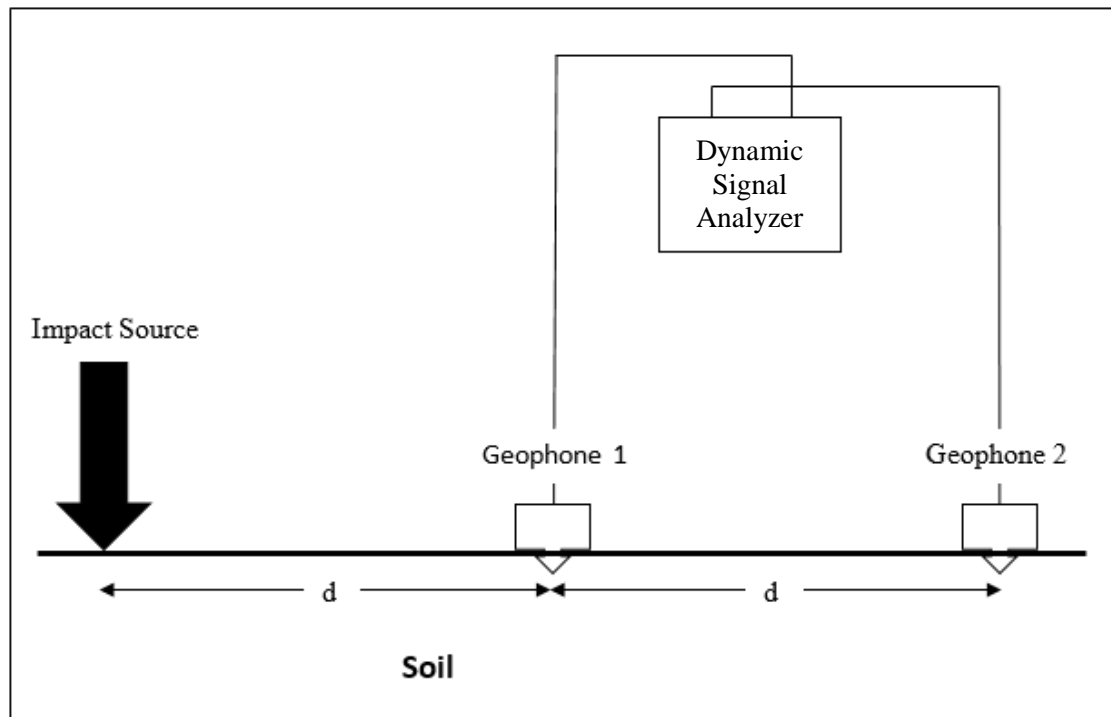


Figure 8. Basic setup for SASW testing.

2.2.2 Dispersion Curve

Impacting the soil generates a spectrum of Rayleigh surface waves with different frequencies (Stokoe et al. 1994). The receivers (typically geophones) monitor the passing waves and then the signals are digitized and recorded by a dynamic signal analyzer. This time signal can be decomposed into a sum of cyclic functions, with each of function having a different frequency, amplitude, and phase also referred to as its spectrum. This process of decomposition is called spectral analysis (Foti et al. 2015) and is shown in Figure 9.

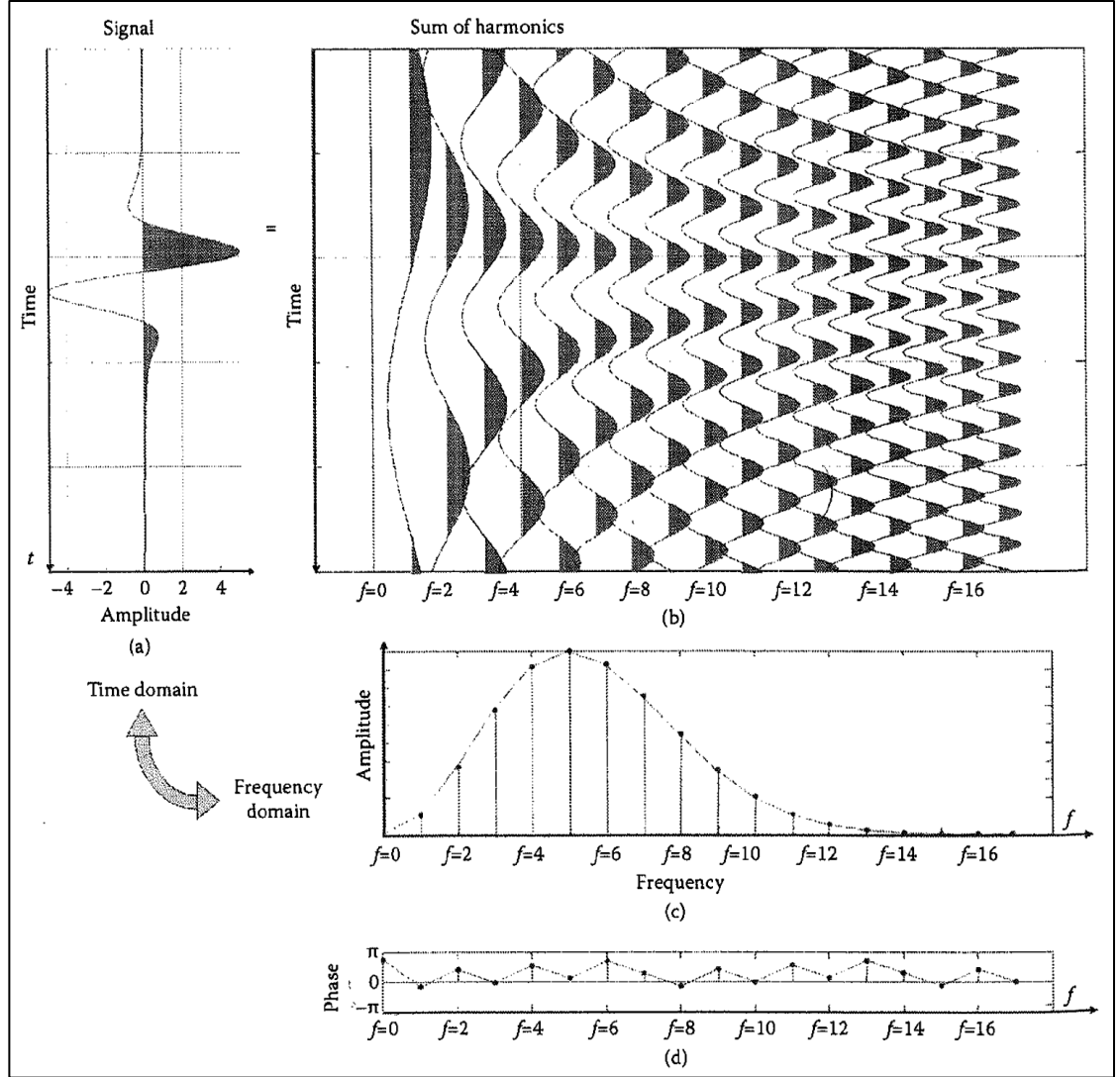


Figure 9. (a) A generic non-periodic signal can be decomposed in (b) the sum of simple cyclic functions. The amplitude and phase of the elementary cyclic signal are the frequency-domain representation of the signal, or its spectrum, consisting of the (c) amplitude and (d) phase (Foti et al. 2015).

For both receivers each time signal is transformed to the frequency domain using a Fast Fourier Transform to determine each frequency with its amplitude and phase angle. The phase difference $\phi(f)$ of each frequency f between the receivers is

then calculated. With this the travel time $t(f)$ of each frequency between the two receivers can be computed by

$$t(f) = \frac{\phi(f)}{2\pi f}. \quad (1)$$

The distance between the receivers is known ($\Delta d = d_2 - d_1$), so the Rayleigh wave phase velocity V_R arises from

$$V_R = \frac{\Delta d}{t(f)}. \quad (2)$$

Finally, the wavelength can be calculated by

$$\lambda_R = \frac{V_R}{f}. \quad (3)$$

These calculations are performed for each frequency of the time signals recorded by all receivers and the results are plotted as velocity vs. frequency or velocity vs. wavelength; this plot is called a dispersion curve and two examples are shown in the following two figures.

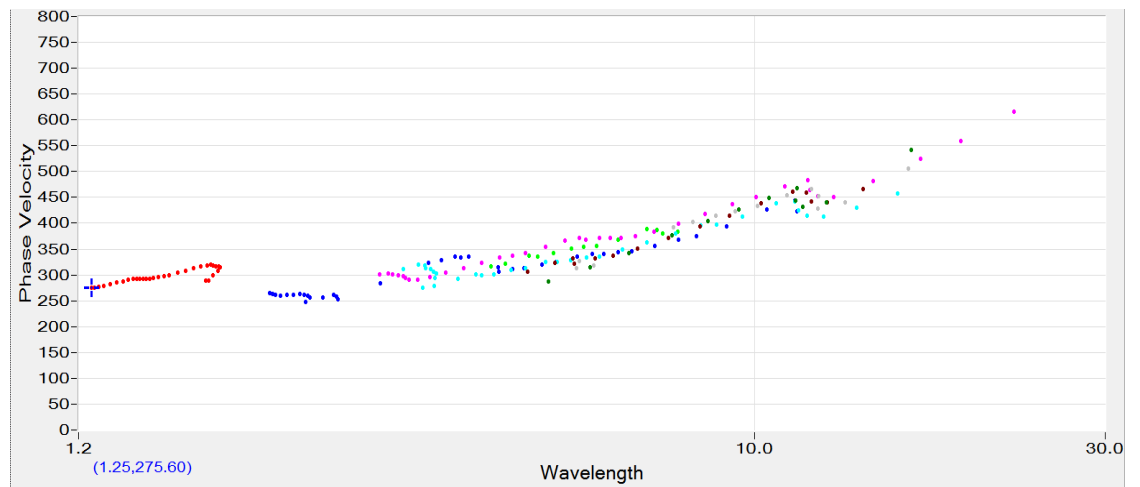


Figure 10. Example of a dispersion curve plotted as phase velocity vs. wavelength. Phase velocity is in m/s and wavelength is in m.

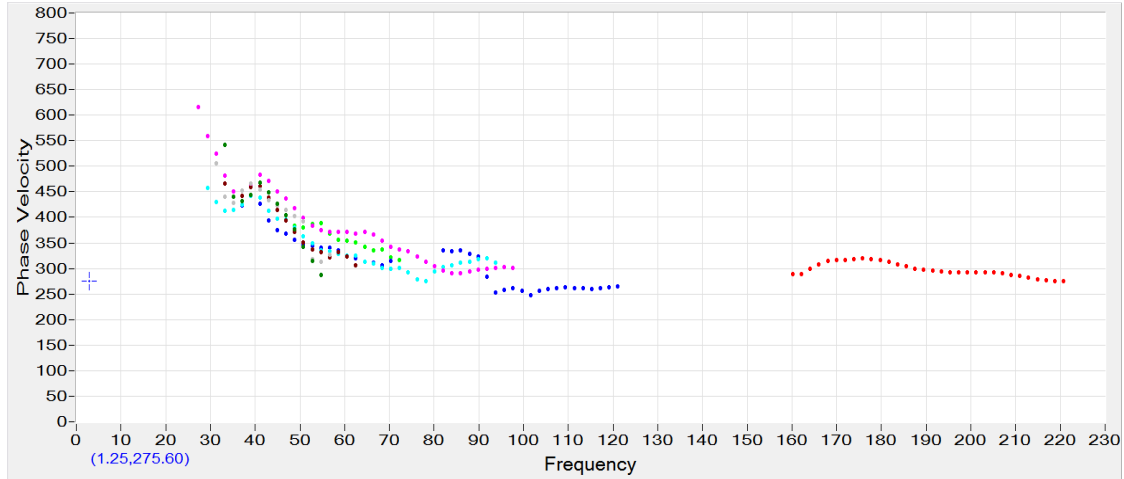


Figure 11. Example of a dispersion curve plotted as phase velocity vs. frequency. Phase velocity is in m/s and frequency is in Hz.

The ratio of the Rayleigh wave phase velocity (V_R) to shear wave velocity (V_s) ranges from 0.874 to 0.955 depending on the value of Poisson's ratio (0 to 0.5). A value of 0.92 is commonly used to convert the Rayleigh wave velocity to shear wave velocity (Stokoe et al. 1994).

2.2.3 Forward Modelling

The next step for the SASW is a forward modelling process, in which a theoretical dispersion curve is calculated from an assumed soil profile. The dynamic stiffness matrix method (Kausel and Roesset 1981; Kausel and Peek 1982) is typically utilized. This model solves for the response of a soil profile due to a vertical load and includes a half space solution and a layered system solution (Stokoe et al. 1994).

The half space solution is used for a homogenous soil profile with no change in stiffness with depth and it relates the displacements at the top of the profile to the forces at the top of the profile with the dynamic stiffness matrix. For this case the

Rayleigh wave velocity is only dependent on the shear and compressional wave velocity of the estimated profile.

The layered system solution is used for the case where the stiffness properties vary with depth and Rayleigh waves are affected by these layers depending on their wavelengths. For this problem the stiffness matrix relates the loads and displacements at the top and bottom of each layer, with an assumed half space below the deepest layer. The model solves, for a reasonable range of wavelengths, the Rayleigh wave velocities with an initially assumed soil profile including again shear and compressional wave velocities. Details and equations for this procedure can be found in Kausel and Roesset (1981) or Stokoe et al. (1994).

The calculated phase velocities as a function of wavelengths form the so-called theoretical dispersion curve which is compared to the experimental dispersion curve. The shear wave velocity which has the greatest impact on the Rayleigh phase velocity and the compressional wave velocity are changed iteratively to obtain a better match of the theoretical dispersion curve to the experimental dispersion curve. When finally an accurate match is made, the assumed shear wave velocities for the layers are used to plot a shear wave velocity profile vs. depth. This iterative procedure is called inversion (Stokoe 1994; Joh 1996). The entire SASW process is summarized in Figure 12.

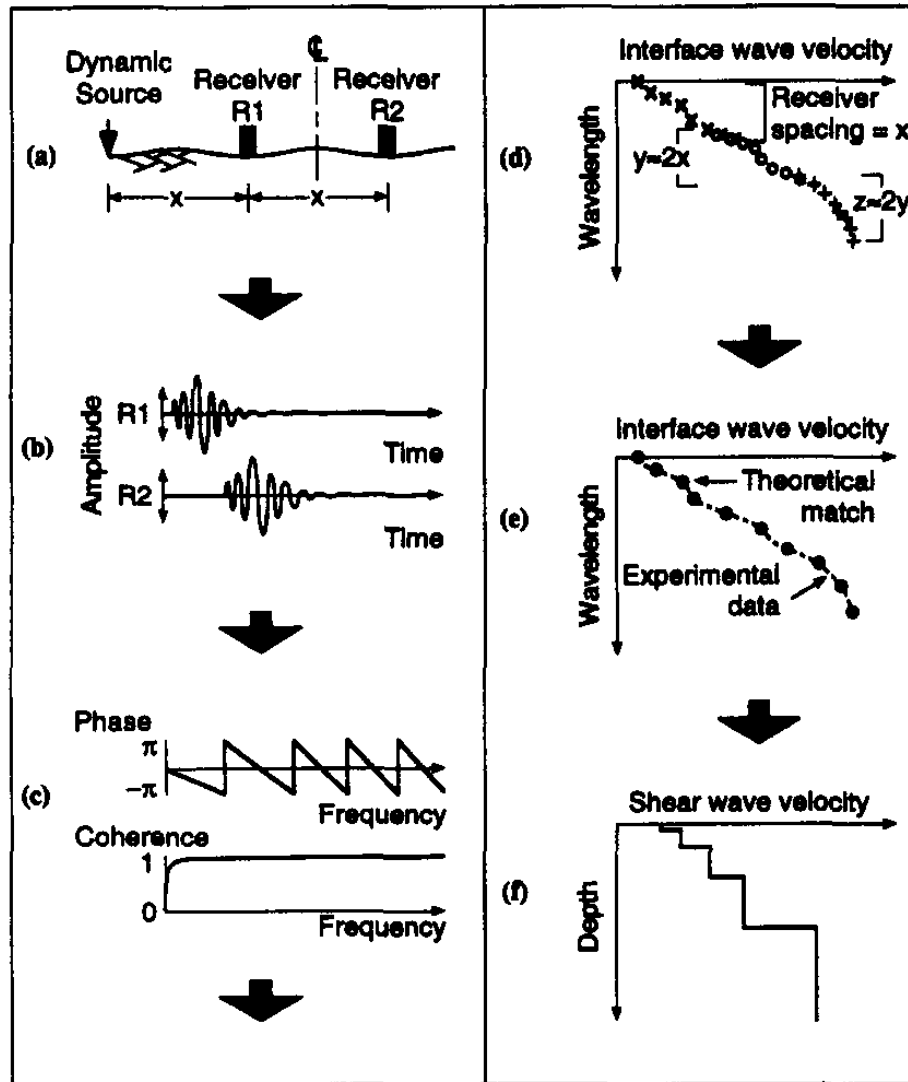


Figure 12. Schematic representation of SASW measurement process: (a) Linear array is placed in field; (b) Time records are collected at various spacings; (c) Phase difference and signal coherence are calculated in frequency domain; (d) Experimental dispersion curve ("signature" of site) is generated from measurements at four to six spacings x ; (e) Inverse theory is applied to develop (f) Shear wave velocity profile (Luke and Stokoe, 1998).

2.2.4 Multi-Channel Analysis of Surface Waves (MASW)

Besides the normal SASW method where two receivers are used during the acquisition phase, another method called Multi-channel Analysis of Surface Waves (MASW) exists. As the name implies, this approach uses more receivers, typically 6-48. Hence, the MASW approach is much quicker to collect data of a site as the receivers are set up once and do not necessarily have to be moved. This is due to the fact that with the geophones that are typically all set up with the same spacing already cover the whole range of different distances to collect the desirable wavelengths (Giard 2013). A typical setup of a MASW system is presented in Figure 13.

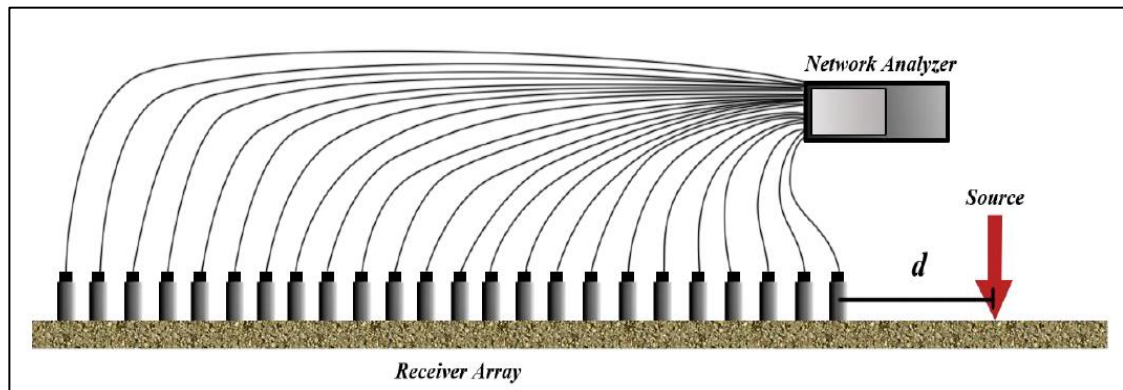


Figure 13. Basic setup for a MASW system (McCaskill 2014).

Another advantage in comparison to the SASW method with only two receivers is the effective identification and isolation of noise during testing according to trace-to-trace coherence (Park et al. 1997). Therefore the MASW approach is an easier method than SASW, but it is still possible to test and get the same results with a system that only uses two receivers.

2.3 Challenges Associated with SASW testing

SASW testing is a complex process at every stage, from producing and measuring surface waves to the final inversion to determine a shear wave velocity profile with depth. Different problems and challenges can occur throughout this process.

For the determination of the dispersion curve, it can occur that the system measures different modes of Rayleigh waves. This usually happens if the variation of stiffness over depth is very high as parts of the Rayleigh waves are reflected at the interface of two different layers producing additional groups of phase velocities. Instead of only the fundamental mode, higher modes can also be generated and be measured. This can cause difficulties in determining a dispersion curve, as it is sometimes not clear which curve is the fundamental mode (Foti et al. 2015).

Another problem that can appear is the near field effect which can be caused by body wave interference with the cylindrical wavefront of the Rayleigh wave. As described earlier, body waves attenuate faster than surface waves, but within the range of one or two wavelengths from the source they can still influence the measurements. This is also the case for the shape of the wavefront. Close to the source, the wavefront of the Rayleigh wave is cylindrical, however at greater distances the wavefront becomes planar. These near field effects are accounted for by using appropriate distances between the source and the first receiver as well as using forward modelling models that can calculate the complex wavefield close to the source (Foti et al. 2015).

Another aspect that should be taken into consideration is that the model to calculate the dispersion curve during the inversion process assumes a lateral

homogenous medium whereas in reality this is not always the case (Foti et al. 2015). Additionally, a three-dimensional heterogeneity may also have an impact on the system as boulders or fundaments can reflect seismic waves even if they are not directly in between the source and the receivers.

The last problem with SASW testing is that the vertical resolution of shear wave velocity decreases with depth. A thin layer with a different stiffness can be easily distinguished if it is found in the top layers but not easily identified if it is located at a greater depth. A “rule of thumb” is that the SASW systems can only resolve layers adequately as long as they are thicker than 20% of the depth (Stokoe 1994).

3. Details of Olson Instruments, Inc. SASW System

Olson Instruments, Inc. developed a commercial SASW system for site investigations. The most important components of the system include the following: 1.) the NDE 360 platform which is used for data acquisition, analysis and display of SASW data; and 2.) a pair of 4.5 Hz geophones (Geospace Technologies, SNG 11D/PC-21OPEN-100') and a pair of 2 Hz geophones (Geospace Technologies, HS1 2.0-225 VERT) with appropriate cable lengths. The different types of geophones are shown in Figure 14. The system also includes two software packages, WinTFS 2.5.2 and WinSASW 3.2.6 for post-processing of the acquired data of the tests. This chapter describes details of the hardware set up and post-processing software, as well as the steps involved in generating a dispersion curve and then the inversion process to obtain a shear wave velocity profile.



(a.) (b.)
Figure 14. Geophones used for the testing of this study: (a.) 4.5 Hz Geophones,
(b.) 2 Hz Geophones.

3.1 Hardware/Set Up

The two geophones and the source are set up in a linear array with a certain spacing, d , between the two geophones and between the first geophone and the source (Figure 15). Different spacings should be used to collect surface wave data over a range of wavelengths (8 or more spacings). This is due to the fact that longer wavelengths are easier to measure with bigger spacings (Lin et al., 2014). The first geophone (or Geophone 1) is meant to be the closer one to the source. Signals from the geophones are acquired using the Olson Instruments, Inc. NDE 360 platform, which is described in the next section. Geophone 1 is connected to Channel 1 (and set as the Trigger Channel) and the other geophone is connected to Channel 4 of the NDE 360 platform. Channel 2 and 3 do not work for this version of the Olson Instruments, Inc. system.

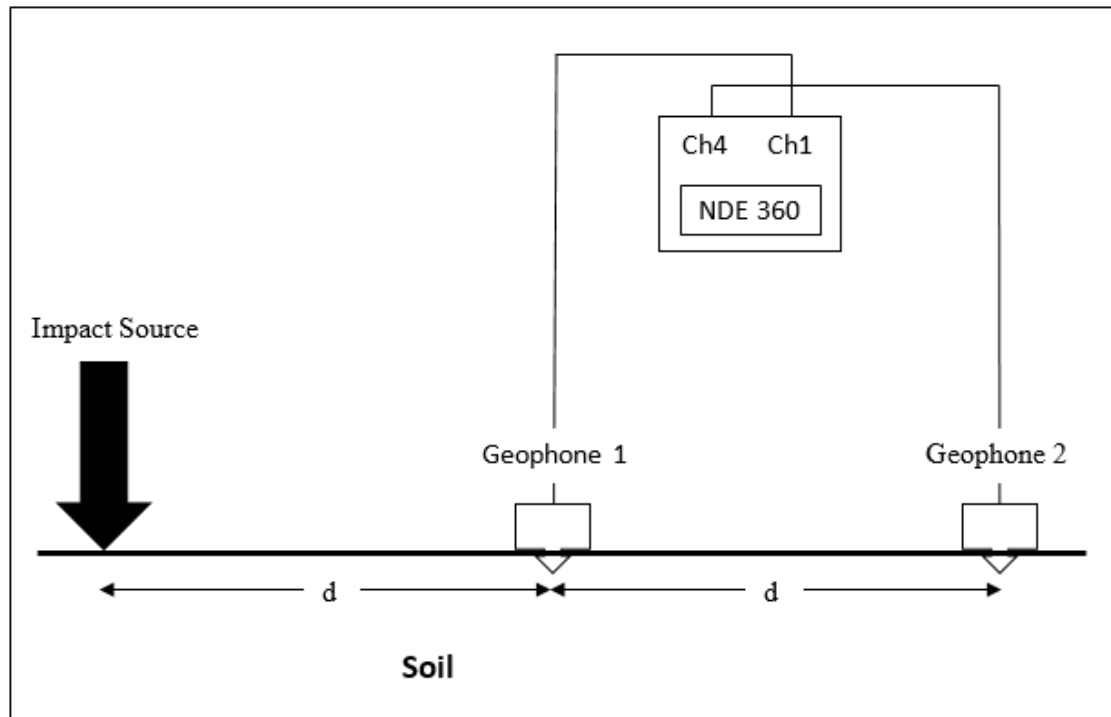


Figure 15. SASW test setup with NDE 360 acquisition system.

3.2 NDE 360 Non-Destructive Testing Platform

The NDE 360 platform must be configured properly before performing a SASW test. There are two testing modes: SASW-S (“structures”) and SASW-G (“geotechnical”). Unfortunately, at this time the SASW-G setting is not functional in the NDE 360 platform (Olson Instruments, Inc., personal communication), and therefore the SASW-S mode must be chosen. Settings within the SASW-S mode can be changed so that testing of soil profiles is possible, as will be explained later. The gain amplifies the measured signals from the geophones. It is set for the two channels according to the particle source, spacing of the receivers, and strength of the received signals. The options the gain can be set to are 1, 10, 100 and 1000 which represents the factor the original signal is multiplied by.

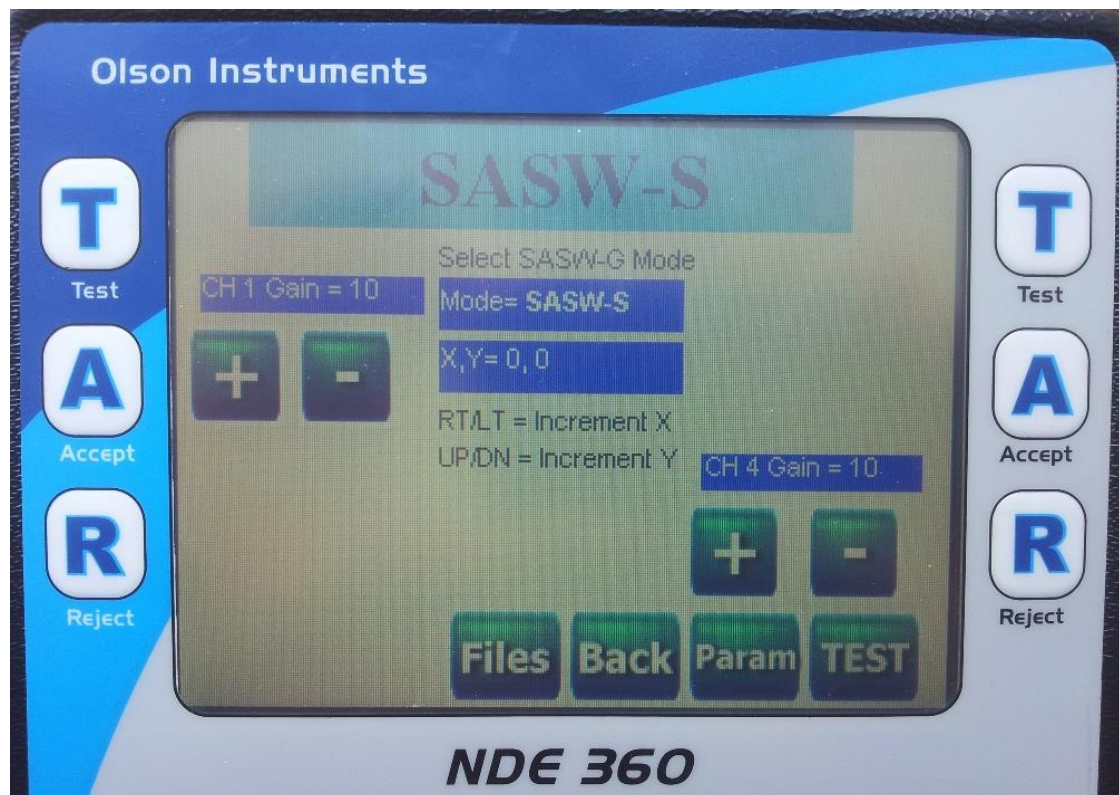


Figure 16. Photograph of the front screen of the NDE 360 platform showing the Mode and gain settings.

Table 1. List of relevant parameters that need to be set in the NDE 360 platform.

Parameter	Settings	Notes
Testing Mode	SASW-S, SASW-G	SASW-S (structures) is the only available setting.
Gain	10 to 1000	100 and 1000 used most times
Time/Point; Sampling Rate	200 μ s or 500 μ s	500 μ s used for larger spacings
Spacing		Not used by the software
Trigger Channel		Channel for geophone that is closer to the source
Number of Records	4 to 6	

The Time/Point or Sampling Rate describes the length of the time between data points and is adjusted based on the velocity and frequency content of the surface waves. As the velocity in soil is lower than in structures the value should be increased so that a frequency span with a lower maximum frequency is obtained. For testing up to geophone spacings of 15 meters, a value of 200 μ s is reasonable. For greater spacing distances, the Time/Point or Sampling should be set to the maximum of 500 μ s. The spacing does not need to be changed because the function is not used by the program. The Trigger Channel (TRIG) should be the channel where Geophone 1 is connected to (normally set to Channel 1). The other parameters do not need to be changed.



Figure 17: NDE 360 platform parameter settings.

After all settings are adjusted, the NDE 360 platform is ready to collect data. The system waits until an impact of the soil is strong enough to trigger the data acquisition. The NDE 360 platform then records the signal and displays a plot of signal amplitude vs. time of the first channel and the phase difference between the data from the two geophones. Based on visual inspection of these plots, the record can be accepted or rejected before the system is ready for the next impact of the soil.

The visual inspection is based on two aspects. The primary aspect is a clear saw tooth pattern of the phase plot which implies good quality data. The second factor that can be taken into consideration is the shown scales of the two geophones, which give an idea of how strong the recorded signal is. If the scale is too high (around 90%)

the signal might be clipped. In this case the strength of the source impact or the gain should be decreased to reduce the amplitude. If the value is too low (under 35%), the system might record too much background noise which lowers the data quality. Experience has shown that a scale for the first geophone of about 75% often provides the clearest saw tooth pattern in the phase difference plot for a certain spacing if the source impact is well and no background noise disturbs the measurement. This data should then be accepted.

This process is repeated until a set number of records is accepted. It is desirable that the accepted data for one spacing look similar to each other on the two plots as these are averaged. At this point the coherence function of the averaged collected records is displayed, which shows how the measured particle motions between the two receivers are correlated. A value close to unity means the records are not affected by noise and is desirable (Foti et al. 2015). If that is the case for the desired frequency range, the data is then saved. Otherwise, the test can be repeated with either a different source or by moving the location of the source slightly.

3.3 Post Processing

After data has been acquired in the field, post-processing of the data is performed using two software programs provided by Olson Instruments, Inc. The first program is WinTFS, which is used to window and review the records and to accept or reject them again. It is also possible but not mandatory to generate a dispersion curve for each spacing. The data is then imported to the second program WinSASW to create an experimental dispersion curve from all the data collected and to perform the inversion to estimate the variation of shear wave velocity vs. depth.

3.3.1 WinTFS

In WinTFS (version 2.5.2), each saved data file can be reviewed. Records that are accepted are averaged and saved as one file for the particular spacing. It is also possible to window the data. “Windowing” means that the portions of the time series that do not have relevant information about the surface wave are filtered out. For SASW-G testing, Olson Instruments, Inc. recommends to use no windowing or an exponential cut with a decay factor of 200-500 from the point with the largest negative amplitude. The decay factor is the exponent on the e^x -factor which is applied to the signal. Thus, the higher the factor the faster the cutoff (Olson Instruments, personal communication). As the surface waves have the biggest amplitude and are at the front of the measured waveform, the data in the latter portion of the record are gradually eliminated (Olson Instruments Inc. 2013).

Figure 18 shows the output of two geophone records for a given spacing in WinTFS. The upper two records show the signals from each geophone in the time domain. The middle graph shows the coherence of the averaged, accepted records and the lower graph shows the phase difference of the averaged data. If the coherence of two records is low, the records should be rejected.

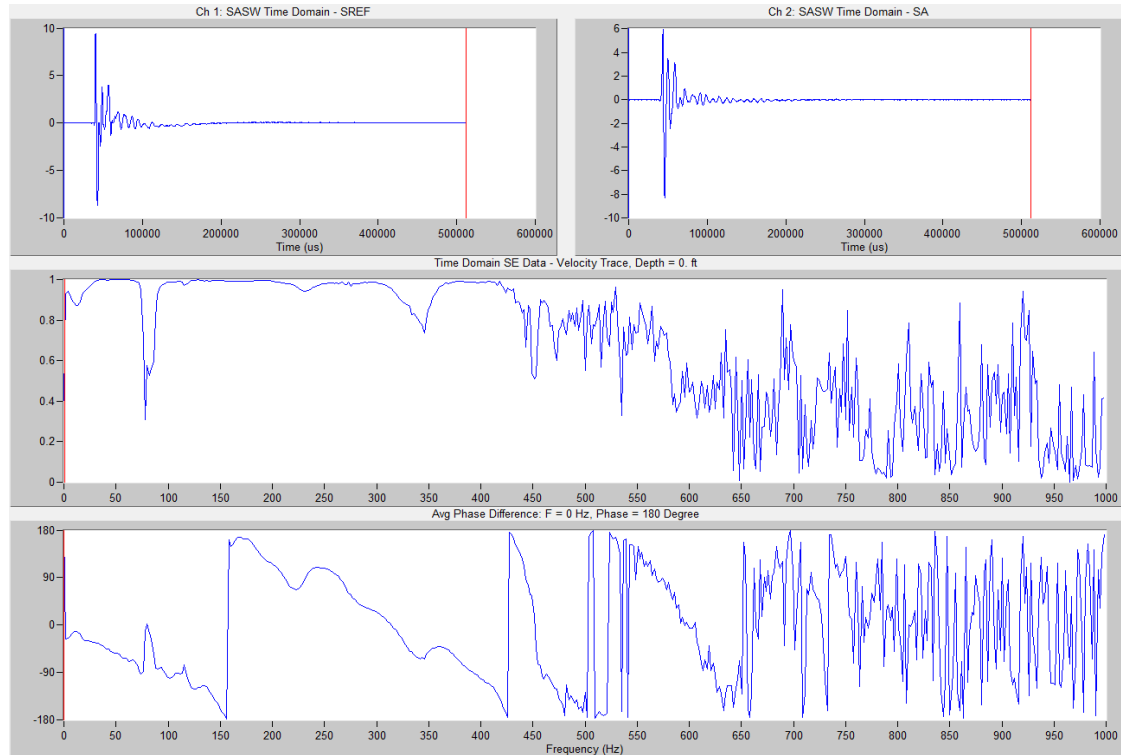


Figure 18. Overview of WinTFS. The upper two records show the signals from each geophone in the time domain. The middle graph shows the coherence of the averaged, accepted records and the lower graph shows the phase difference of the averaged data.

3.3.2 WinSASW

The procedure for the analysis of the records in WinSASW 3.2.6 can be divided into three steps. At first the data for each spacing is masked so that only “clean” areas are used for the calculation of the experimental dispersion curve. Second, these curves of the different spacings are then combined and a composite experimental dispersion curve is created. The third step is the inversion, in which a theoretical dispersion curve is generated that iteratively tries to match the experimental dispersion curve best so a reasonable shear wave velocity profile for the site can be determined. These three steps will be described in detail in the following sections.

3.3.2.1 Masking

Masking is a process in WinSASW in which windows of data are selected or eliminated based on the frequency range of interest (based on the geophone spacing), and the frequency-phase angle relationship between the two geophones (e.g. upper plot in Figure 19). Before masking can be initiated, the data files from the averaged records of WinTFS are loaded into the program. The data file for a certain spacing is selected and is named in the program (for example “1 m” for the data of the spacing 1 m). Then the spacing of the source to the first geophone and the second geophone is inserted before the file is finally loaded into the program. This step is repeated for all the different spacing datasets of the site including data from the different Geophones (4.5 Hz and 2 Hz). The masking process is performed in a window as shown in Figure 19, where the upper figure is a plot of frequency vs. phase difference (frequency response) and the lower figure is a plot of the Gabor Spectrum (shown) or amplitude. The Gabor Spectrum (shown) or the frequency response amplitude show the frequencies where most of the energy of the surface wave is concentrated. In the Gabor Spectrum the additional information of time is included so that higher amplitudes (yellow to red areas) and their arrival in time is shown. This suggests for the example in Figure 19 that two wave groups with a low frequency of about 50 Hz arrived at different times.

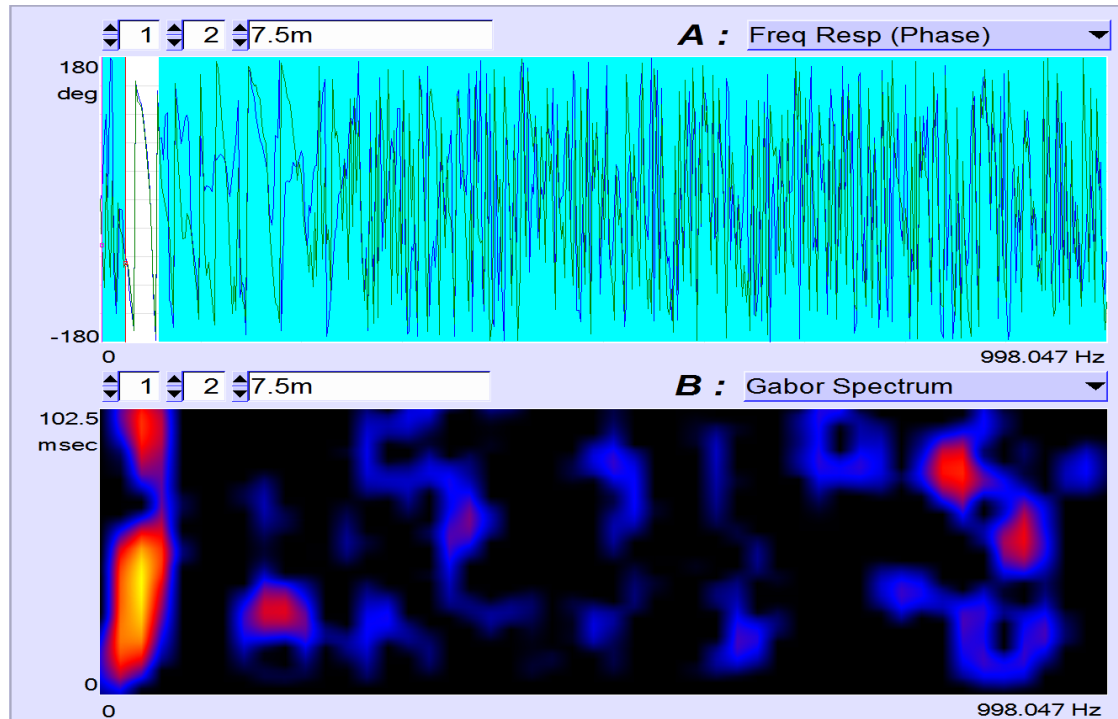


Figure 19. Example of masking procedure in WinSASW. The unshaded area on the left side in the upper figure is the only portion of the signal to be saved for calculation of the dispersion curve (i.e. that part of the signal is “unmasked”).

From both plots, the signal in a reasonable frequency range is chosen for use in determining the dispersion curve; the rest of the signal is “masked.” Therefore, the following frequency ranges should be masked and not be used to construct the phase velocity dispersion curve:

- where the phase angle-frequency relationship does not follow a descending sawtooth pattern (i.e. not “clean”), such as messy phase angles from random noise, undulating phase angles and backward saw tooth shaped phase angles which indicate reflections (Joh, 1996);
- where the energy distribution indicated by the Gabor Spectrum is low (Foti et al, 2015);

- $\lambda \geq 2 * d$, where λ is the wavelength and d is the geophone spacing; and
- $\lambda \leq 4 * R_d$, where R_d is the radius of the geophone. (4.5 Hz geophone: $R_d=3.5$ cm; 2 Hz geophone: $R_d=5$ cm)

In addition to masking the signal, the proper number of phase angle jumps (also called cycle) has to be identified to unwrap the phase spectrum for the calculation of the dispersion curve (Foti et al. 2015). It is common to wrap the frequency-phase angle data by jumping from $-\pi$ to π , which appears as a saw tooth shape. An example of wrapped and unwrapped data can be seen in Figure 20.

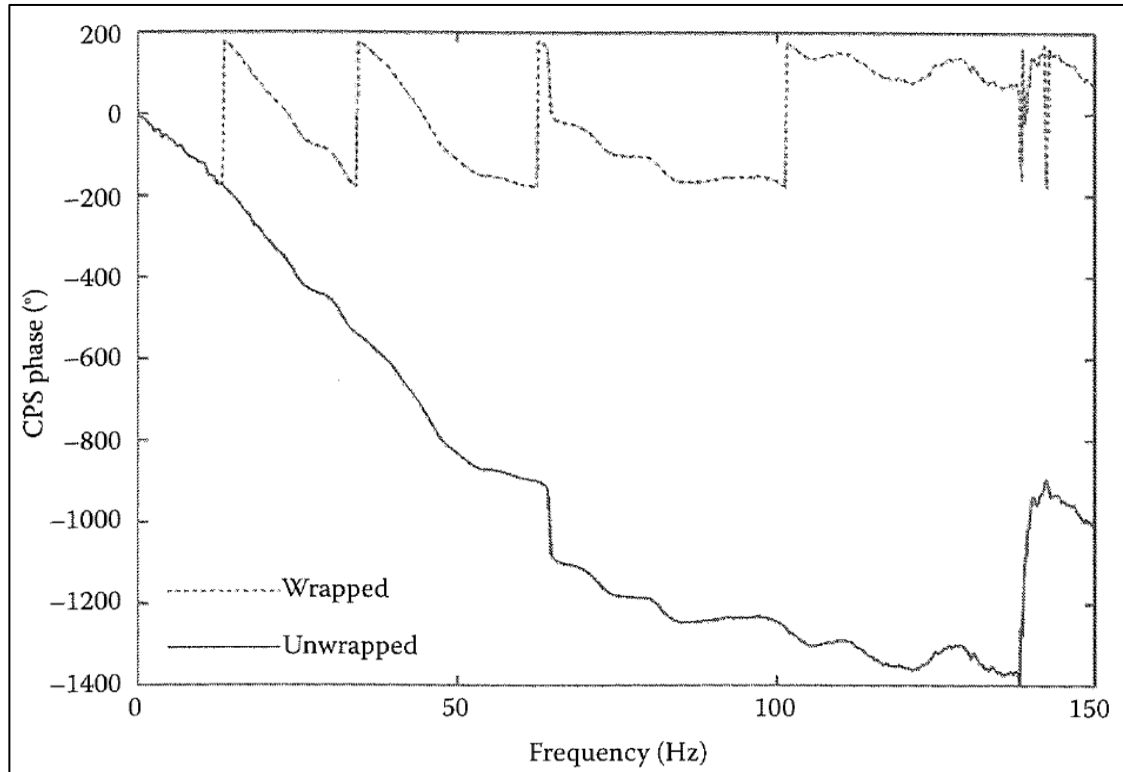


Figure 20. Example of phase unwrapping for a cross power spectrum. At about 140 Hz, the anomaly represents a typical example of failure of the unwrapping procedure in identifying phase jumps (Foti et al., 2015).

The process of masking and identification of the proper number of jumps to the start of the unmasked data is the most difficult part of the post-processing as it is sometimes difficult to identify the jumps. Considerable judgement is necessary which can be a source of mistakes as the setting of the proper jump number has a significant impact on the calculation of the dispersion curve. The entire masking process is repeated for each receiver spacing before the theoretical dispersion curve can be determined.

3.3.2.2 *Generation of the Dispersion Curve*

The experimental dispersion curve from each geophone spacing is calculated with the unwrapped cross power spectrum (f and ϕ) and the receiver spacing d by the following equation:

$$V_R = f * \lambda = f * \frac{d}{\phi/360^\circ} \quad (4)$$

Within WinSASW, all the computed dispersion curves for the different spacings (different colors) are shown in one plot, as shown in Figure 21. Dispersion curves from different spacings can be deleted if they do not match globally with the rest of the data. Considerable judgement and iteration is required to generate a reasonable dispersion curve.

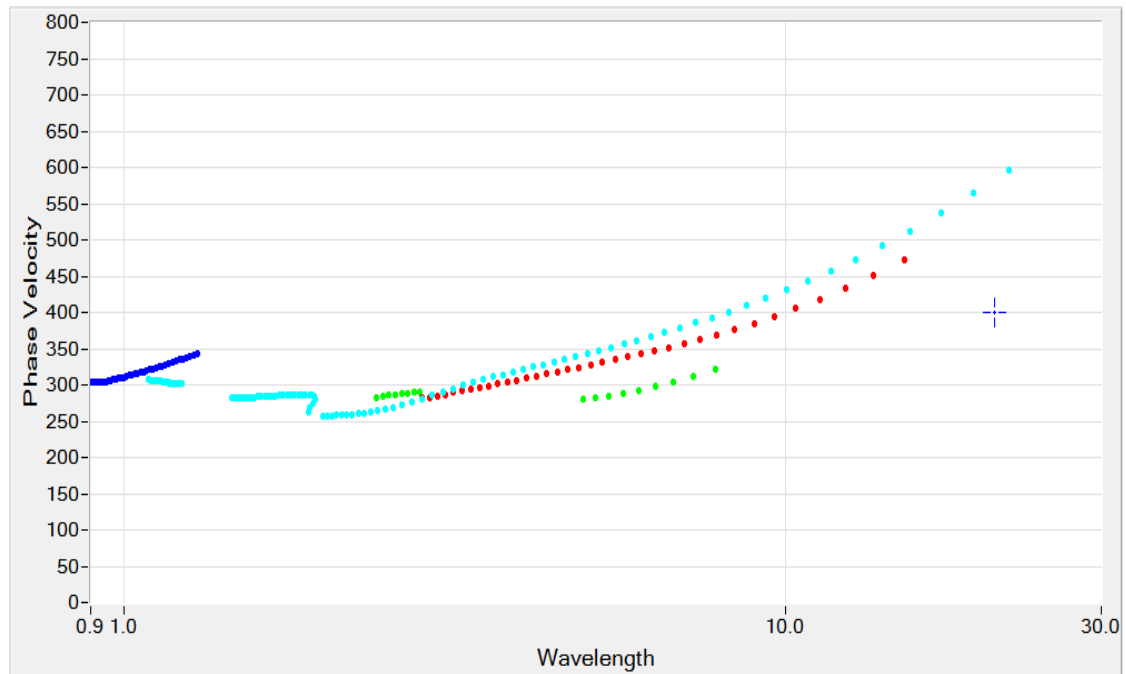


Figure 21. Example of a composite experimental dispersion curve of a test. Phase velocity is in m/s and wavelength is in m.

Once a composite dispersion curve has been generated, the representative dispersion curve can be determined. For this process the program WinSASW uses an averaging algorithm from Joh (1996) where it is possible to choose how many points this curve should have and where the focus of the distribution of these points should be located. This is a helpful feature as there might be areas where the experimental dispersion curve has more points or is better matched by the preceding dispersion curves of different spacings. After this is determined a global representative dispersion curve and an array representative dispersion curve are created, which can both be used for the inversion analysis as will be explained later. The global representative dispersion curve is one curve that averages the composite dispersion curve and so follows its trend, whereas the array representative dispersion curve creates an average

curve for each individual experimental dispersion curve from certain receiver spacings/data files that were included in the composite dispersion curve. The array representative dispersion curve consists therefore of more points than the global representative dispersion curve. Figure 22 shows an example of a global representative dispersion curve (in blue) generated in WinSASW to match a composite experimental dispersion curve and Figure 23 shows an array representative dispersion curve (different colors for different included receiver spacings/data files) to match the individual experimental dispersion curves.

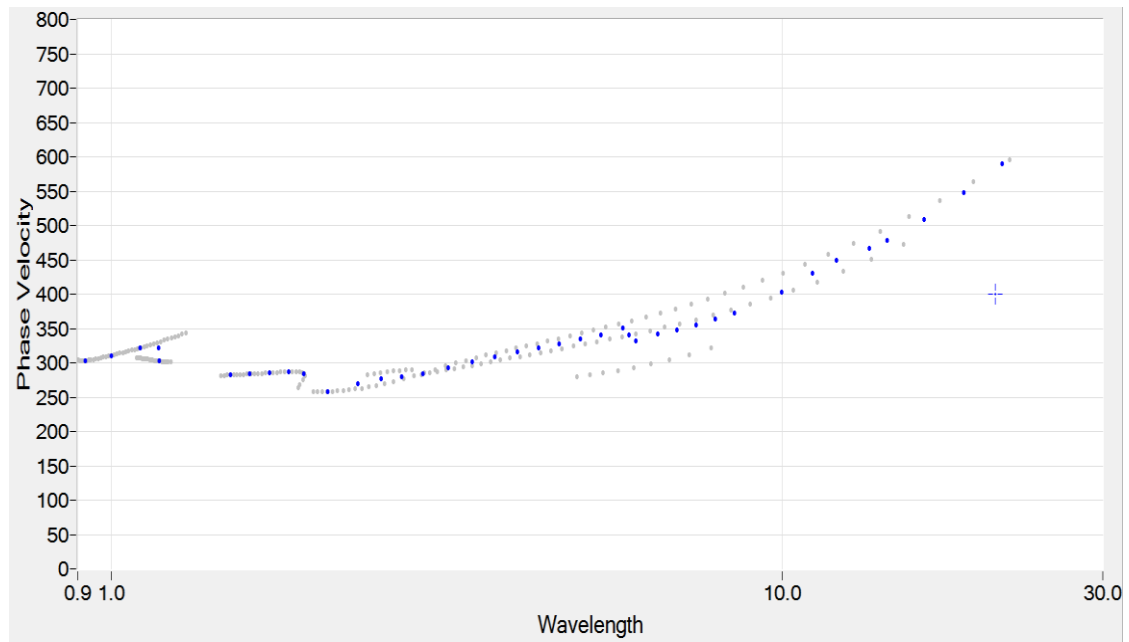


Figure 22. Example of a global representative dispersion curve (in blue) generated in WinSASW to match a composite experimental dispersion curve (in gray). Phase velocity is in m/s and wavelength is in m.

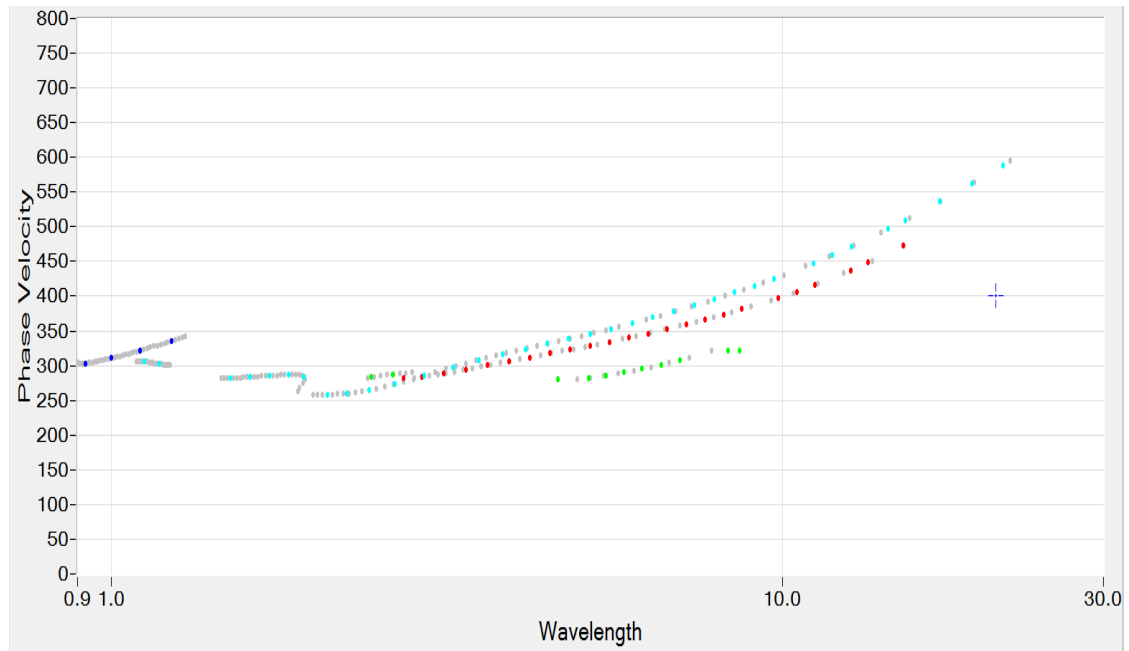


Figure 23. Example of an array representative dispersion curve (different colors) generated in WinSASW to match individual experimental dispersion curves (gray). Phase velocity is in m/s and wavelength is in m.

3.3.2.3 Inversion Analysis

WinSASW uses the maximum likelihood method (Joh 1996) for the inversion to determine the best match of the theoretical dispersion curve to the experimental one and therefore the shear wave velocity profile. The model which describes the theoretical response of the soil to a source is the dynamic stiffness matrix method, which was described in Chapter 2. At first the subsurface layering has to be assumed for the investigated depth of the geotechnical site. Soil layers (at least 10 suggested by the program) should be estimated with layer thickness (thinner on the top and thicker on the bottom), P-Wave Velocity (all set to 0), S-Wave Velocity (all set to 150 m/s as start values), Density (all set to 1900 kg/m^3), Poisson's Ratio (set to 0.3333) and a Damping Factor (all set to 0.02). The last layer is assumed to be thicker than the

maximum wavelength as this represents a half space for the dynamic stiffness matrix as explained in section 2.2.3. Figure 24 shows an input table showing these initial values for a 10-layer system.

Analysis Type: 2D 3D Enhanced 3D

F. of Displ. Bulb: 1.00
SubLayers: 16

Soil Profile No. of Layers: 10

	Thickness	P-Wave Vel.	S-Wave Vel.	Density	Poisson's R.	Damping F.
L1	0.5000	0.0000	150.0000	1900.0000	0.3333	0.0200
L2	0.5000	0.0000	150.0000	1900.0000	0.3333	0.0200
L3	0.5000	0.0000	150.0000	1900.0000	0.3333	0.0200
L4	0.5000	0.0000	150.0000	1900.0000	0.3333	0.0200
L5	1.0000	0.0000	150.0000	1900.0000	0.3333	0.0200
L6	1.0000	0.0000	150.0000	1900.0000	0.3333	0.0200
L7	2.0000	0.0000	150.0000	1900.0000	0.3333	0.0200
L8	4.0000	0.0000	150.0000	1900.0000	0.3333	0.0200
L9	8.0000	0.0000	150.0000	1900.0000	0.3333	0.0200
L10	700.0000	0.0000	150.0000	1900.0000	0.3333	0.0200
Dflt	0.0000	0.0000	150.0000	1900.0000	0.3333	0.0200

Apply All Apply All Apply All Apply All Apply All Apply All

Insert a Layer before Layer 10 Copy from INV 1 Clear All

Delete Layer.....

Figure 24. Example of a soil profile with 10 layers in WinSASW.

For the analysis type two different options can be chosen. The first option is a 2D analysis that assumes that the waves are planar. The second option assumes the wavefront of the surface wave is cylindrical and also considers a hemispherical wavefront of the body waves. It therefore considers the modes of all stress waves and represents the superposition of them. This approach is considered to be 3-dimensional and is recommended by Joh (1996) to be the best solution to represent the SASW measurements. Hence, it is used in this study.

Another option deals with the dispersion curve. It can be selected whether the analysis is based on the representative global average dispersion curve or the representative array dispersion curve. Both have their advantages for different conditions. The inversion over a global average dispersion curve suits better when there are no significant changes in stiffness or when there is significant lateral variability. If this does not suit for the site, the array average dispersion curve is considered to be the preferred approach, although it needs more computation power (Joh 1996).

The next step for the inversion is to determine the best matching starting model parameters that are obtained from different depth-to-wavelength ratios. This is done in two phases. In the first phase a certain layer thickness for each phase velocity point of the representative dispersion curve is assumed by a certain ratio of the corresponding wavelength to depth. With the dynamic stiffness matrix approach the shear wave velocity of each layer is determined. In the second phase the amount of layers from the temporary profile is reduced with increasing thick layers from top to bottom and a half space at the bottom. The shear wave velocities of the combined layers from Phase 1 are determined by a weighted average. With the obtained profile a theoretical dispersion curve is calculated with the corresponding root-mean-squared (RMS) error. The RMS error represents the difference between the representative dispersion curve and the theoretical dispersion curve. This whole process is repeated a determined amount of times with different depth-to-wavelength ratios (Joh 1996).

From the obtained preliminary shear wave velocity profiles the one which matches best to the theoretical dispersion curve is selected; this is identified by a

measure of the least RMS error. This is the starting model parameter for the following inversion analysis.

For the actual inversion analysis there are three model parameters that can be varied to reduce error: the shear wave velocity profile, the thickness of the soil layers, or both. At first only one model parameter should be varied until a reasonable profile is generated before varying other parameters. After a set of inversions are generated, the one with the lowest error in comparison to the theoretical dispersion curve is picked and its soil profile is taken for the next starting model parameter. Some other parameters can be changed manually to improve the results, such as density and Poisson's Ratio (especially for the deeper layers).

For the density the recommendations of Stokoe et al. (2005) are taken. It is suggested to change the unit weight to about 2000 kg/m^3 if the computed shear wave velocity is higher than 610 m/s, and to 2100 kg/m^3 if it is higher than 914 m/s. As long as the shear wave velocity is lower than 610 m/s it is set to the start parameter of 1900 kg/m^3 . Poisson's ratio should be changed to approximately 0.5 if the soil layer is below the water table. This depth is reached if the calculated P-wave velocity is above 1500 m/s (Lin et al. 2014). Nevertheless, these values are just recommendations and can be changed if reasonable as the final effect on the shear wave velocity is minor (Stokoe et al. 2005).

This whole process is repeated until the best match between the theoretical and representative dispersion curve is obtained, which is indicated by the lowest achievable RMS error (Department of Civil Engineering Chung-Ang University

2002). The resulting shear wave velocity vs. depth profile that is obtained represents a reasonable profile for the site, and an example profile is shown in Figure 25.

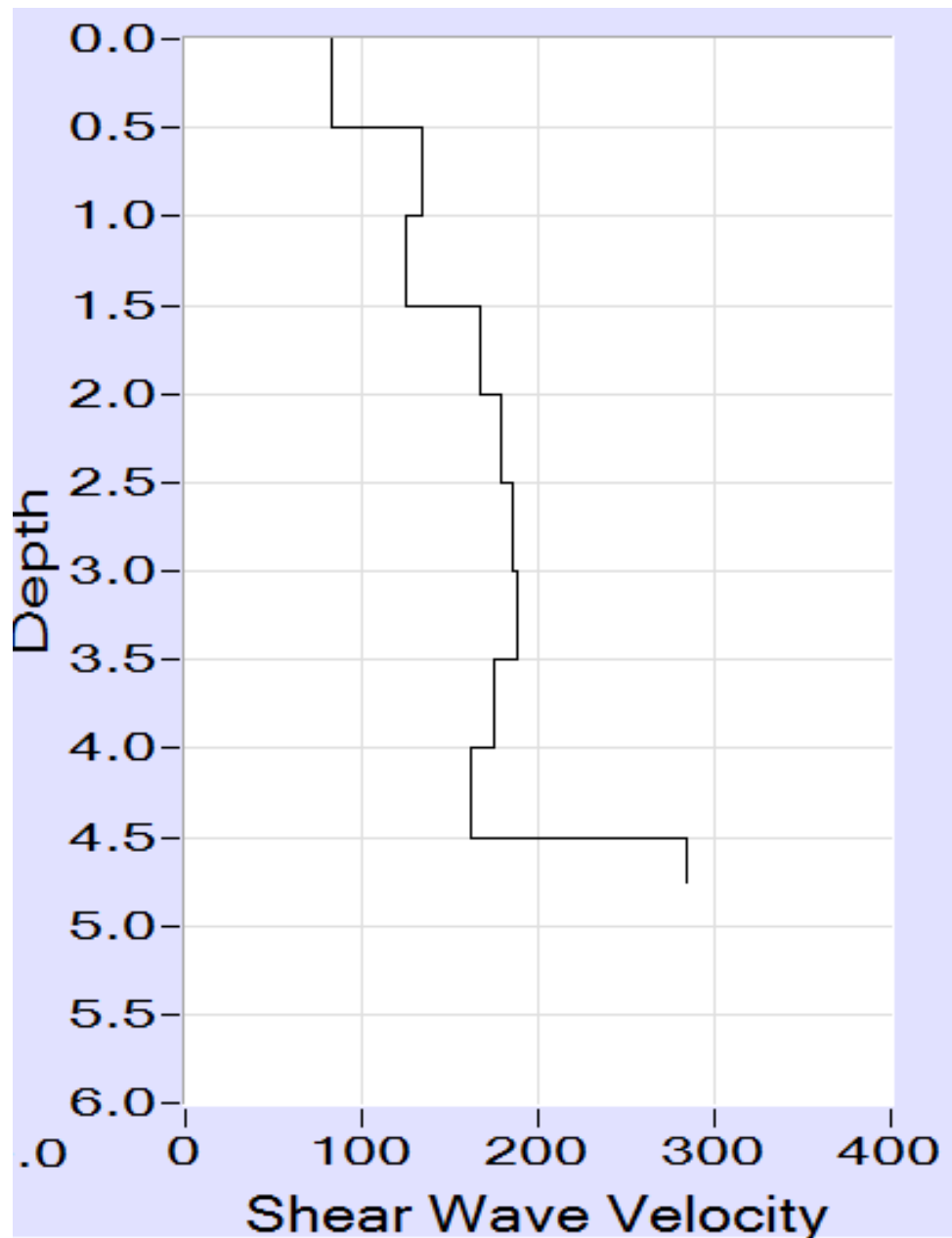


Figure 25. Example shear wave velocity profile vs. depth. Depth is in m and shear wave velocity is in m/s.

4. SASW Testing and Results

This chapter presents details about the five different sites in Rhode Island where SASW testing was performed with the Olson Instruments, Inc. system. Testing was performed at the Gainer Memorial Dam in Scituate, the old Farmer's Market site in Providence, the Middleton building site on the URI Bay Campus, Misquamicut Beach, and Quonochontaug Beach. The locations are shown in Figure 26.



Figure 26. Locations of the different test sites. (Source: Rhode Island Base and Elevation Maps. (n.d.). Retrieved January 7, 2016, from http://www.netstate.com/states/geography/mapcom/ri_mapscom.htm)

The Old Farmer' Market, Gainer Dam and the Middleton sites were chosen as tests with the ASARS system were conducted there. Misquamicut Beach is a

replenished beach while Quonochontaug Beach is a natural beach. Hence, these two sites were chosen to estimate shear wave velocity profiles and find out if there are differences due to the different nature of these two sites. The condition of each site and details of the testing will be described before the results are presented in each section.

4.1 Gainer Memorial Dam, Scituate, RI

The Gainer Memorial Dam was constructed to create a fresh water reservoir for the inhabitants of Rhode Island. The dam is about 975 m long and with a maximum height of 33 m. The estimated cross section for the location of the test, which is the same location of a previous test with the ASARS system as well as a boring, is shown in Figure 27.

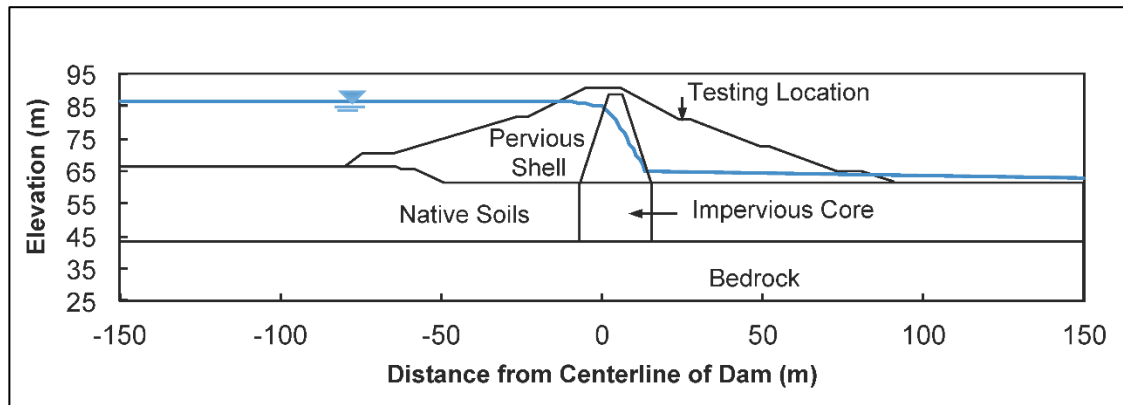


Figure 27. Cross section of Gainer Memorial Dam (Reyes et al. 2016).

The estimated geological setting from a SPT-test as well as the ASARS test is presented in Figure 28. As can be seen, the pervious shell at the test location consists of sand, gravel and cobbles to a depth of about 22.5 m (~74 ft.). Below is a 7.5 m

(~24.5 ft.) sand (outwash) layer before at a depth of 30 m (~98 ft.) granite bedrock is present (Reyes et al. 2016).

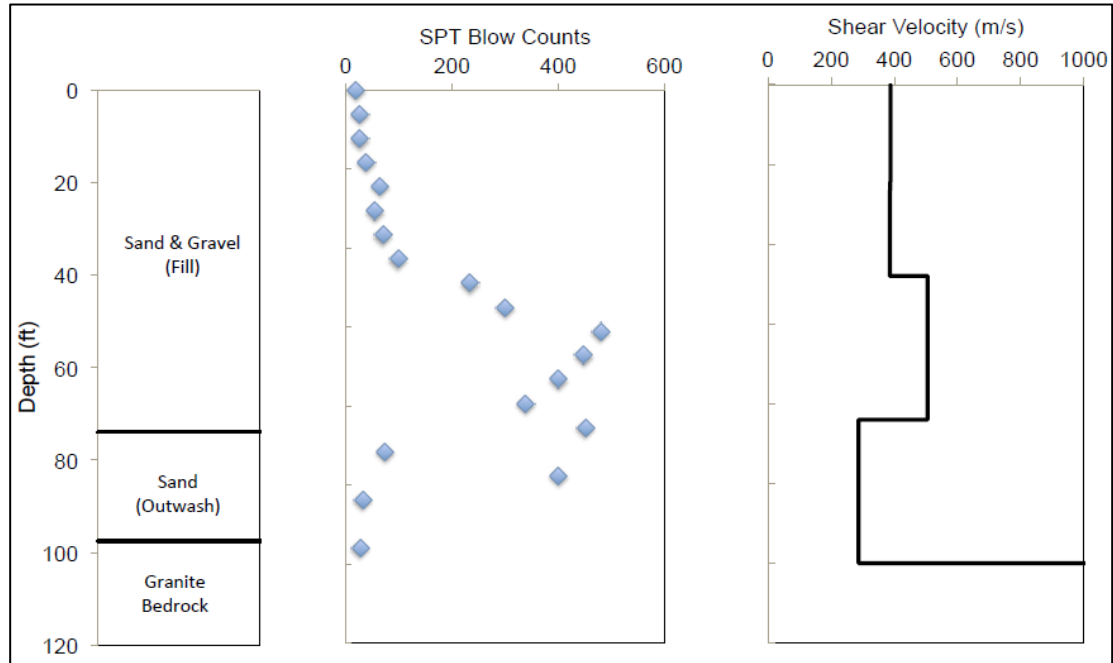


Figure 28. Geological setting of Gainer Memorial Dam (Bradshaw and Reyes 2015).

SASW testing was conducted at the Gainer Dam in Scituate, Rhode Island on September 22, 2015. Testing was performed on the grass-covered downstream face on the second “bench” of the slope, northeast of the concrete stairs between two drains spaced approximately 100 m apart (Figure 29). Testing was performed with 4.5 Hz geophones up to a spacing of 12 m, and with 2 Hz geophones up to a spacing of 80 m.



Figure 29. Locations of the SASW array on the Gainer Memorial Dam (red line indicates use of 4.5 Hz geophones; blue line indicates use of 2 Hz geophones) (Google Maps).

A 1 kg sledge hammer, 4 kg sledge hammer, and a 50 kg drop weight suspended from a tripod were used as impact sources (Figure 30). Occasionally a steel plate and/or rubber plate were used as a striker plate on the ground surface.



(a.) (b.) (c.)
 Figure 30. a.) 1 kg sledge hammer; b.) Rubber pad, steel plate and 4 kg sledge hammer; and c.) Tripod with 50 kg dropping weight.

Spikes attached to the bottom of the 4.5 Hz geophones were used to fix them better to the ground so they can measure the Rayleigh Waves more accurately. For the 2 Hz geophones no spikes were available so it was made sure that they were in contact with the ground as best as possible. The geophones and the source were set up in a linear array with different spacings between the two geophones and between the first geophone and the source. The geophones were connected to the NDE 360 platform to acquire the data. Geophone 1 was connected to Channel 1 (and set as the trigger channel) and the other geophone was connected to Channel 4.

The location of the source was fixed for all the testing at a distance 8 m away from the eastern drain. The geophones were placed in a linear array from the source and were moved to the next greater spacing after each test. Spacings of 0.5 m, 1 m, 1.5 m, 2 m, 3 m, 4 m, 5 m and 6 m were used for the 4.5 Hz geophones. For the 2 Hz

geophones, spacings of 5m, 7.5m, 10m, 12.5m, 15m, 20m, 25m, 30m and 40m were used. Figure 31 illustrates the smallest and the largest spacing of testing with the 2 Hz geophones.

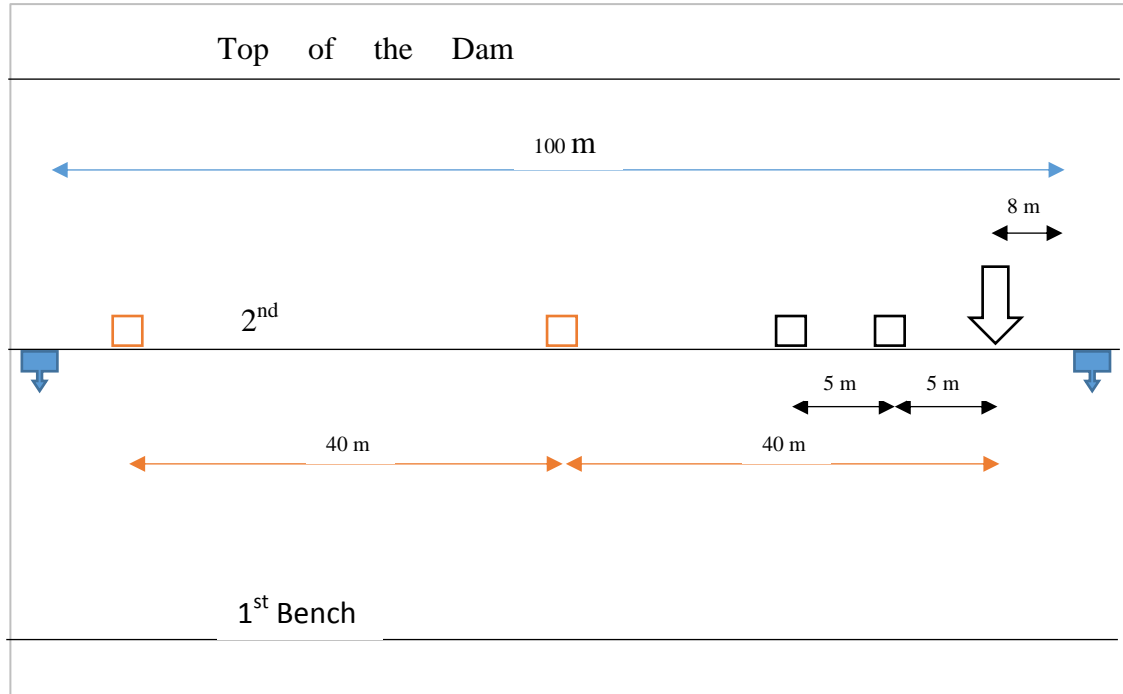


Figure 31. Setup with different spacing for the 2 Hz Test.

For some cases different sources were used at the same spacing to make sure the acquired data was as good as possible. The settings and parameters for each spacing, including source and scale of the channels, the saved filename and if it was used for the calculation of the dispersion curve can be seen in Tables 2 and 3 for testing with 4.5 Hz geophones and with 2 Hz geophones, respectively; the number of records was always set to 4.

Table 2. Summary of testing details at the Gainer Dam site with the 4.5 Hz geophones.

Test #	Spacing d (m)	Gain	Time/pt (μs)	Source	Plate type	Scale	NDE File	Disp. Curve
1	0.5	10	200	S	-	-	NDE77	Yes
2	1	10	200	B	-	-	NDE78	No
3	1	100	200	B	-	-	NDE79	Yes
4	1	100	200	B	Rubber + Steel	~ 80%	NDE80	No
5	1.5	100	200	B	Rubber + Steel	~ 85%	NDE81	Yes
6	2	100	200	B	Rubber + Steel	~67%	NDE82	Yes
7	3	100	200	B	Rubber + Steel	~52%	NDE83	Yes
8	4	100	200	B	Rubber + Steel	-	NDE84	Yes
9	4	1000	200	B	Rubber + Steel	~85%	NDE85	Yes
10	5	100	200	B	Rubber + Steel	~40%	NDE86	Yes
11	5	1000	200	B	Rubber + Steel	~77%	NDE87	Yes
12	6	100	200	B	Rubber + Steel	~36%	NDE88	Yes
13	6	1000	200	B	Rubber + Steel	~70%	NDE89	Yes
14	6	100	200	DW	Rubber	~75%	NDE90	Yes

Note: 1. S=Small Sledgehammer
2. B=Big Sledgehammer
3. DW= Drop Weight

Table 3. Summary of testing details at the Gainer Dam site with the 2 Hz geophones.

Test #	Spacing d (m)	Gain	Time/pt (μs)	Source	Plate type	Scale	NDE File	Disp. Curve
1	5	100	200	DW	Rubber	~70%	NDE91	No
2	5	100	200	DW	Rubber	~80%	NDE92	Yes
3	7.5	100	200	DW	Rubber	~67%	NDE93	Yes
4	10	100	200	DW	Rubber	~ 46%	NDE94	Yes
5	12.5	100	200	DW	Rubber	~ 33%	NDE95	No
6	12.5	1000	200	DW	Rubber	~79%	NDE96	No
7	12.5	1000	200	B	Rubber + Steel	~65%	NDE97	No
8	15	1000	200	B	Rubber + Steel	~70%	NDE98	No
9	15	1000	200	DW	Rubber	~78%	NDE99	No
10	20	1000	200	DW	Rubber	~70%	NDE100	No
11	25	1000	200	DW	Rubber	~70%	NDE101	Yes
12	25	1000	200	DW	Rubber	~70%	NDE102	No
13	30	1000	200	DW	Rubber	~74%	NDE103	No
14	30	1000	200	DW	Rubber	~70%	NDE104	No
15	40	1000	500	DW	Rubber	~72%	NDE105	No

Note: 1. S=Small Sledgehammer
2. B=Big Sledgehammer
3. DW= Drop Weight

4.1.1 Results for Gainer Dam

The first step of the post-processing consisted of a review of the data in the program WinTFS. To improve the data quality, windowing with the exponential cut filter and a decay of 200 was used. During the procedure certain files were excluded if the measurement was bad and if there was a better quality file for the same spacing. Hence, the files NDE 78, NDE 80, NDE 91, NDE 95, NDE 96 and NDE 103 were removed from further analysis.

In the second step, the program WinSASW was used to mask undesired portions of the phase vs. frequency plot of the files if these did not match the requirements that were described in section 3.3.2.1. Within this process, additional data were completely excluded so that finally only the following NDE files were used: NDE 77, NDE 79, NDE 81, NDE 82, NDE 83, NDE 84, NDE 85, NDE 86, NDE 87, NDE 88, NDE 89, NDE 90, NDE 92, NDE 93, NDE 94 and NDE 101. On the basis of these files the following composite dispersion curves were calculated.

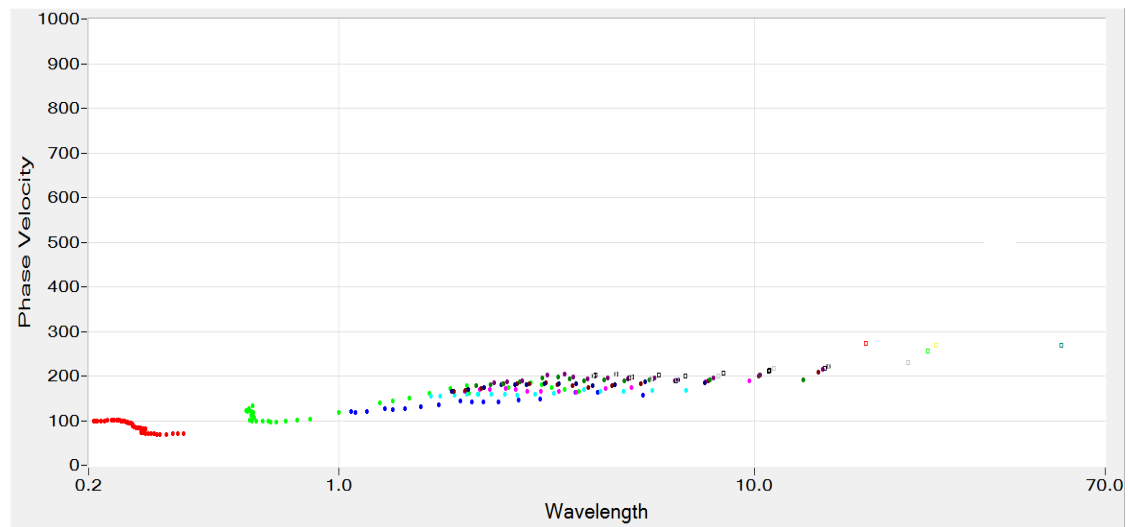


Figure 32. Composite dispersion curve (phase velocity vs wavelength) for the Gainer Dam site. Phase velocity is in m/s and wavelength is in m.

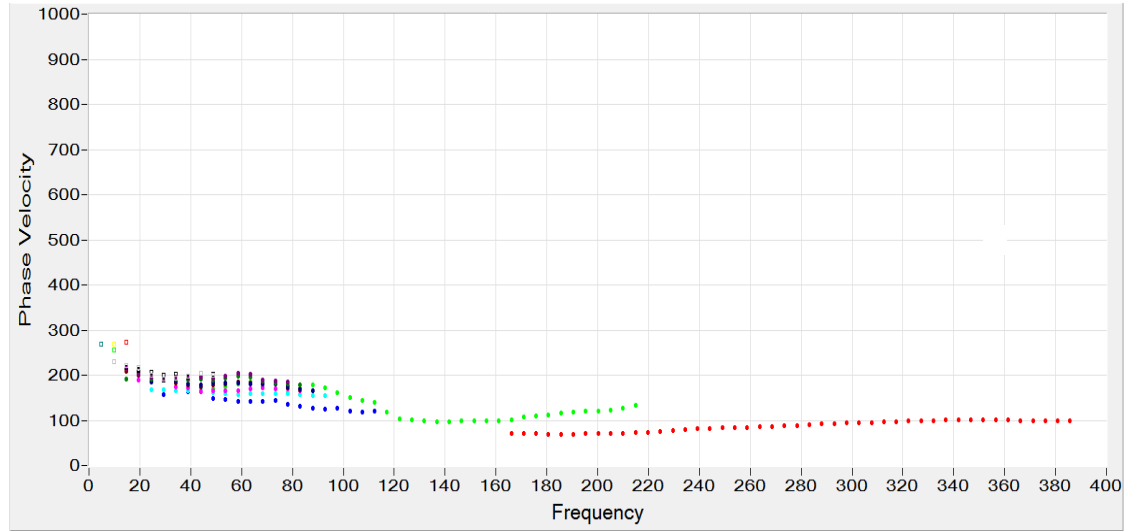


Figure 33. Composite dispersion curve (phase velocity vs frequency) for the Gainer Dam site. Phase velocity is in m/s and frequency is in Hz.

In the following step, the global and array representative dispersion curves of the composite experimental dispersion curve were estimated to be used for the following inversion. As can be seen in Figure 34 (solid blue circles), the maximum wavelength that is included in the global representative dispersion curve is about 40 m, hence the maximum investigation depth of the site for this approach is 20 m (half the maximum wavelength). However, as shown in Figure 36, the maximum wavelength for the array representative dispersion curve (solid blue circles) is about 50 m which determines a maximum investigation depth of 25 m for this approach. The starting soil profile was estimated as suggested in section 3.3.2.3. The inversion process was conducted two times, once with the global representative dispersion curve and one time with the array representative dispersion curve. The more accurate 3D method was used in both cases.

The suggested soil profile was adjusted if the shear wave velocity or primary wave velocity exhibited certain values as described in section 3.3.2.3. As soon as a reasonable match between the representative and theoretical dispersion curve and no further improvement of the RMS error could be achieved, the inversion and adjustment process was finished. The match of the theoretical and global representative dispersion curves for this site is shown in Figures 34.

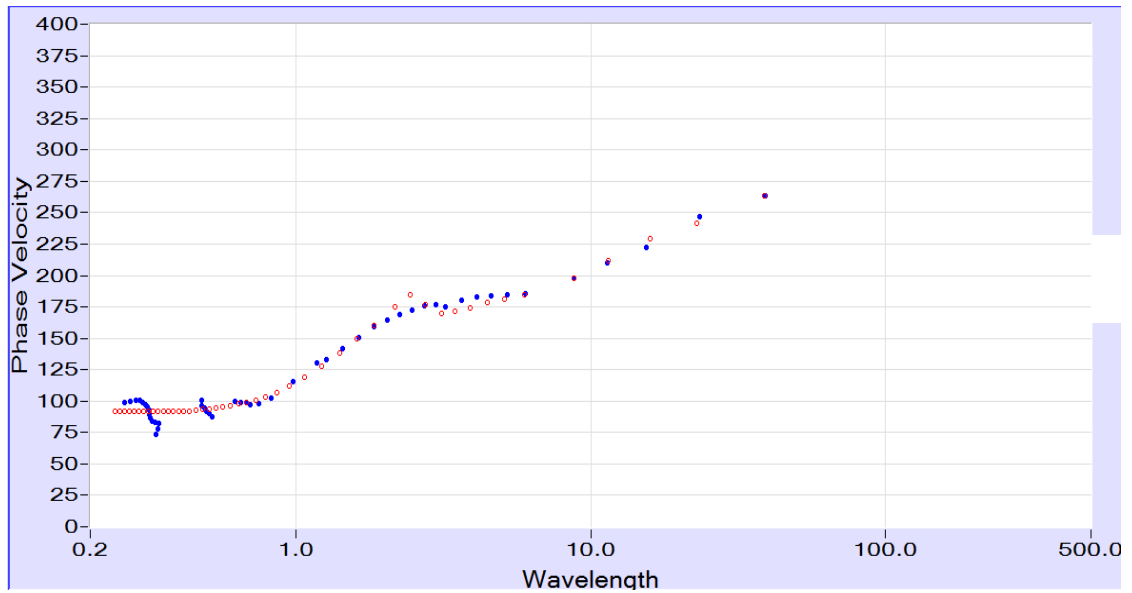


Figure 34. Global representative (solid blue circles) and theoretical dispersion curve (empty red circles) for Gainer Dam. Phase velocity is in m/s and wavelength is in m.

The shear wave velocity profile based on the theoretical dispersion curve is presented in Figure 35. In addition to the best possible inversion, five other inversions are shown that had a higher RMS error to evaluate the variety. Typical shear wave velocities of soft sand, silt and clay as well for dense gravel were included according to estimations from Lin et al. (2014).

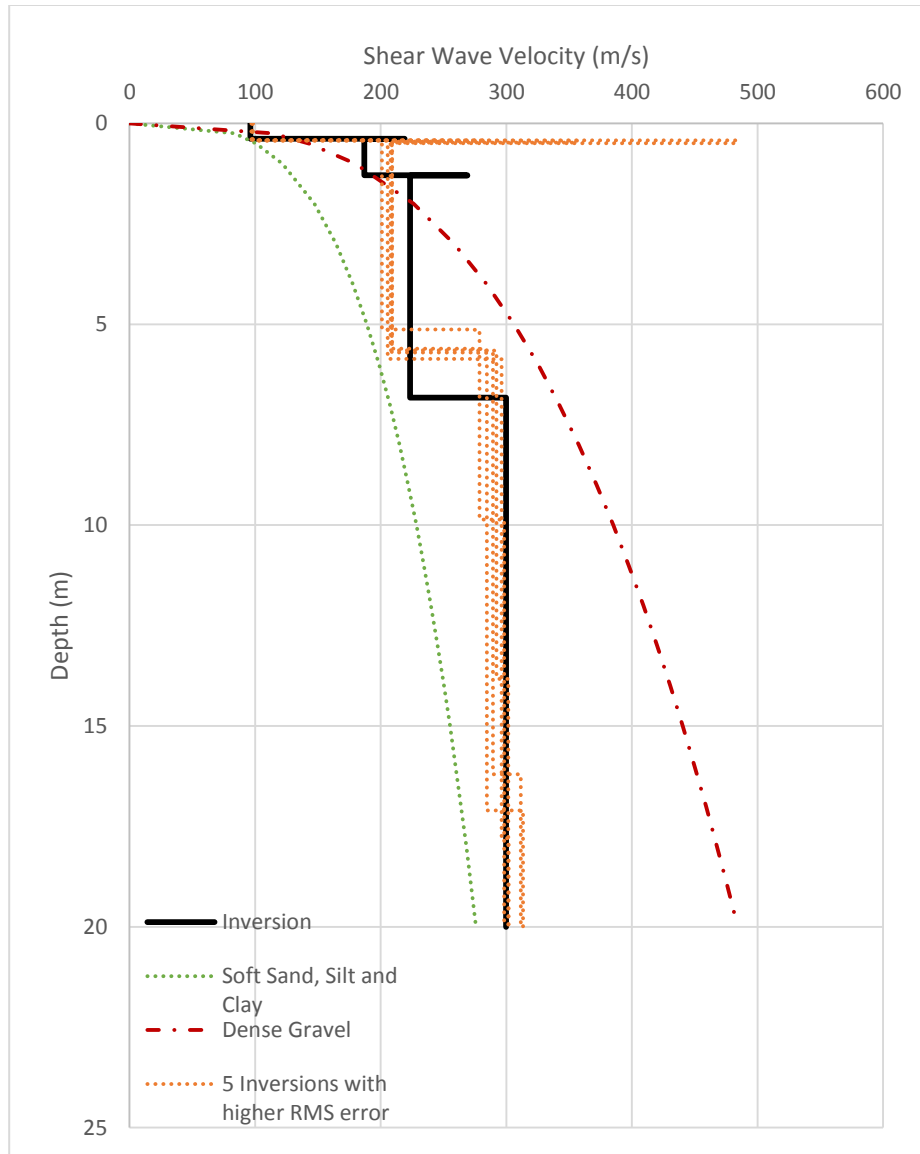


Figure 35. Estimated shear wave velocity profile for the Gainer Dam site based on global array dispersion curve.

The match of the theoretical dispersion curve and the array representative dispersion curve is shown in Figure 36 with a resulting shear wave velocity profile presented in Figure 37.

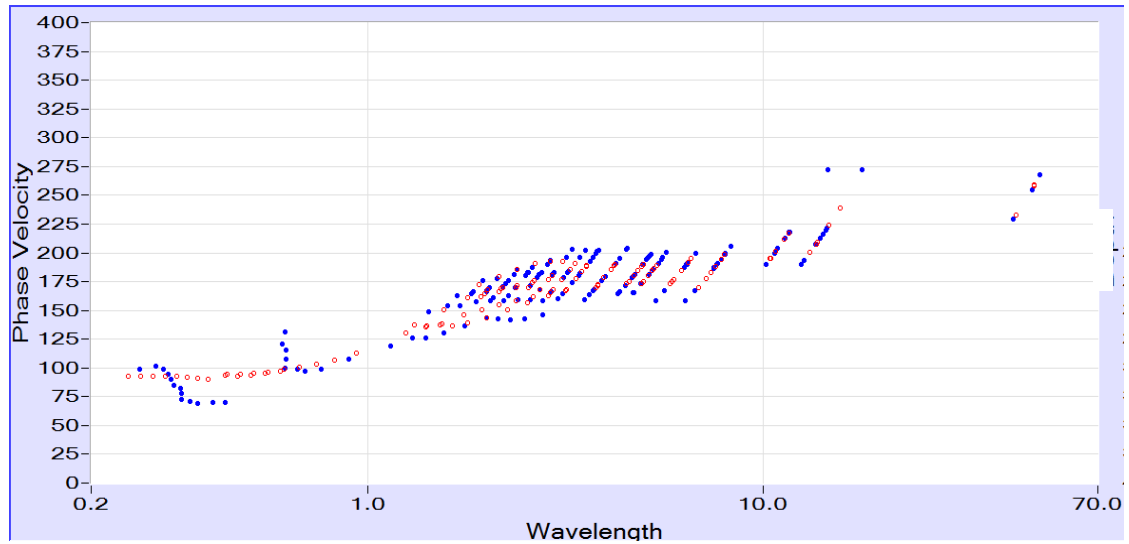


Figure 36. Array representative (solid blue circles) and theoretical dispersion curve (empty red circles) for Gainer Dam. Phase velocity is in m/s and wavelength is in m.

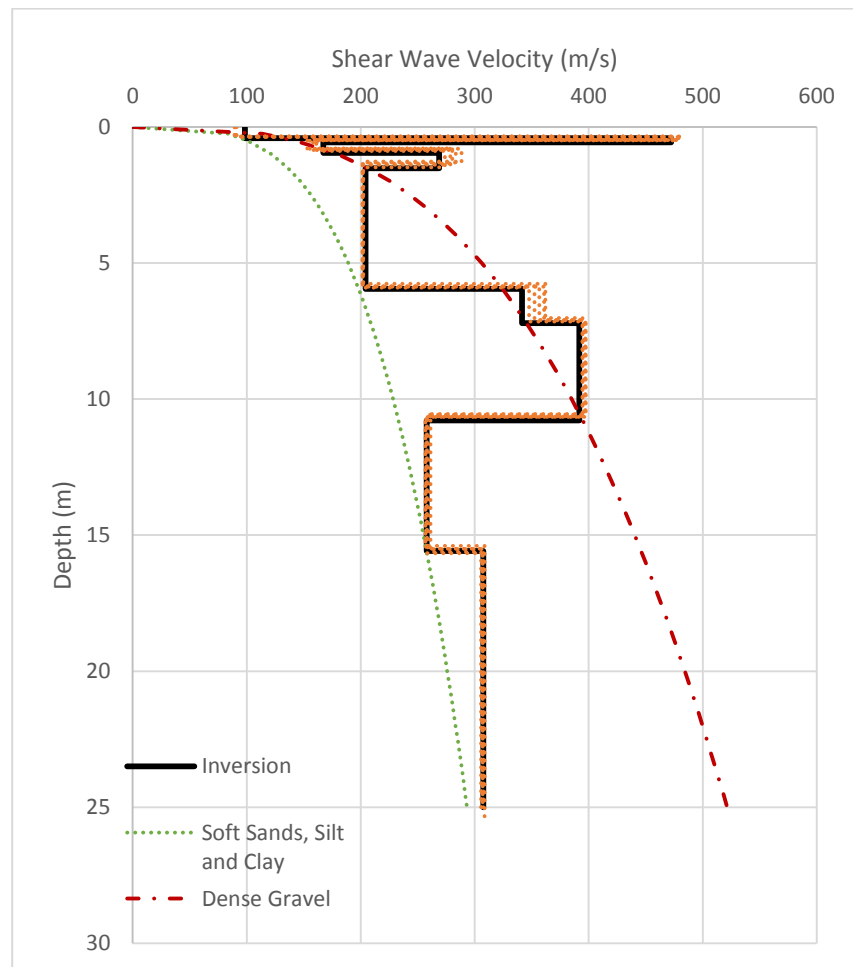


Figure 37. Estimated shear wave velocity profile for the Gainer Dam site based on array representative dispersion curve.

The shear wave velocity profile based on the array representative dispersion curve is more detailed than the other profile. The SPT-blow counts in Figure 28 show an increase to a maximum value at about 15 m and then a drop in blow counts below this layer. This trend is picked up more reasonable by the array approach although the depths are not the same. The shear wave velocity profile based on the global approach shows a steady increase in stiffness and no decrease in stiffness as predicted by the SPT-blow count profile. Hence, for the rest of the study only the array representative dispersion curve should be used for the analysis as it shows more accurate results.

4.2 Old Farmer's Market, Providence, RI

Different tests have been conducted to estimate the geologic setting (Figure 38) of the Old Farmer's Market before. The upper 5 m consist of fill material, underlain by a thick inorganic silt layer which is typical for the Providence area (Bradshaw et al. 2007).

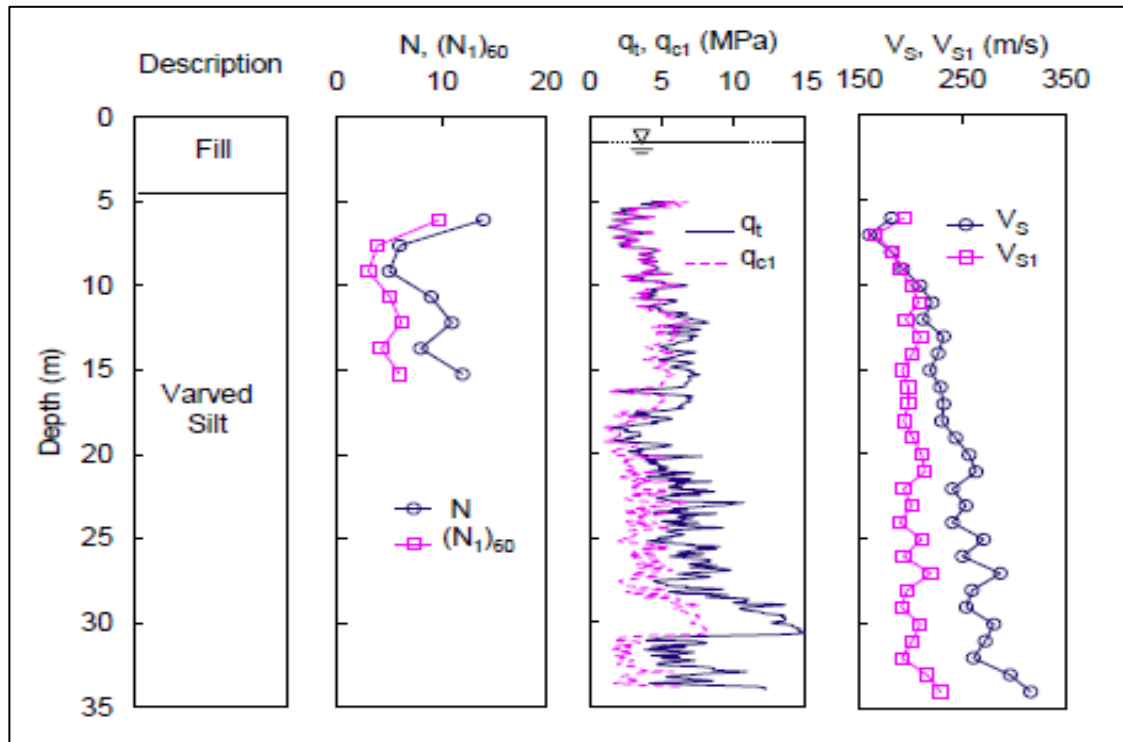


Figure 38. Geological setting of the Old Farmer's Market site (Bradshaw et al. 2007).

The field test was conducted at the site of the old Farmer's Market in Providence, Rhode Island on October 16, 2015. The test site was overgrown by plants and the ground was covered in most areas with gravel. A nearby elevated highway and railroad tracks with considerable traffic created a lot of noise and sometimes triggered the SASW system unexpectedly. The site location is shown in Figures 39 and 40. The center geophone was placed across from the 7th pier of the elevated highway, which can be seen in Figure 30. Both the 4.5Hz and 2 Hz geophones were used.

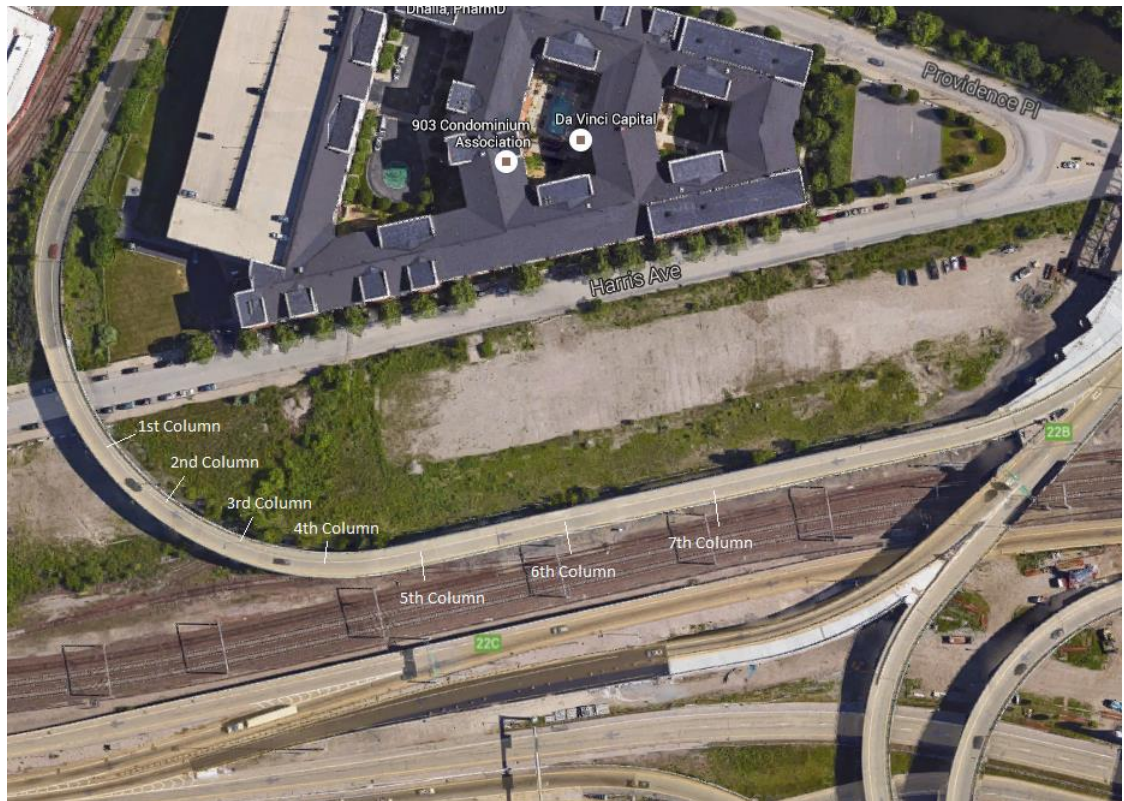


Figure 39. Old Farmer's Market site in Providence, RI with the highway piers marked.

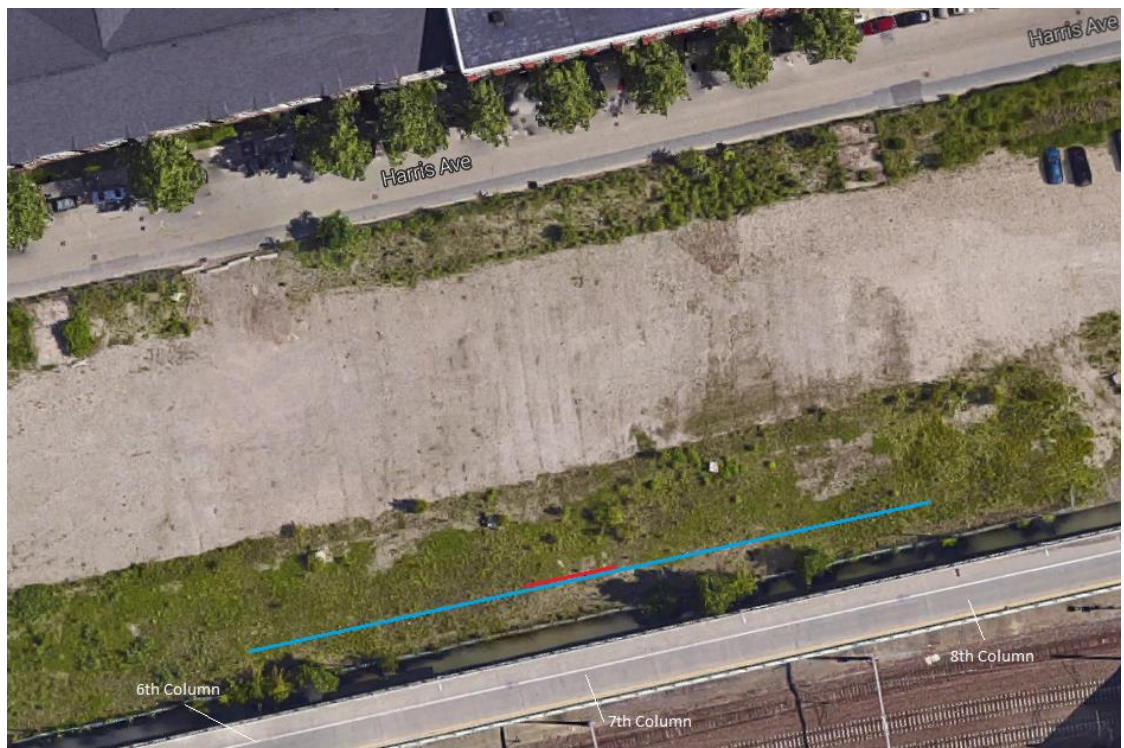


Figure 40. Location of the 4.5 Hz geophone array (red line) and the 2 Hz array (blue line) at the old Farmer's Market site.

The coordinates of the test site are 41.827073° North and 71.420966° West. The linear array was aligned parallel to the fence at a distance of 2.2 meters. The center geophone was placed in line with the 7th pier of the elevated highway. The first geophone was kept in the same location while the second geophone and the source was moved to test at different spacings. The test was conducted with spacings of 0.5 m, 1 m, 2 m, 3 m, 4 m, 5 m and 6 m with the 4.5 Hz geophones and 10 m, 20 m, 30 m and 40 m with the 2 Hz geophones. 6 records were collected for every test. Tables 4 and 5 summarize the testing details for the tests performed with the 4.5 Hz and 2 Hz geophones, respectively.

Table 4. Summary of testing details at the old Farmer's Market site with the 4.5 Hz geophones.

Test #	Spacing (m)	Gain	Source	Plate type	Scale	Trigger %	NDE File	Disp. Curve
1	0.5	100	S	-	-	6	NDE 135	No
2	0.5	100	B	Rubber	-	6	NDE 136	No
3	1	100	S	Rubber + Steel	-	6	NDE 137	No
4	1	100	S	Rubber + Steel	-	6	NDE 138	Yes
5	2	100	B	Rubber + Steel	~70%	6	NDE 139	Yes
6	3	100	B	Rubber + Steel	~50%	6	NDE 140	No
7	3	100	B	Rubber + Steel	~50%	6	NDE 141	No
8	4	100	B	Rubber + Steel	~47%	6	NDE 142	No
9	4	1000	S	Rubber + Steel	~75%	6	NDE 143	No
10	4	1000	S	Rubber + Steel	~80%	10	NDE 144	No
11	5	1000	S	Rubber + Steel	~80%	10	NDE 145	Yes
12	5	100	B	Rubber + Steel	~35%	10	NDE 146	No
13	6	100	B	Rubber + Steel	~40%	10	NDE 147	No
14	6	1000	S	Rubber + Steel	~85%	10	NDE 148	No
15	6	100	DW	Rubber + Steel	~65%	10	NDE 149	No

Note: 1. S=Small Sledgehammer

2. B=Big Sledgehammer

3. DW= Drop Weight

Table 5. Summary of testing details at the old Farmer's Market site with the 2 Hz geophones.

Test #	Spacing (m)	Gain	Source	Plate type	Scale	Trigger %	NDE File	Disp. Curve
1	10	100	DW	Rubber + Steel	~25%	6	NDE 150	No
2	10	1000	DW	Rubber + Steel	~80%	14	NDE 151	Yes
3	10	1000	B	Rubber + Steel	~75%	14	NDE 152	Yes
4	20	1000	DW	Rubber + Steel	~75%	14	NDE 153	No
5	20	1000	B	Rubber + Steel	~70%	14	NDE 154	No
6	30	1000	B	Rubber + Steel	~35%	14	NDE 155	No
7	30	1000	DW	Rubber + Steel	~75%	14	NDE 156	No
8	40	1000	DW	Rubber + Steel	~40%	14	NDE 157	No

Note: 1. S=Small Sledgehammer
2. B=Big Sledgehammer
3. DW= Drop Weight

4.2.2 Results of Farmer's Market

The data was imported into the program WinTFS and windowed using the exponential cut filter with a decay of 200. The files NDE 136, NDE 143, NDE 147, NDE 149 and NDE 150 were excluded after reviewing.

After further review and masking in WinSASW, only NDE 138, NDE 139, NDE 145, NDE 151 and NDE 152 were selected for the calculation of the composite experimental dispersion curves (Figure 41 and 42) which was used subsequently to determine a representative dispersion curve.

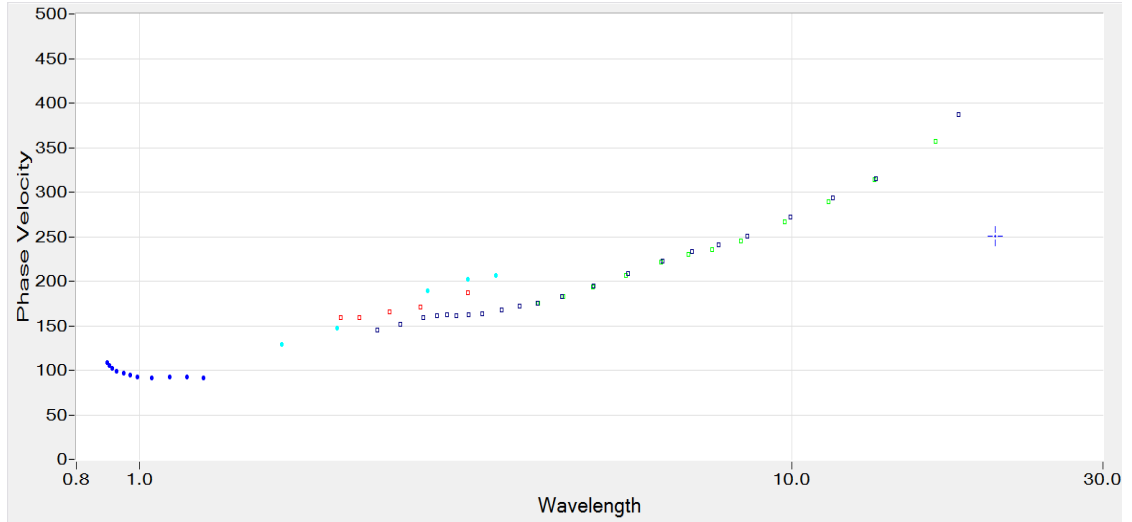


Figure 41. Composite dispersion curve (phase velocity vs wavelength) for the old Farmer's Market site. Phase velocity is in m/s and wavelength is in m.

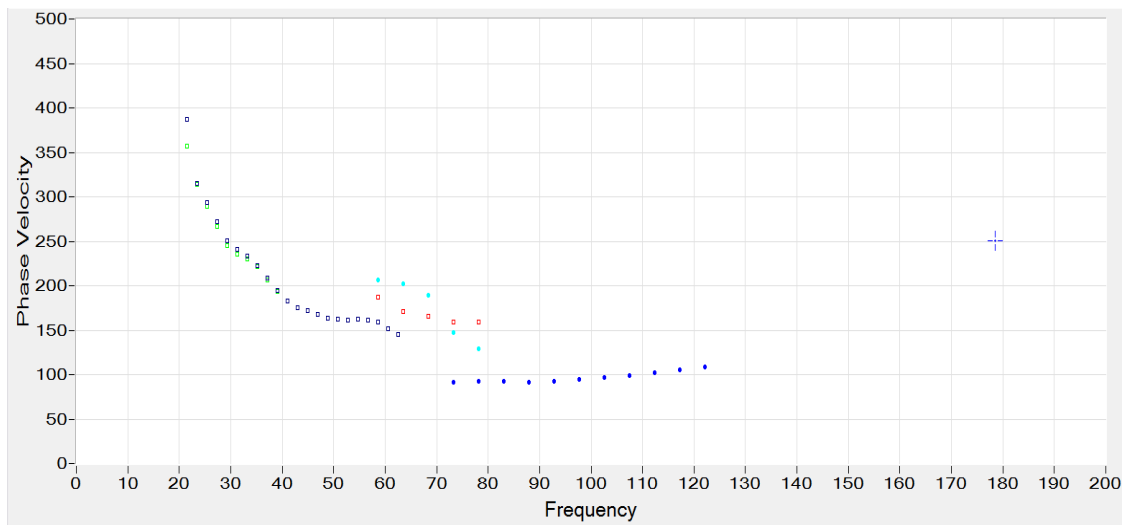


Figure 42. Composite dispersion curve (phase velocity vs frequency) for the old Farmer's Market site. Phase velocity is in m/s and frequency is in Hz.

Based on the representative curve (solid blue circles in Figure 43) the inversion was performed using the representative array dispersion method with the 3D analysis. The maximum investigation depth is approximately 7 m due to the maximum

wavelength of 14 m of the representative dispersion curve. Figure 43 shows the match between the representative dispersion curve and the theoretical dispersion corresponding to the estimated shear speed profile as shown in Figure 44.

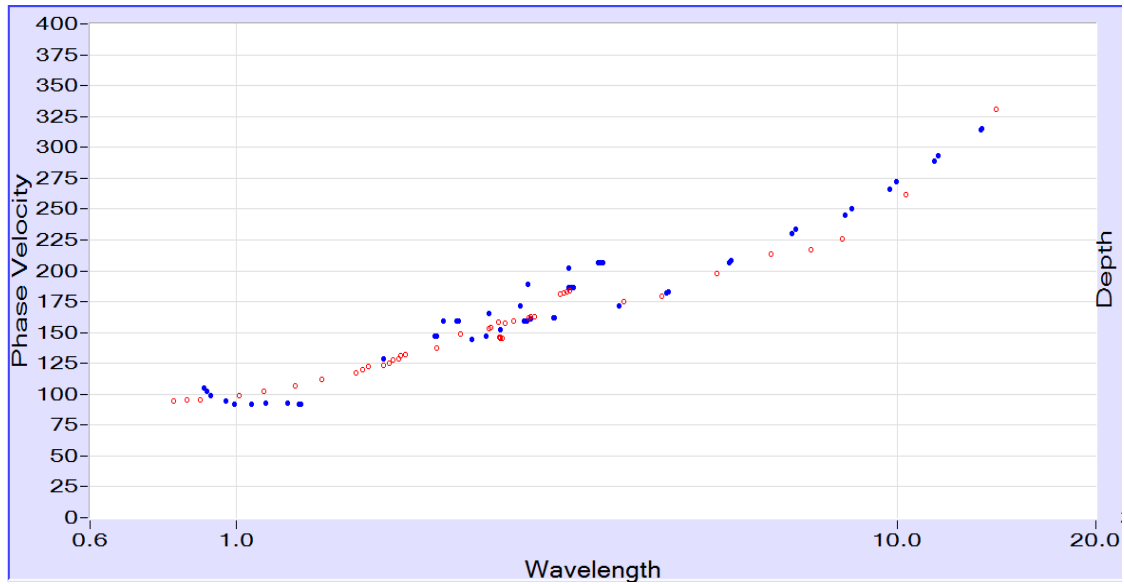


Figure 43. Representative (solid blue circles) and theoretical dispersion curve (empty red circles) for the old Farmer's Market site. Phase velocity is in m/s and wavelength is in m.

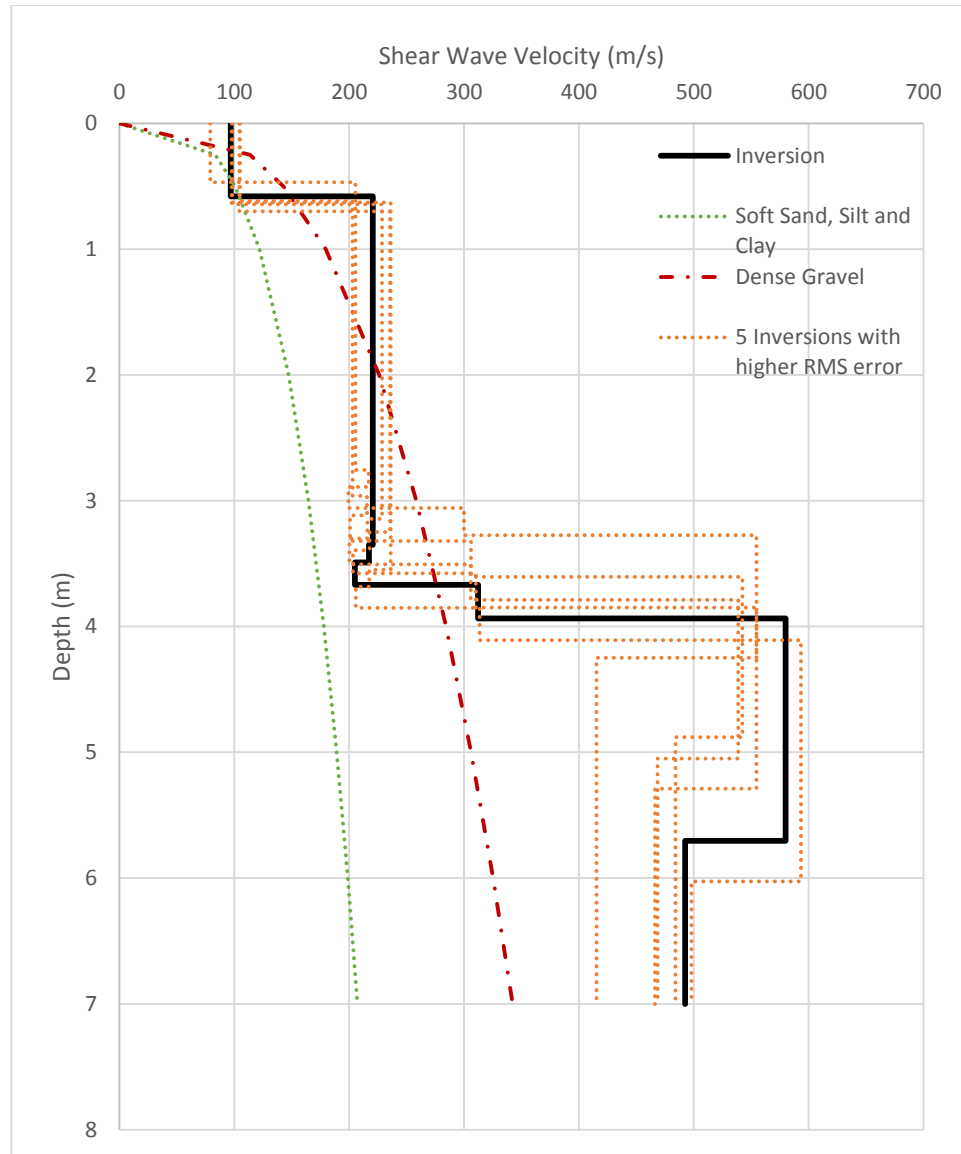


Figure 44. Estimated shear wave velocity profile for the old Farmer's Market site.

4.3 Middleton Building, URI Bay Campus

The geological setting of the URI Bay Campus is estimated by boring tests that were conducted as part of construction of the Watkins building in 1975. The results of these boring tests are attached in the Appendix. They show bedrock at a depth of about 3.5 to 6 m overlain by fine to medium sand, some silt and gravel.

For this study, a number of SASW tests were performed in a grassy area immediately east of the parking lot of the Middleton Laboratory building on the URI Narragansett Bay Campus. Tests # 1 and #2 were performed with 4.5 Hz geophones at spacings up to 6 m and Test #3 were performed with 2 Hz geophones at spacings up to 15 m. Test #1 was conducted on June 10, 2015, Test #2 on July 22, 2015 and Test #3 on August 14, 2015. The location of the arrays are shown in Figure 45. Spikes were mounted on the bottom of the 4.5 Hz geophones to fix them better to the ground.



Figure 45. Location of SASW arrays at the Middleton Building site (Red Lines - 4.5 Hz geophones; Blue Line – 2 Hz geophones) (Google Maps).

A 4 kg sledge hammer and a tamper with a 5.858 kg weight dropped from a height of up to 57.5 cm were used (Figure 46). A steel plate covered with a rubber pad were used as a striker plate on the ground.



(a.) (b.)
Figure 46. Impact sources for the tests performed at the Middleton building: a.) Sledge hammer; and b.) Tamper.

For these tests, the first geophone was kept at the same location while the source and the second geophone were moved for each spacing. Details of the tests are summarized in Tables 6-8 for the three arrays.

Table 6. Summary of testing details for Test #1 at the Middleton building site with the 4.5 Hz geophones.

Test	Spacing	Gain	Time/pt	Source	Plate type	NDE File	Disp. Curve
------	---------	------	---------	--------	------------	----------	-------------

#	(m)		(μ s)				
1	1	100	20	B	-	NDE 20	No
2	1	100	500	B	-	NDE 21	Yes
3	2	100	500	B	-	NDE 22	Yes
4	4	100 and 1000	500	B	-	NDE 23	Yes
5	4	1000	500	B	-	NDE 24	Yes
6	6	1000	500	B	-	NDE 25	Yes

Note: 1. B=Big Sledgehammer

Table 7. Summary of testing details for Test #2 at the Middleton building site with the 4.5 Hz geophones.

Test #	Spacing (m)	Gain	Time/pt (μ s)	Source	Plate type	NDE File	Disp. Curve
1	1.5	10	100	B	Steel + Rubber	NDE 29	-
2	1.5	10	100	B	Steel + Rubber	NDE 30	-
3	1.5	100	200	T	Steel + Rubber	NDE 31	-
4	1.5	100	200	T	-	NDE 32	-
5	1.5	10	200	B	Steel + Rubber	NDE 33	-
6	1.5	100	200	B	Steel + Rubber	NDE 34	-
7	1.5	100	200	T	Steel + Rubber	NDE 35	-
8	3	100	200	T	-	NDE 36	-
9	3	1000	200	T	-	NDE 37	-
10	4.5	1000	200	T	-	NDE 38	-
11	4.5	100	200	T	-	NDE 39	-
12	6	1000	200	T	-	NDE 40	-

Note: 1. B=Big Sledgehammer
2. T=Tamper

Table 8. Summary of testing details for Test #3 at the Middleton building site with the 2 Hz geophones.

Test #	Spacing (m)	Gain	Time/pt (μ s)	Source	Plate type	Scale	NDE File	Disp. Curve
1	5	1000	500	B	Steel + Rubber	-	NDE 41	Yes
2	5	1000	500	FS	Steel + Rubber	-	NDE 42	No

3	5	100	500	B	Steel + Rubber	~ 12%	NDE 43	No
4	5	100	500	B	Steel + Rubber	~ 20%	NDE 44	Yes
5	7.5	1000	500	B	Steel + Rubber	~ 71%	NDE 45	No
6	7.5	1000	500	B	Steel + Rubber	~ 35%	NDE 46	Yes
7	10	1000	500	B	Steel + Rubber	~ 75%	NDE 47	No
8	10	1000	500	B	Steel + Rubber	~ 75%	NDE 48	No
9	12.5	1000	500	B	Steel + Rubber	~ 65%	NDE 49	No
10	12.5	1000	500	B	Steel + Rubber	~ 65%	NDE 50	No
11	15	1000	500	B	Steel + Rubber	~ 38%	NDE 51	No
12	15	1000	500	B	Steel + Rubber	~ 38%	NDE 52	No

Note: 1. B=Big Sledgehammer
2. FS=Foot Stamp

4.3.2 Results for Middleton Building Site

The variation of shear wave velocity vs. depth was estimated at this site using data collected as part of Test #1 and #3 (described above) because these tests were performed along the same line (Figure 45). The data was first processed in WinTFS to determine which data should be used for the further analysis in WinSASW. Data files NDE 42 and NDE 43 were eliminated from further processing because other files contained better quality data for the same spacing.

Additional data files were eliminated from the determination of a dispersion curve based on the various criteria described in section 3.3.2.1. In some cases, data were removed simply because the resulting dispersion curve did not match the trends of the rest of the data. Finally, only the following files were used for the composite dispersion curve that formed the basis for the determination of a representative dispersion curve: NDE 21, NDE 22, NDE 23, NDE 24, NDE 25, NDE 41, NDE 44 and NDE 46. The resulting composite dispersion curves (phase velocity vs frequency and phase velocity vs wavelength) are shown in Figures 47 and 48.

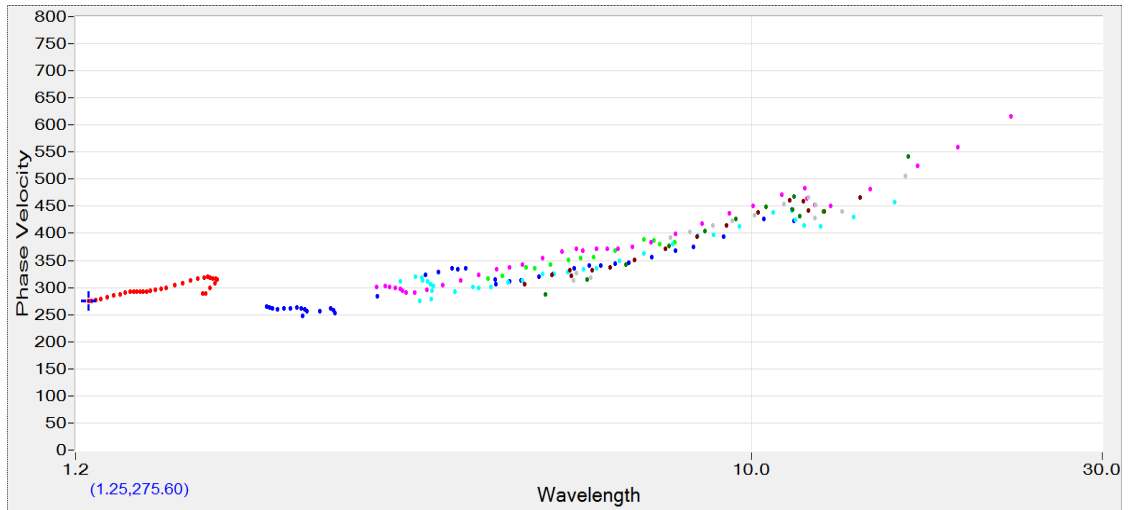


Figure 47. Composite dispersion curve (phase velocity vs wavelength) for the Middleton building site. Phase velocity is in m/s and wavelength is in m.

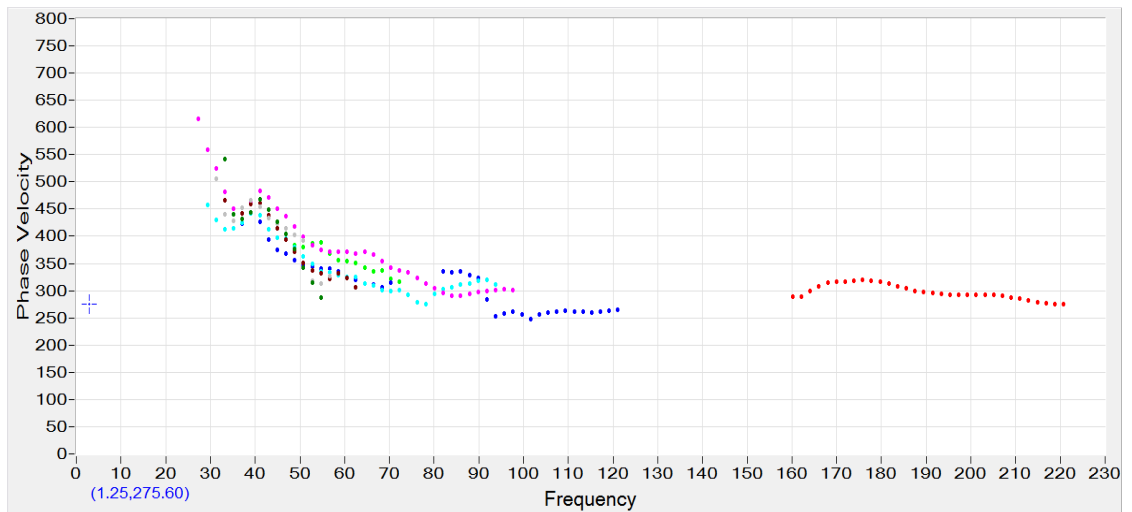


Figure 48. Composite dispersion curve (phase velocity vs frequency) for the Middleton building site. Phase velocity is in m/s and frequency is in Hz.

The representative dispersion curve was then used for the inversion. As can be seen in Figure 40, the maximum wavelength captured is about 18m and therefore the approximate maximum depth of investigation is 9 m (half the maximum wavelength). The other parameters of the soil profile were set to the same values as suggested in Section 3.3.2.3. The inversion was then conducted using the representative array

dispersion curve (solid blue circles shown in Figure 49) and the more accurate 3D analysis method.

The suggested soil profile was again adjusted following the previously described criteria. The match of the theoretical and representative dispersion curves and the final shear wave velocity estimated by the system for this site are shown in Figures 49 and 50.

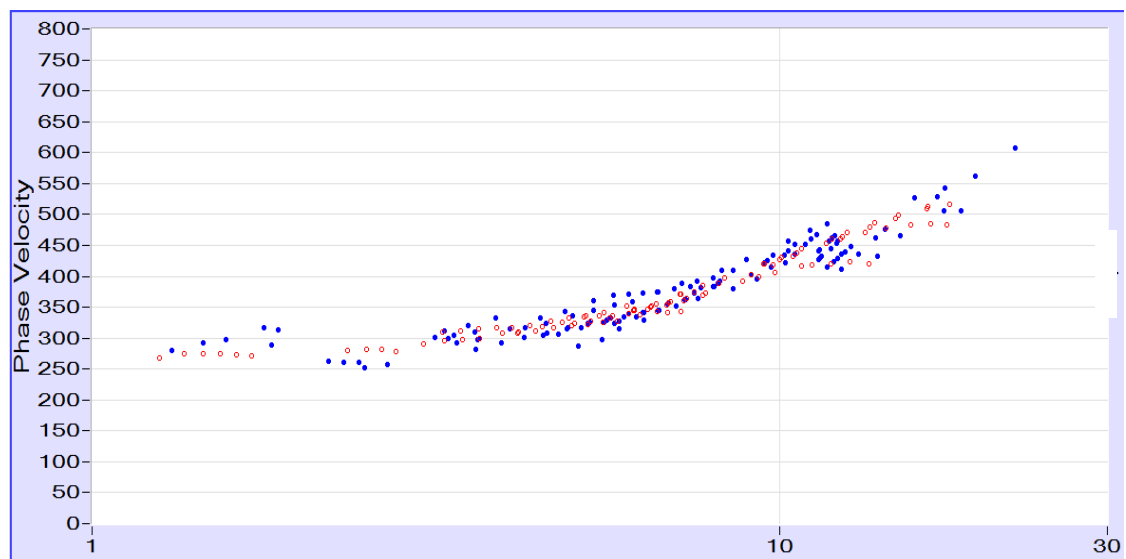


Figure 49. Representative (solid blue circles) and theoretical dispersion curve (empty red circles) for the Middleton Building site. Phase velocity is in m/s and wavelength is in m.

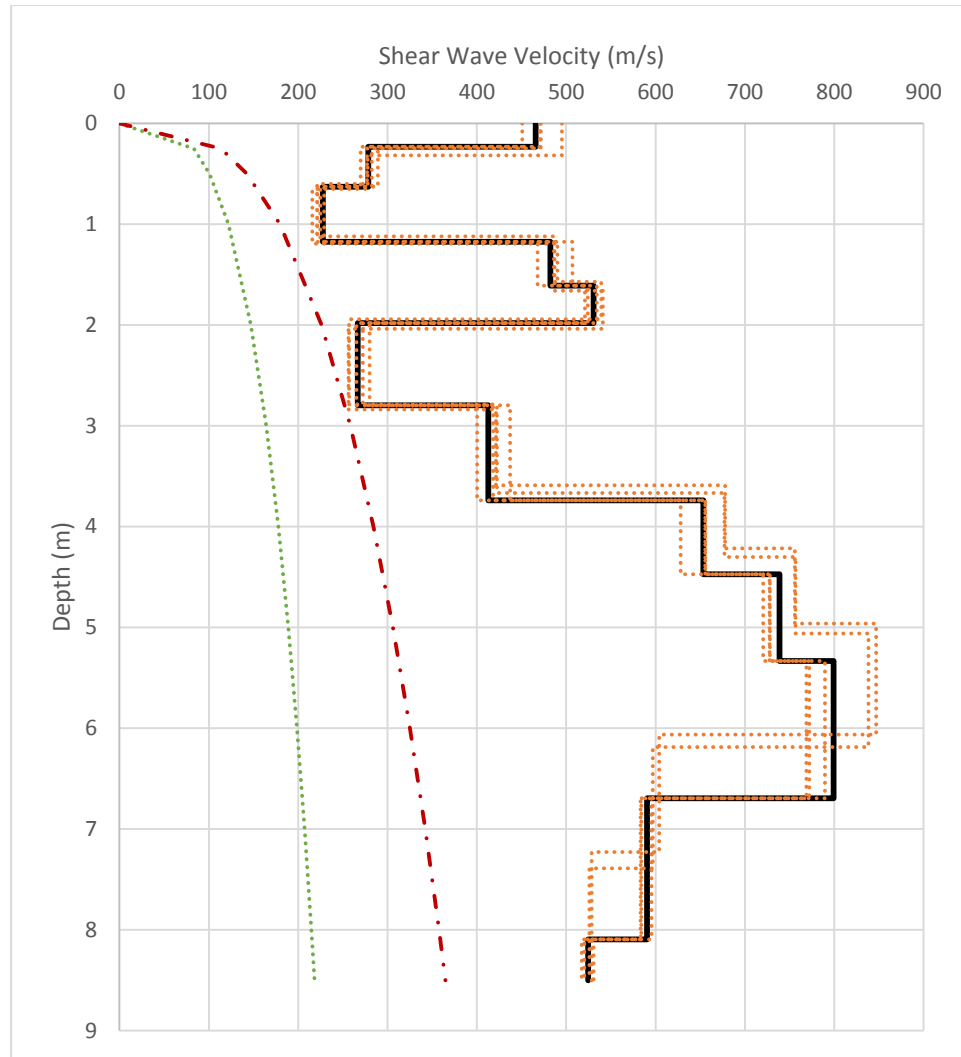


Figure 50. Estimated shear wave velocity profile for the Middleton Building site.

4.4 Quonochontaug Beach, Weekapaug, RI

Quonochontaug Beach's geological setting is outwash consisting of medium to coarse sand and gravel, as well as layers of fine sand, silt or clay as stated by a groundwater map from a geological survey which is attached in the Appendix. The SASW test was conducted on Quonochontaug Beach in Weekapaug, Rhode Island on October 3, 2015. The coordinates of the first Geophone are 41.332576° North and

71.725850° West and the location is shown on Figures 51 and 52. Only the 4.5 Hz geophones were used for this test.

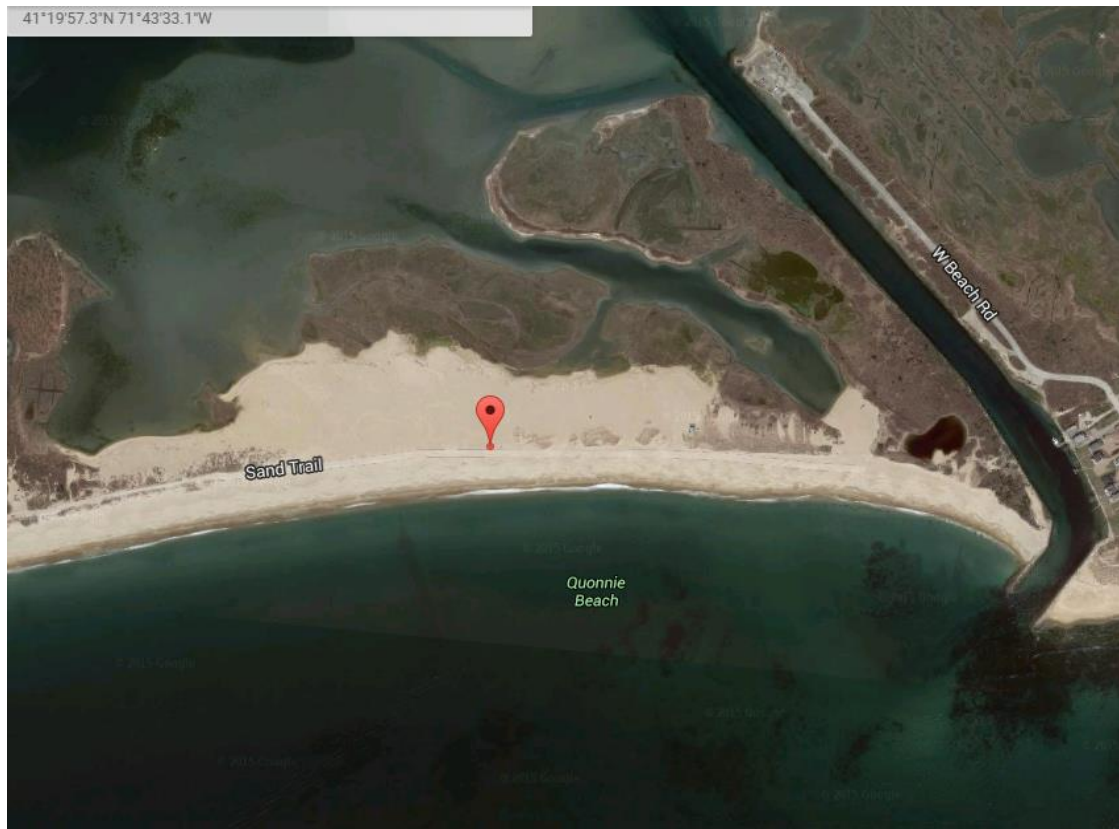


Figure 51. Location of SASW test at Quonochontaug Beach; the marker shows the location of the first geophone.

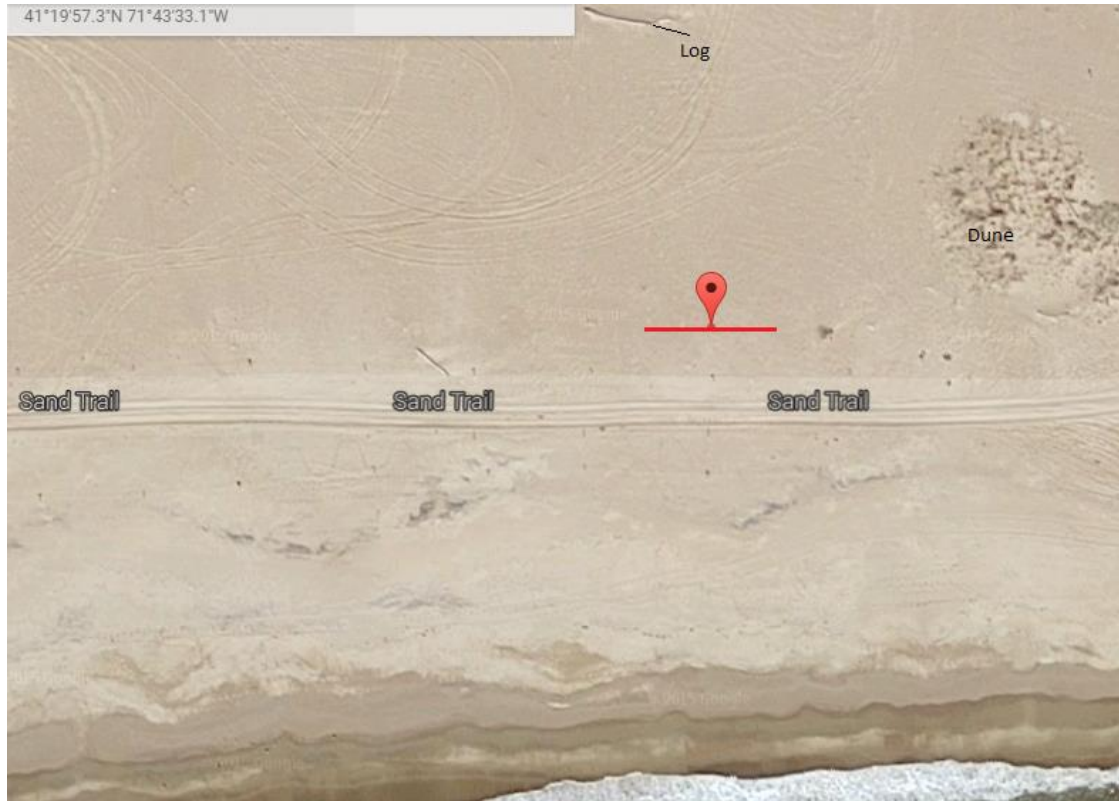


Figure 52. Location of test at Quonochontaug Beach with a spacing up to 6m between the geophones and the source.

The test was conducted parallel to the Sand Trail and Atlantic Ocean. The distance to the fence (steel line) was 10 m. The first geophone was kept in place for each spacing while both the source and the second geophone were moved. The test was conducted for spacings of 0.5 m, 1 m, 2 m, 3 m, 4 m, 5 m and 6 m. 6 Records were made for every test. Details of the test are summarized in Table 9; the time/pt was always set to 200 μ s.

Table 9. Summary of testing details for SASW test at Quonochontaug Beach.

Test #	Spacing (m)	Gain	Source	Plate type	NDE File	Disp. Curve
1	0.5	100	S	-	NDE 106	Yes
2	0.5	100	S	Rubber	NDE 107	Yes
3	0.5	100	S	Rubber + Steel	NDE 108	No
4	1	100	S	Rubber + Steel	NDE 109	Yes
5	1	100	B	Rubber + Steel	NDE 110	Yes
6	2	100	B	Rubber + Steel	NDE 111	Yes
7	3	100	B	Rubber + Steel	NDE 112	Yes
8	4	100	B	Rubber + Steel	NDE 113	Yes
9	4	1000	S	Rubber + Steel	NDE 114	Yes
10	5	1000	S	Rubber + Steel	NDE 115	No
11	5	100	B	Rubber + Steel	NDE 116	No
12	6	1000	S	Rubber + Steel	NDE 117	No
13	6	100	B	Rubber + Steel	NDE 118	No

Note: 1. S=Small Sledgehammer
2. B=Big Sledgehammer

4.4.1 Results for Quonochontaug Beach

Based on an evaluation of coherence in WinTFS, all the records were used for the further analysis in WinSASW. After masking the records within WinSASW, the following files were used to develop the composite experimental dispersion curve: NDE 106, NDE 107, NDE 109, NDE 110, NDE 111, NDE 112, NDE 113 and NDE 114. The resulting composite dispersion curves are shown in Figures 53 and 54.

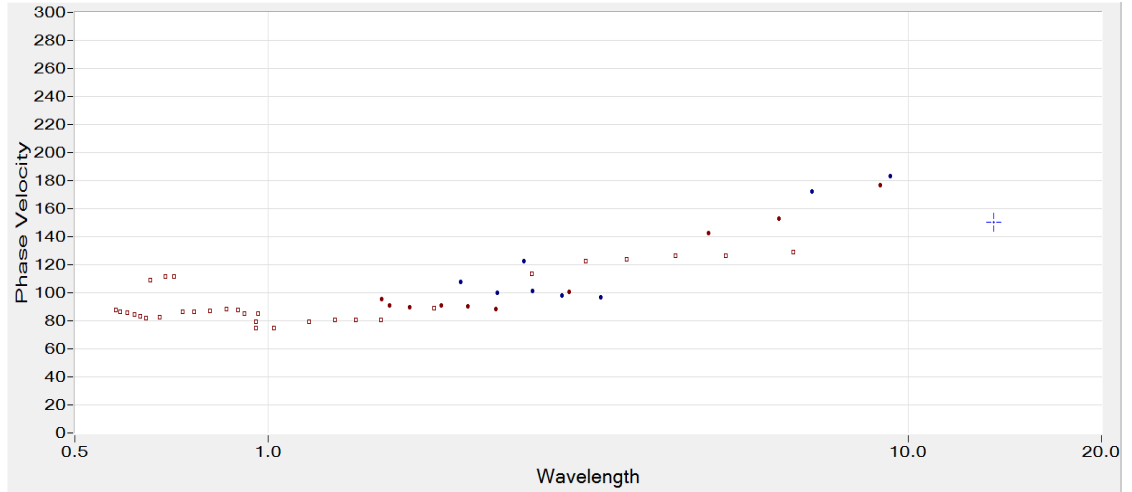


Figure 53. Composite dispersion curve (phase velocity vs wavelength) for the Quonochontaug Beach site. Phase velocity is in m/s and wavelength is in m.

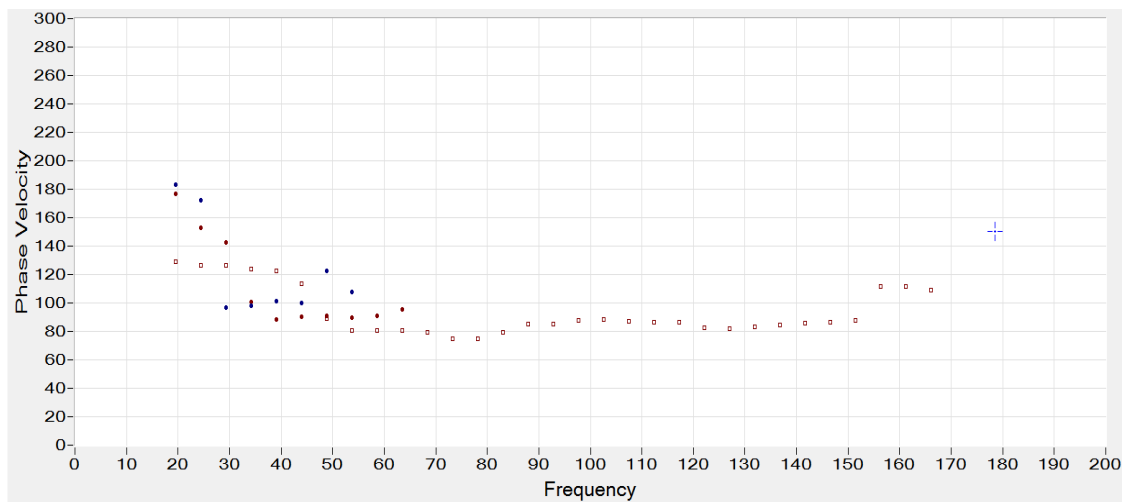


Figure 54. Composite dispersion curve (phase velocity vs frequency) for the Quonochontaug Beach site. Phase velocity is in m/s and frequency is in Hz.

The representative dispersion curve was then determined based on the composite dispersion curves. The maximum wavelength of the dispersion curve was about 9 m, and therefore the maximum reasonable depth for the inversion is approximately 4.5 m. The other parameters of the soil profile were again set to the

same values as suggested in section 3.3.2.3. The inversion was then conducted using the representative array dispersion curve and the more accurate 3D analysis method. The process was the same as described in the previous section.

The match of the theoretical and representative dispersion curves and the final shear wave velocity of the inversion for this site are shown in Figures 55 and 56.

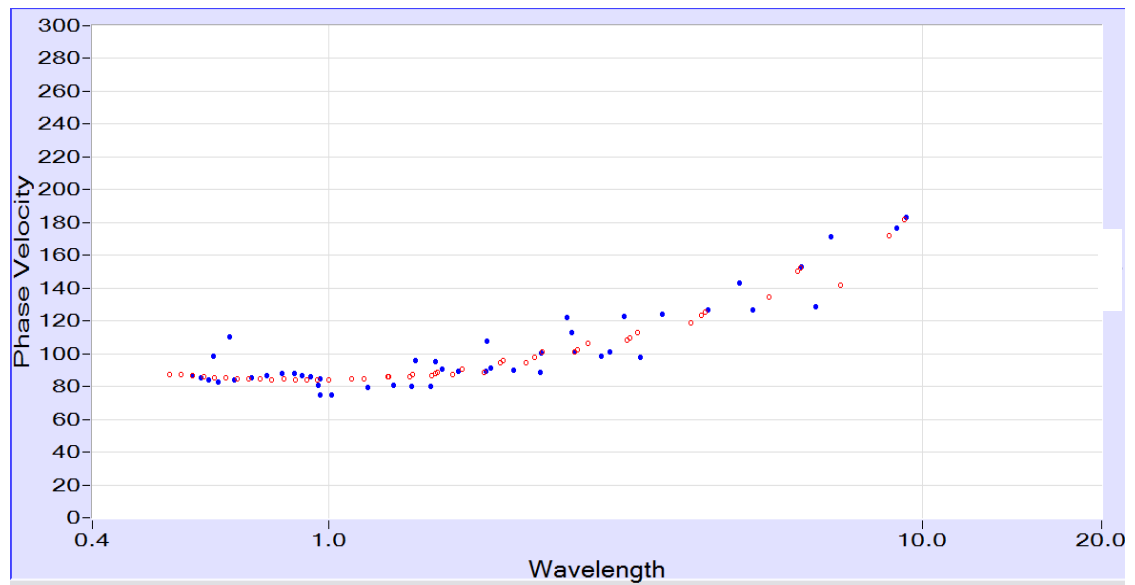


Figure 55. Representative (solid blue circles) and theoretical dispersion curve (empty red circles) for the Quonochontaug Beach site. Phase velocity is in m/s and wavelength is in m.

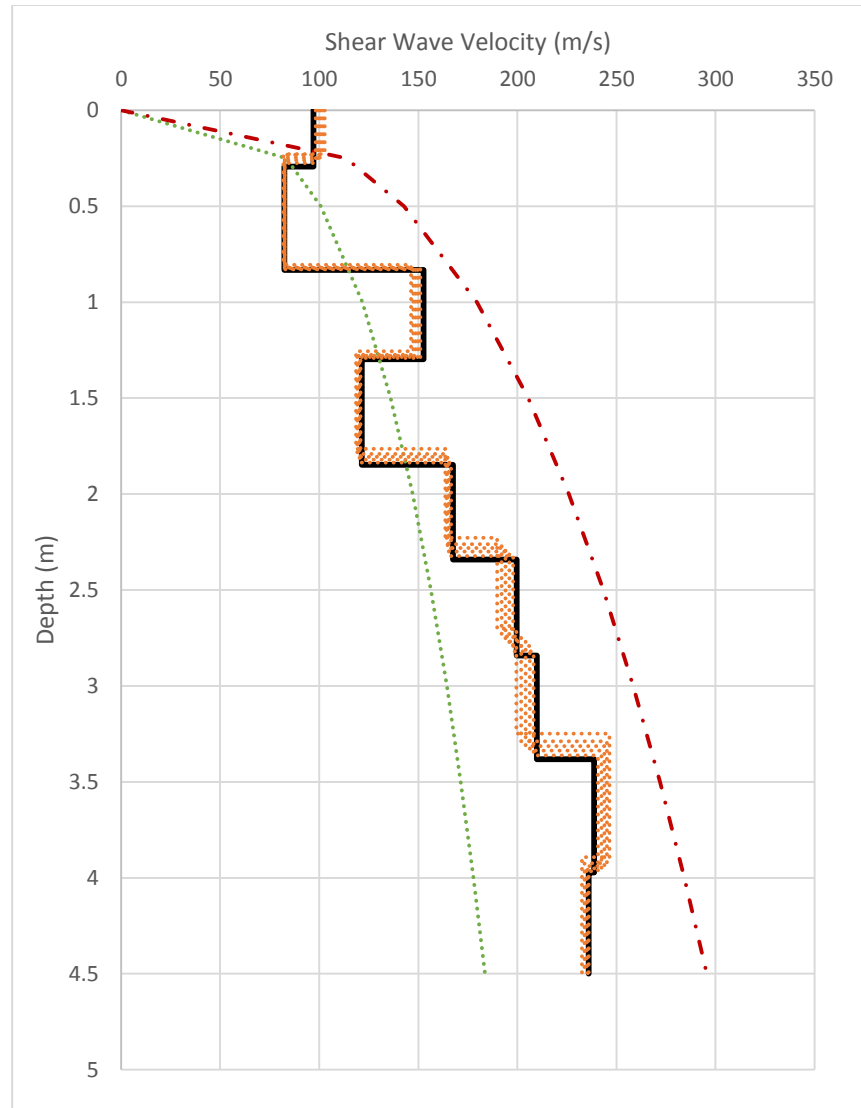


Figure 56. Estimated shear wave velocity profile for the Quonochontaug Beach site.

4.5 Misquamicut Beach, Westerly, RI

The second Test on a Beach was conducted on the Misquamicut Beach in Westerly, Rhode Island on October 3, 2015. The geologic setting consists of outwash with medium to coarse sands and gravel and fine sands, silts and clays. The beach was replenished in 2013 by the U.S. Army Corps of Engineers following significant erosion during Hurricane Sandy. The coordinates of the first Geophone are

41.322667° North and 71.805001° West and the location can be seen in Figures 57 and 58. For this test only the 4.5 Hz geophones were used.



Figure 57. Test Location on Misquamicut Beach with the marker on the first geophone.

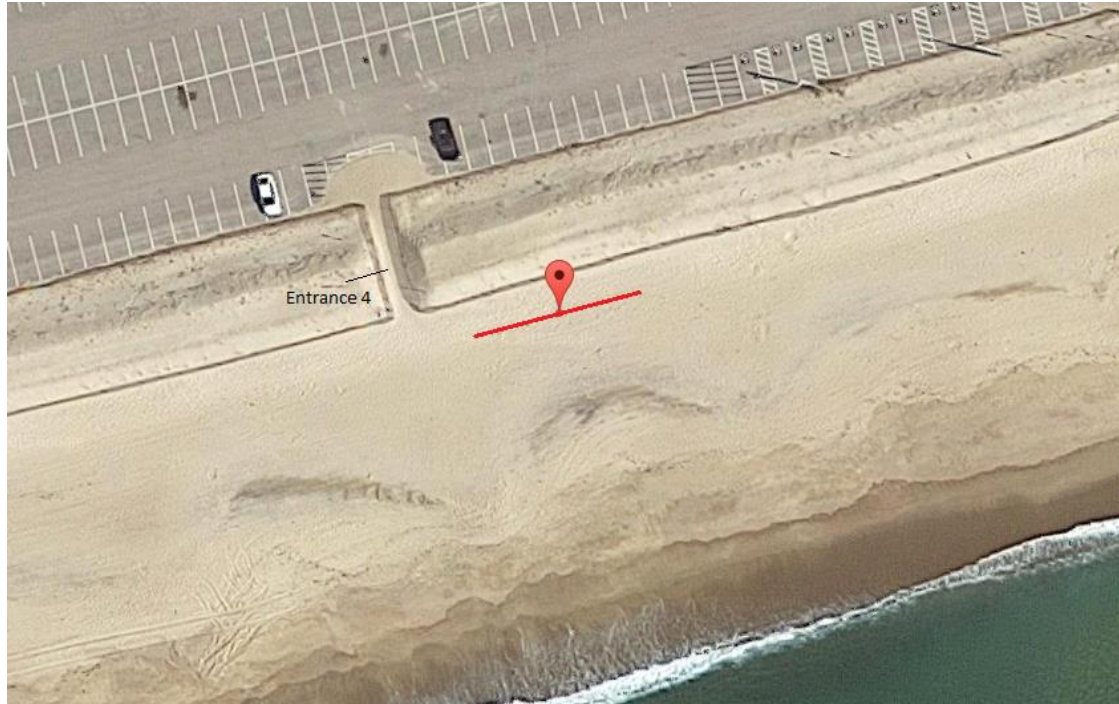


Figure 58. Location of the test (red line) with the marker on the first geophone.

The marker in Figures 57 and 58 is set at the point where the first Geophone was located. It was about 13.1m away from the beginning of Entrance 4. The linear array was set up parallel to the fence at a distance of 2.8m. The first Geophone was kept on the same spot during the tests for different spacings and the source and the second geophone were moved instead. The test was conducted for the spacings 0.5m, 1m, 2m, 3m, 4m, 5m, 6m and 7m. 6 Records were made for every test. In the following Table 10 an overview for the different spacings, parameters and names of the equivalent NDE data files is given. The time/pt was always set to 200 μ s.

Table 10. Summary of testing details for SASW test at Misquamicut Beach.

Test #	Spacing (m)	Gain	Source	Plate type	Scale	NDE File	Disp. Curve
1	0.5	100	S	Rubber + Steel	-	NDE 119	Yes
2	0.5	10	B	Rubber + Steel	-	NDE 120	No
3	1	100	S	Rubber + Steel	-	NDE 121	Yes
4	1	100	S	Rubber + Steel	~70%	NDE 122	Yes
5	2	100	B	Rubber + Steel	~70%	NDE 123	Yes
6	3	100	B	Rubber + Steel	~65%	NDE 124	No
7	4	100	B	Rubber + Steel	~50%	NDE 125	No
8	4	100	B	Rubber + Steel	~65%	NDE 126	No
9	5	100	B	Rubber + Steel	~45%	NDE 127	No
10	5	100	B	Rubber + Steel	~55%	NDE 128	No
11	6	100	B	Rubber + Steel	-	NDE 129	Yes
12	7	100	B	Rubber + Steel	-	NDE 130	No
13	7	100	B	Rubber + Steel	-	NDE 131	No
14	7	1000	S	Rubber + Steel	-	NDE 132	No

Note: 1. S=Small Sledgehammer
2. B=Big Sledgehammer

4.5.2 Results for Misquamicut Beach

As for the other beach site, no data were excluded during the processing in WinTFS due to a high coherence in the lower frequency region. Therefore all averaged records for each test were further used in WinSASW. Nevertheless, during the masking procedure certain data files that did not match the desired criteria were disregarded again. Hence only the files NDE 119, NDE 121, NDE 122, NDE 123 and NDE 129 were included for the estimation of the composite dispersion curves which are presented in Figures 59 and 60.

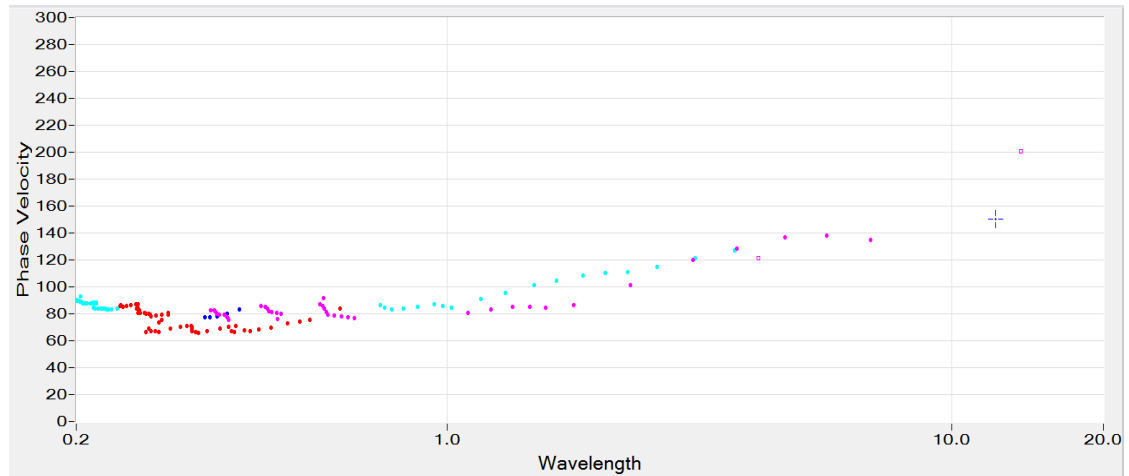


Figure 59. Composite dispersion curve (phase velocity vs wavelength) for the Misquamicut Beach site. Phase velocity is in m/s and wavelength is in m.

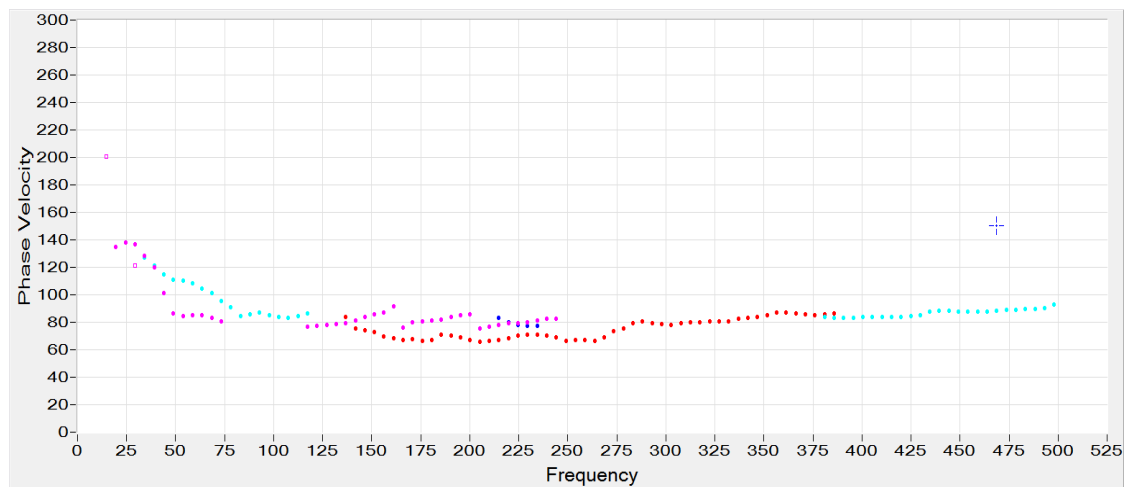


Figure 60. Composite dispersion curve (phase velocity vs frequency) for the Misquamicut Beach site. Phase velocity is in m/s and frequency is in Hz.

The maximum wavelength is again about 9 m (similar to Quonochontaug Beach) and therefore the setup of the layer thicknesses was chosen so that the total depth did not exceed 4.5 m. The other parameters of the soil profile were set to the normal starting values. The inversion was then conducted using the representative

array dispersion curve and the more accurate 3D analysis method. The following inversion process was the same as described in the previous sections.

The match of the theoretical and representative dispersion curves and the final estimated shear wave velocity of the inversion for this site are shown in the following two figures.

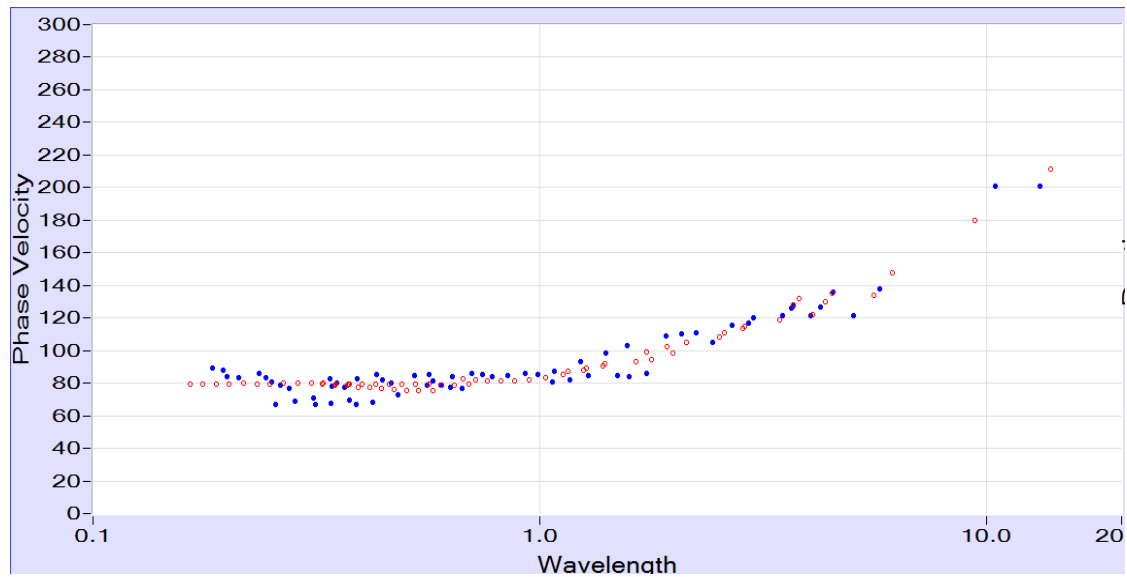


Figure 61. Representative (solid blue circles) and theoretical dispersion curve (red empty circles) for the Misquamicut Beach site. Phase velocity is in m/s and wavelength is in m.

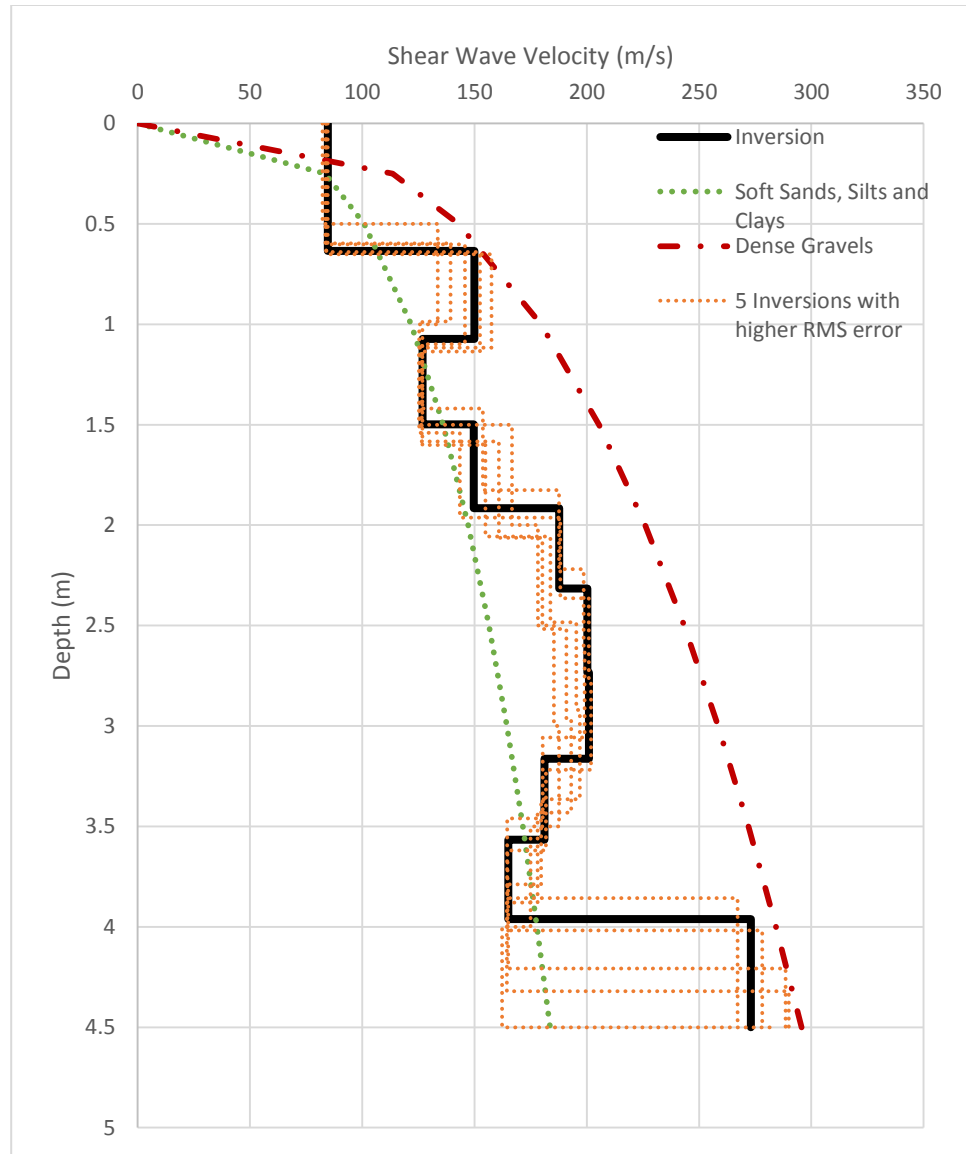


Figure 62. Estimated shear wave velocity profile for the Misquamicut Beach site.

In this chapter the testing procedures for all the tests conducted at different chosen geotechnical sites were presented. In the following chapter the results from these tests are analyzed, compared to previous tests and discussed.

5 Analysis and Discussion

This chapter presents a discussion of the dispersion curves and shear wave velocity profiles developed in the previous chapter. The results from the Gainer Dam, old Farmer's Market and the Middleton Building site are presented first. Dispersion curves had been developed at both of these sites by other researchers using a MASW system called the Amphibious Seismo-Acoustic Recording System (ASARS) designed and built by Drs. James Miller and Gopu Potty of URI's Ocean Engineering department. This is followed by a comparison of the results from the two beach sites. No other measurements have yet been performed at these sites.

5.1 Gainer Dam site

The dispersion curve with phase velocity vs frequency as well as the shear wave velocity profile that were developed in this study are compared to the results of a test that was conducted with the ASARS system (Reyes et al. 2016).

In Figure 63 the plot of the composite dispersion curve measured with the ASARS system is shown for a frequency range of 25 Hz to 60 Hz as well as the curve (representative) that was used for the further inversion. In the area of 40 to 60 Hz, the dispersion curve varies in a range of about 100 to 220 m/s before it increases strongly up to 30 Hz. Below 30 Hz, some data points follow this increasing trend whereas a second curve decreases.

In Figure 64 the composite dispersion curve acquired with the Olson Instruments system in this study is shown again. The curve covers a range of about 10 to 390 Hz. For the interval from 390 to about 120 Hz the dispersion curve ranges around 100 m/s for the shear speed before the scattering increases over a span of about

120 to 200 m/s down to 20 Hz. Below, some more scattered points are in the range of 220 to 280 m/s.

The two composite dispersion curves of the two different tests are slightly different. Whereas the ASARS curve shows a strong increase in phase velocity below 40 Hz above 500 m/s, the curve of this study only slightly increases and stays under 300m/s. A similarity can be seen in the area of 40 to 60 Hz, as both systems measured more scattered data points ranging from about 100 to 200 m/s.

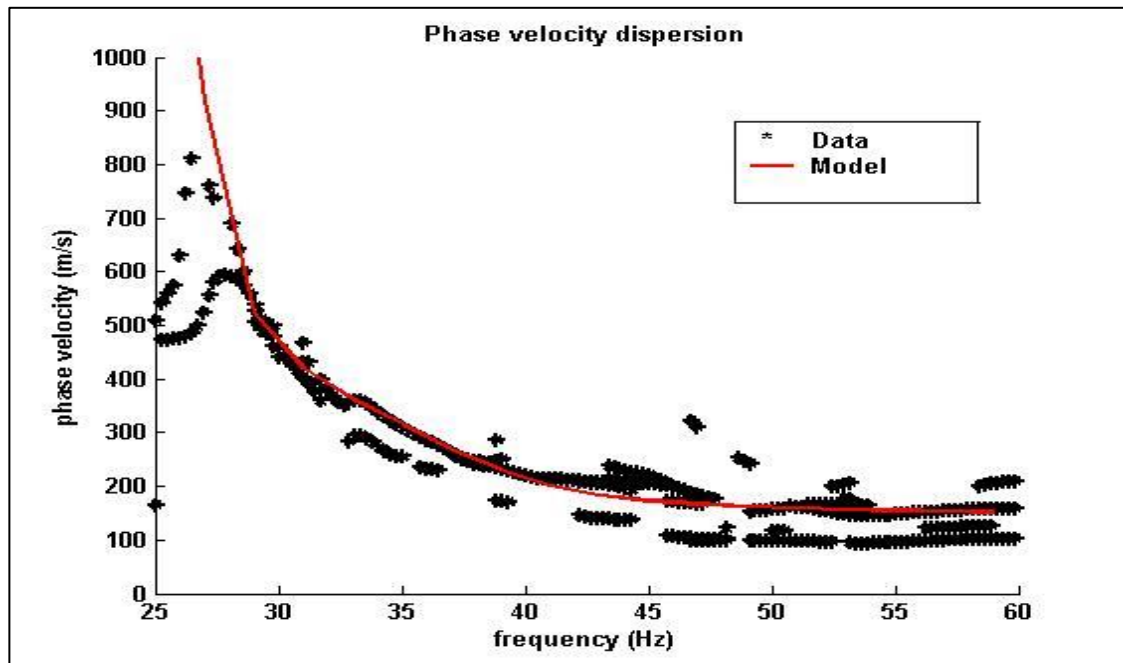


Figure 63. Composite dispersion curve for the Gainer Dam site from the ASARS system (Reyes et al. 2016).

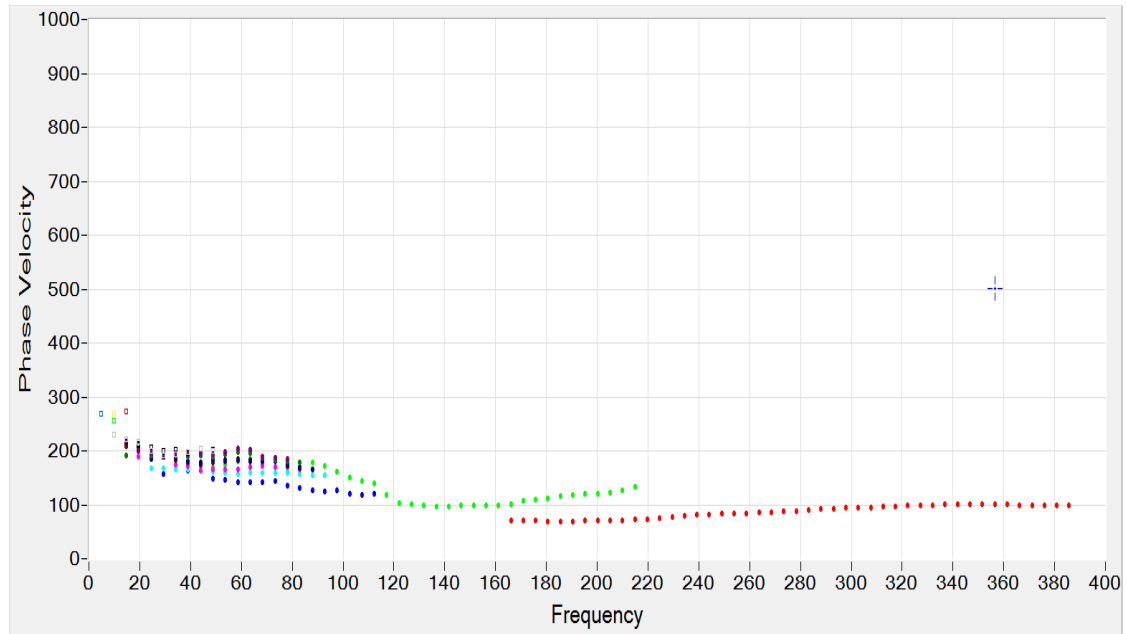


Figure 64. Composite dispersion curve of this study measured with the Olson Instruments system. Phase velocity is in m/s and frequency is in Hz.

On the basis of these dispersion curves, the corresponding shear wave velocity profiles were determined as shown in Figure 65. The inversion process for the profile from the ASARS test was based on the dynamic stiffness matrix approach and a generic algorithm from Potty et al. (2012) to iteratively find the best match to the experimental dispersion curve with a resulting shear wave velocity profile shown in Figure 65a. As can be seen, the shear wave velocity is about 400 to 500 m/s for the top 21 m over a softer layer with about 300 m/s for the next 9 m. At depths greater than 30 m, a strong increase of shear wave velocity was detected which was assumed to be bedrock at this depth (Reyes et al. 2016).

The investigation depth of the test for this study did not exceed a depth of 25 m. In comparison to the ASARS system, the shear wave velocity in these top 25 m is lower with speeds of about 100 m/s at the top, increasing with some outliers until a

depth of 11 m to about 400 m/s. Below, the shear wave velocity drops into the area of soft sand, silt and clay with values of 250 to 310 m/s down to the maximum investigation depth of 25 m.

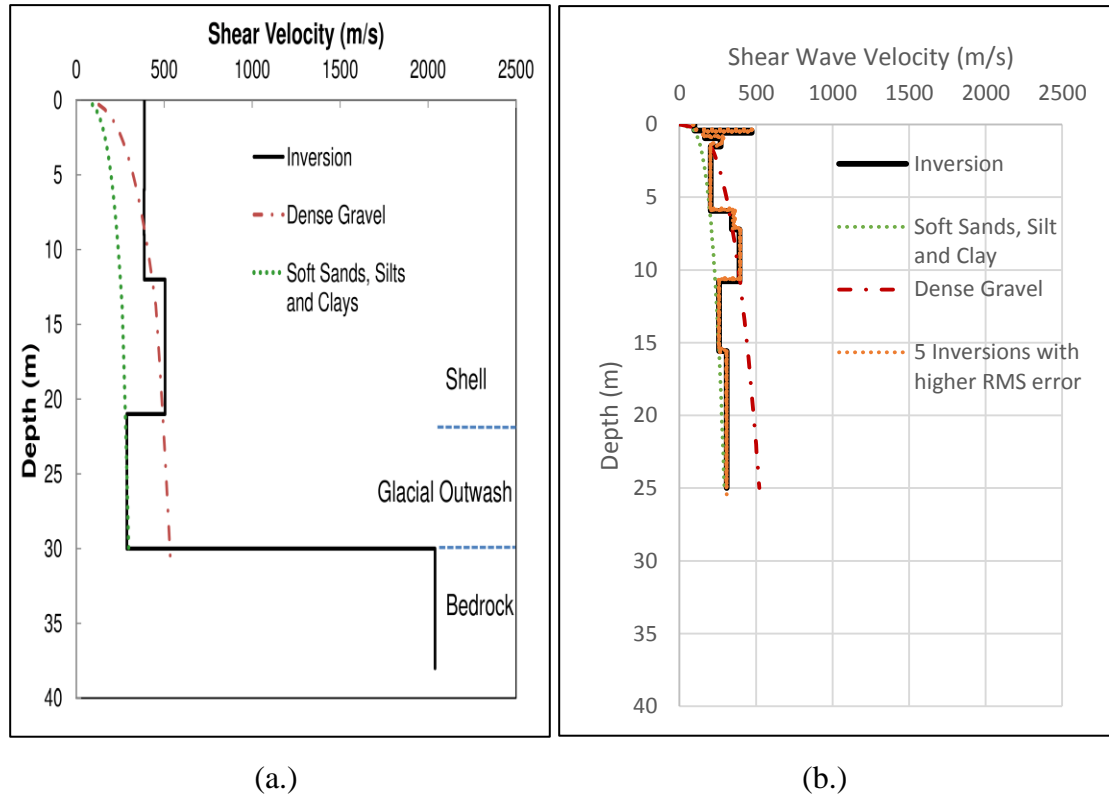


Figure 65. Shear wave velocity profiles for the Gainer Dam site developed from test with (a) ASARS system (Reyes et al. 2016) and (b) the Olson Instrument system in this study.

The shear wave velocity profiles as well as the dispersion curves are different for the two systems, although the basic trend is the same, without taking the depths into consideration. The reason might be the different measurements for the frequency range below 40 Hz which is related to the measurements of larger spacings. Nevertheless, the lower shear wave velocity for the uppermost layers of the profile developed with the Olson Instruments system seems more reasonable, whereas below

5 m, the ASARS profile more reasonably matches the layers of the geologic setting from the Gainer Dam (Figure 28). The ASARS inversion does not provide enough resolution down to 5 m to estimate the thin layers near the top.

5.2 Old Farmer's Market Site

The dispersion curve and shear wave velocity profile developed in section 4.2 were compared to a dispersion curve and a shear wave velocity profile developed using the ASARS system (Potty, personal communication).

The dispersion curve developed with the ASARS system in Figure 66 shows three different curves. One curve increases strongly to a phase velocity of about 900 m/s at a frequency of about 32 Hz. Another curve only varies around phase velocities of about 50 to 150 m/s over the whole frequency range. The third curve lies between the two other described curves, with its highest phase velocity of 400 m/s at a frequency of about 20 Hz.

The dispersion curve developed in this study was shown in Figure 42 and is repeated in Figure 67. For the frequency band from 125 to 80 Hz, the phase velocity is about 100 m/s. In the range of 80 to 40 Hz the composite curve slightly increases and varies around 120 to 200 m/s. For the lower frequency area, the trend of the curve increases up to a phase velocity of about 400 m/s for a frequency of about 20 Hz.

Comparing the two dispersion curves from the different tests, there is a reasonable match between the middle curve of the ASARS test and the dispersion curve of the test for this study. The other two curves are probably different modes that were measured by the ASARS system but not by the Olson Instruments system.

Alternatively, these modes could have been masked out during the process in WinSASW, as they belonged to parts in the frequency response phase that were not considered reasonable.

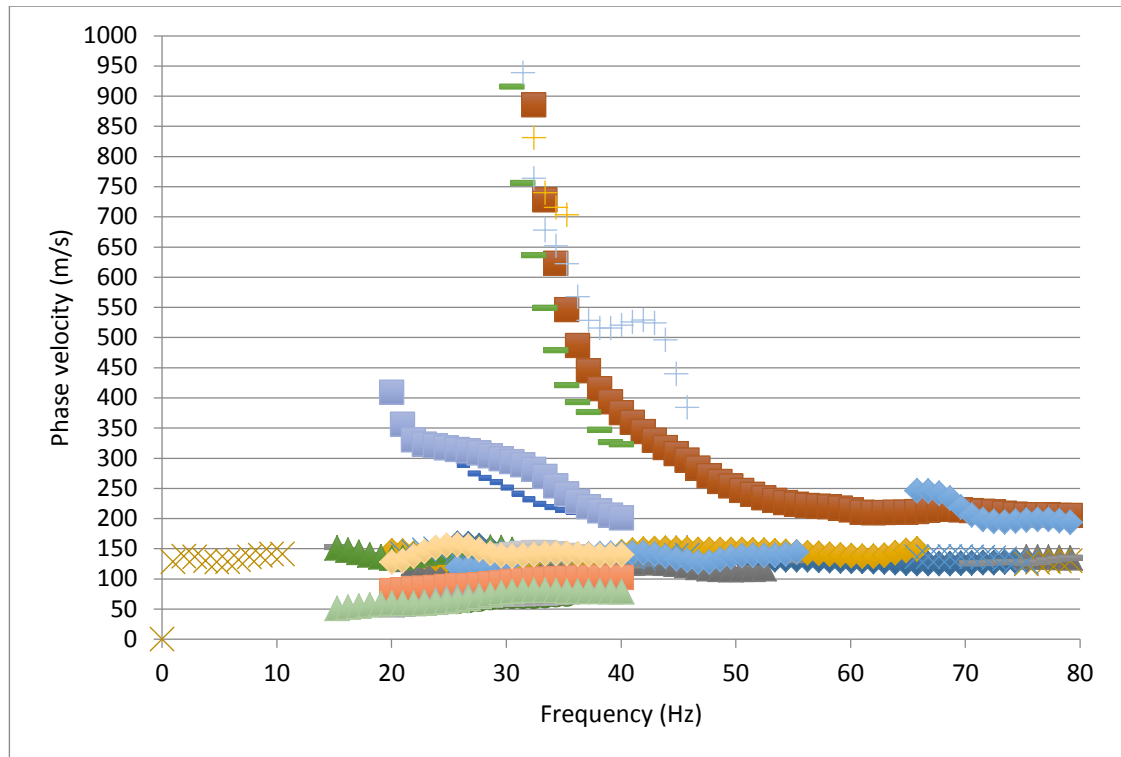


Figure 66. Dispersion curve obtained from the Old Farmer's Market site in Providence, RI using the URI ASARS system (Potty, personal communication).

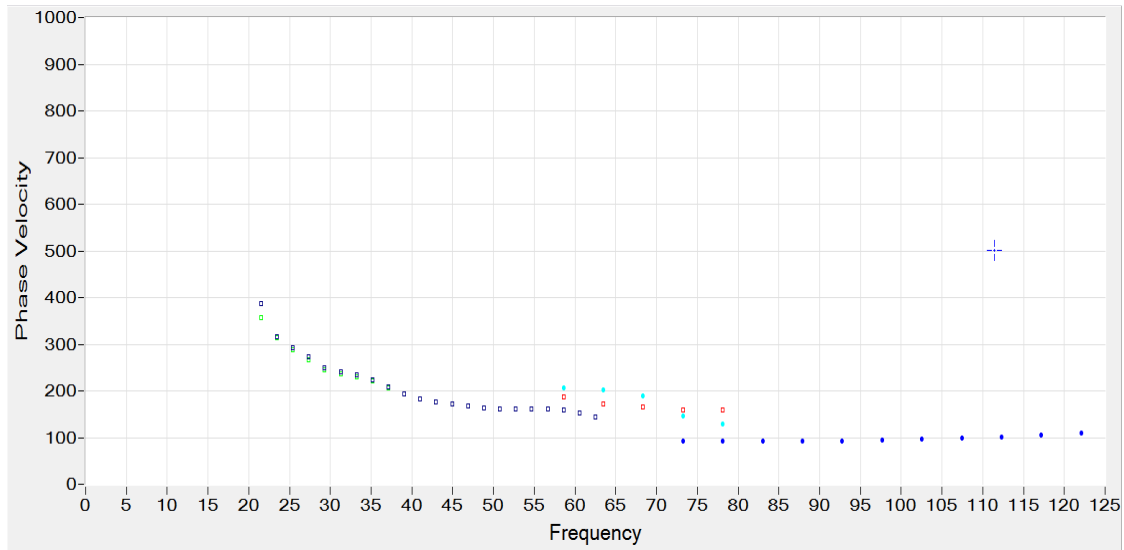


Figure 67. Dispersion Curve obtained from the Old Farmer's Market site in Providence, RI using the Olson Instruments system. Phase velocity is in m/s and frequency is in Hz.

In Figure 68a, the shear wave velocity profile developed with the ASARS system is shown. It can be seen that the shear wave velocity starts at 70 m/s at the top layer and increases to about 200 m/s at a depth of 2 m. Below the upper 2 m, it varies in a range of 150 m/s to 200 m/s to a depth of 8 m where a jump to 250 m/s was determined.

The shear wave velocity profile of the Old Farmer's Market site that was developed in this study was shown in Figure 4 and is repeated in Figure 68b. The top layer has a shear wave velocity of about 93 m/s and increases to 220 m/s at 0.5 m. Below, to a depth of 3.5 m, this value of shear speed does not change with an underlain sharp increase to 580 m/s at about 4 m depth. Below about 5.5 m the profile shows a softer layer of about 500 m/s until the maximum investigation depth of 7 m is reached.

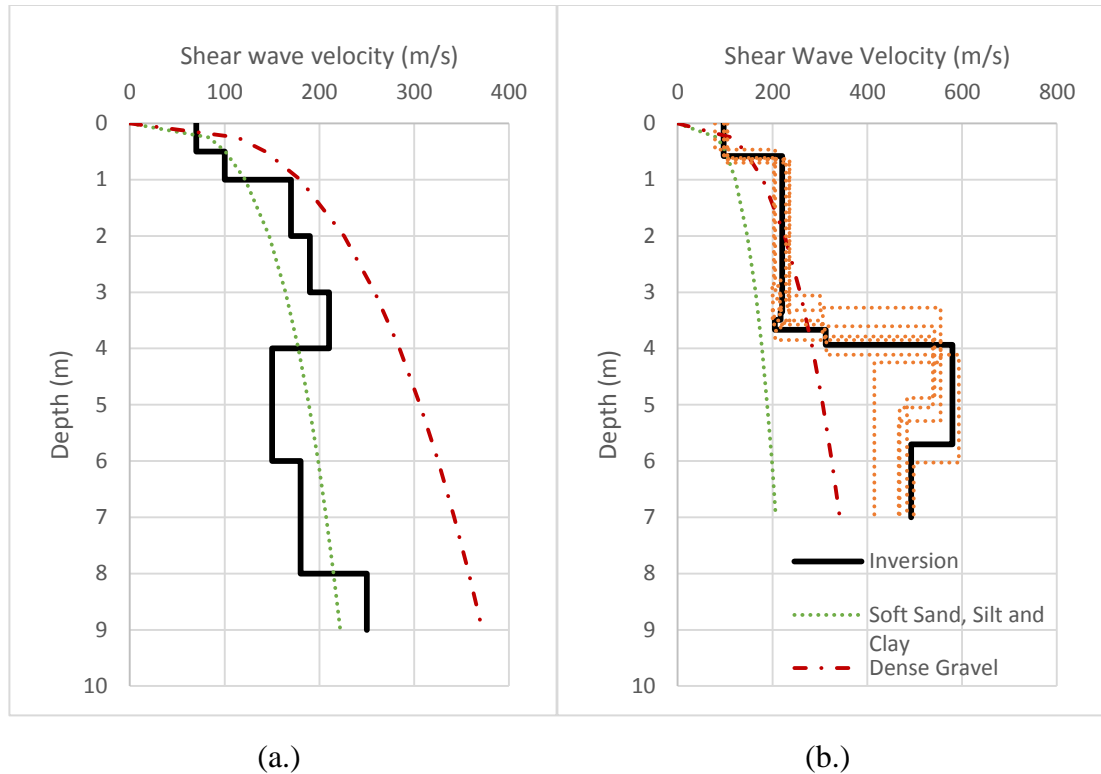


Figure 68. Shear wave velocity profile for the old Farmer's Market site developed with a) ASARS system (Potty, personal communication) and b) Olson Instruments system in this study.

In comparison both profiles show a soft layer at the top and an increase to about 200 m/s up to a depth of 4 m. Below this depth, the profiles are different as the ASARS one slightly decreases in stiffness whereas the profile obtained with the Olson Instruments system has a sharp increase in stiffness. This jump is not reasonable as in these depths fill and silt is expected (Bradshaw et al. 2007) which makes the profile developed with the ASARS system more accurate.

5.3 Middleton Building Site

The dispersion curve developed for the Middleton building site (see section 4.3.1) was compared to a dispersion curve presented by Greene (2011) that was developed using ASARS. No shear wave velocity profiles were presented by Greene (2011).

The dispersion curve developed by Greene (2011) is shown as plots of phase velocity vs. wavelength and phase velocity vs. frequency in Figure 69. There is a clear trend of increasing phase velocity values for higher wavelengths while the variability of the data points is reasonably low. On the other hand, Figure 69b shows large amounts of scatter in the data when plotted as phase velocity vs. frequency.

Figure 70 shows the dispersion curves from this study. A comparison of the plot of phase velocity vs. wavelength with Figure 69a clearly shows that the trend of both curves is the same, although the numerical values are slightly different. For Greene's dispersion curve, the values for a wavelength of 10 m are about 500 to 550 m/s whereas the curve of the test performed for this thesis is lower with values of about 400 to 450 m/s. There is no clear agreement between the plots of the phase velocity vs. frequency.

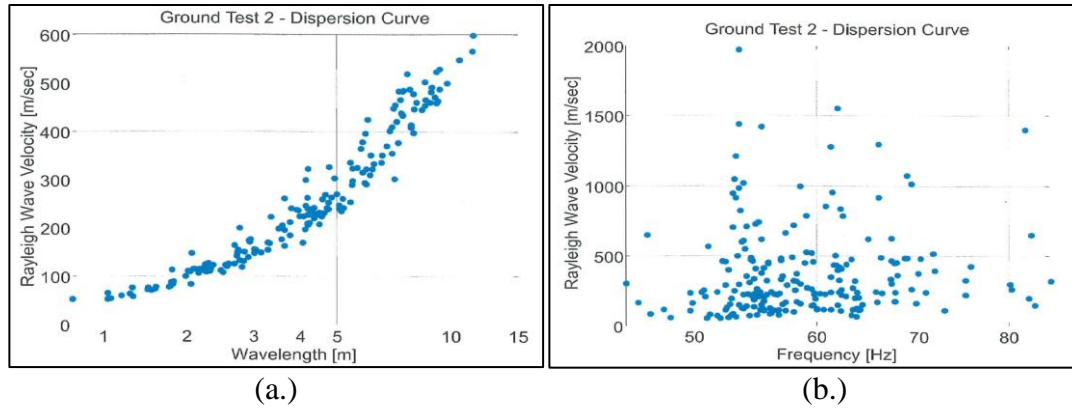


Figure 69. Dispersion curves for the Middleton building site from Greene (2011): a.) phase velocity vs. wavelength; and b.) phase velocity vs. frequency.

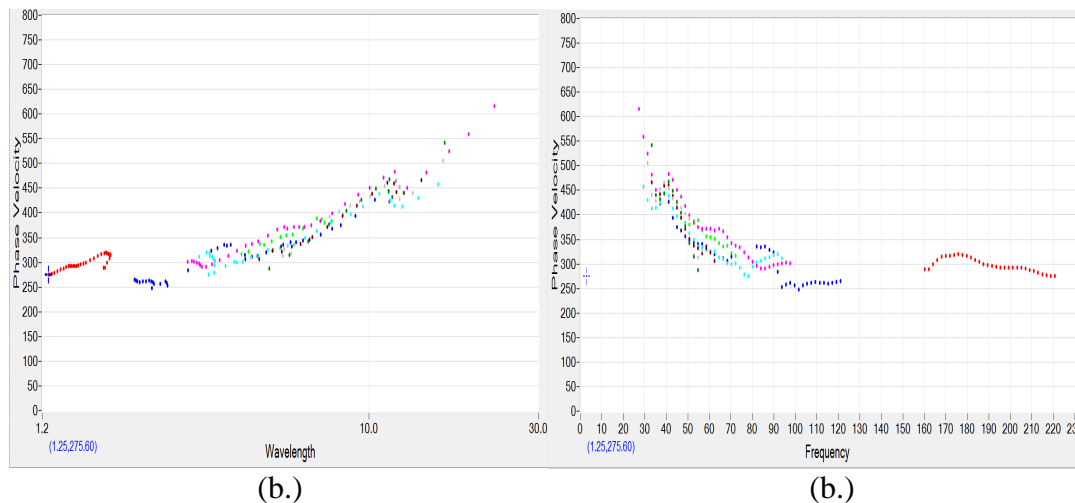


Figure 70. Dispersion curves for the Middleton building site generated from this study: a.) phase velocity vs. wavelength; and b.) phase velocity vs. frequency. Phase velocity is in m/s, wavelength is in m and frequency is in Hz.

The estimated shear wave velocity for this site was shown in Figure 50 and is repeated in Figure 71. The velocities in the upper layer seem not reasonable as they might be only slightly higher than the underlain layer due to grass or a typical consolidation of the most upper layer by human traffic. From about 1 to 2 m, a stiffer layer was detected that is enhanced by two softer layers. From 4 to 7 m, the shear wave velocity highly increases up to 800 m/s which might be due to the presence of

bedrock (shear wave velocity of top 30 m of subsurface profile (V_{s30}) for rock is about 760 m/s to 1500 m/s; Wair et al. 2012) at these depths. However, the decrease at a depth higher than 7 m should be viewed critically as the trend of the stiffness normally increases and bedrock is assumed also in the deeper layers.

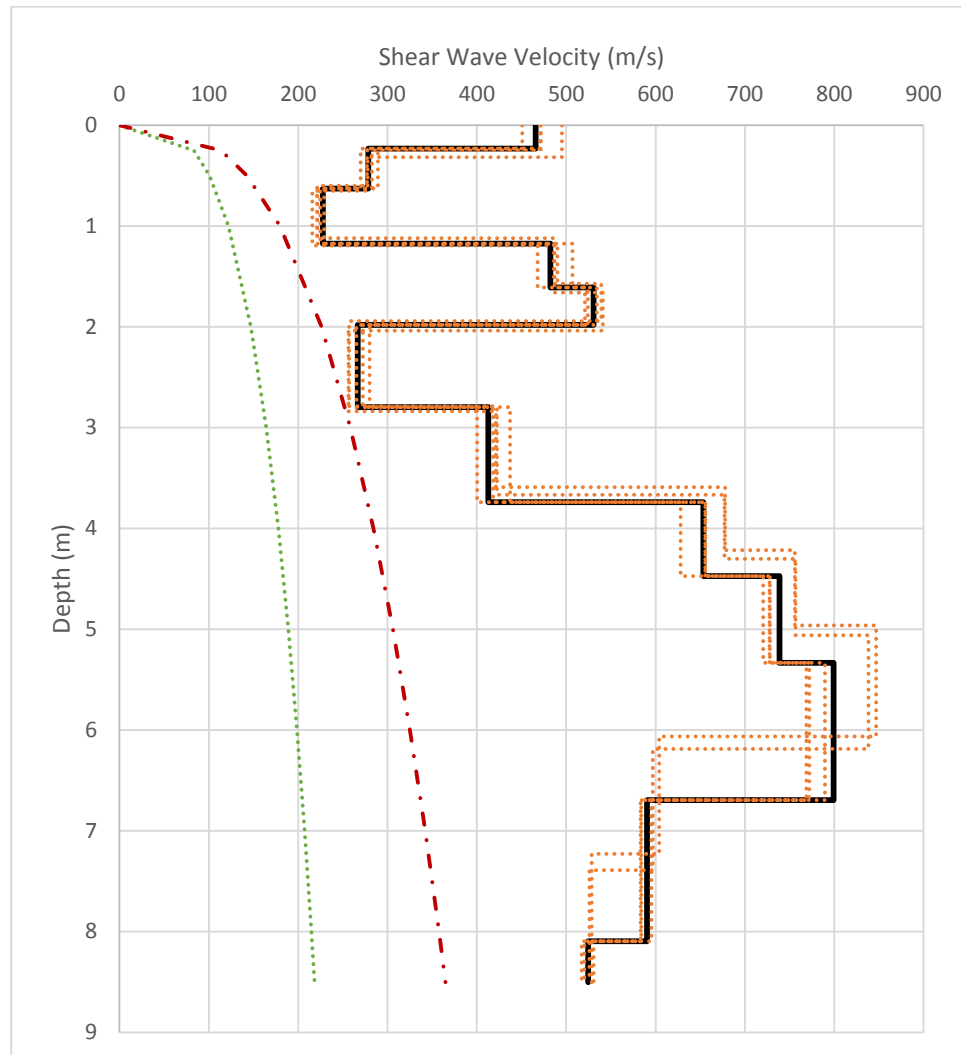


Figure 71. Shear wave velocity profile of the Middleton Building site acquired with the Olson Instruments System.

5.4 Comparison of Beach Sites

For the beach sites, no other shear wave velocity data have been collected; therefore, these two sites are only compared with each other. Figure 72 shows both shear wave velocity profiles.

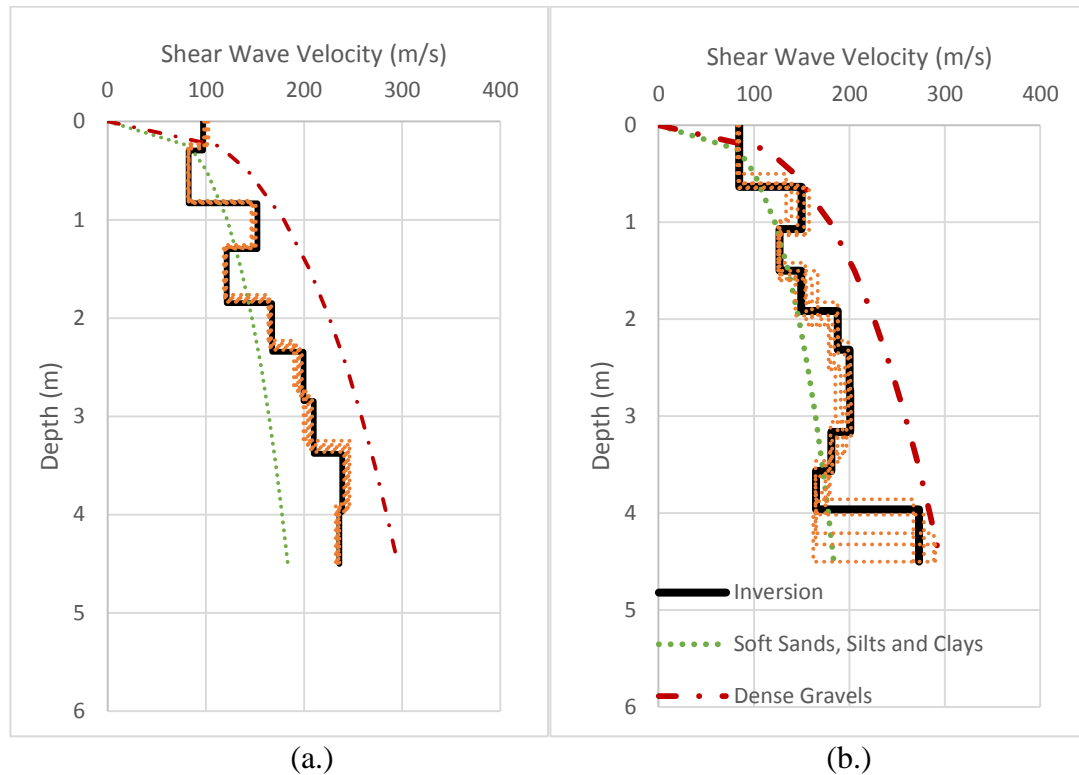


Figure 72. Shear wave velocity profiles from: a.) Quonochontaug Beach; and b.) Misquamicut Beach.

The profile for Quonochontaug Beach shows a loose surficial layer of with shear wave velocity of about 100 m/s for the upper 90 cm and then an increase to about 170 m/s up to a depth of 2.2m. Below this depth, the velocity varies only slightly at around 220 m/s up to the final investigation depth of 5m.

The profile for Misquamicut Beach shows a similar shear wave velocity profile with depth, with a slightly lower velocity in the uppermost layers. The shear wave

velocity at Misquamicut Beach does increase significantly at a depth of 4 m to about 270 m/s. This increase is interesting, but must be viewed critically as it is based on only two data points of the dispersion curve that are at higher wavelengths for this site (Figure 61). However, these two points follow the general trend of the dispersion curve.

Quonochontaug Beach is a natural sand beach whereas the sand on Misquamicut Beach was replenished in 2013 by the U.S. Army Corps of Engineers following significant erosion during Hurricane Sandy. It is hypothesized that the increase in velocity at a depth of 4 m is the erosional boundary between newly placed sand and the existing beach. Clearly more work is needed to be performed at these sites to evaluate this hypothesis.

6. Conclusion

The primary objective of this thesis was to learn how to perform SASW testing with a commercial system and to compare the resulting dispersion curves and shear wave velocity profile to those obtained using the ASARS system developed at URI at several sites. The data from the ASARS system was collected previous to this study (Greene 2011; Reyes 2016) and was analyzed by Dr. Gopu Potty of URI. The SASW system used was manufactured by Olson Instruments, Inc., and consisted of two pairs of geophones (2Hz and 4.5Hz), a data acquisition system (NDE 360 platform), and software for filtering and masking the data and developing the dispersion curves (WinTFS) and performing the inversions (WinSASW). The sites tested for this part of the study included the Gainer Dam in Scituate, RI, the old Farmer's Market in Providence, RI; and adjacent to the Middleton Laboratory building on URI's Narragansett Bay Campus. At each site, different source-to-geophone differences were tested ranging from 0.5 to 40 m. The 4.5 Hz were used for the smaller spacings and the 2 Hz geophones were used primarily for the larger spacings. Three sources were used depending on the receiver spacing: a 1kg and a 4 kg sledge hammer and a 50 kg weight dropped from a height of up to 1.5 m used a tripod/pulley system.

There was not good agreement between the shear wave velocity profiles using the SASW system and the ASARS system at the Gainer Dam site. Specifically, the velocities obtained by the SASW system ranged from 100 to 300 m/s in the upper 20m, which were approximately 200 m/s lower than the velocities at comparable depths obtained with the ASARS system. The values from the ASARS system appear to be high when compared with published relationships for dense sands and gravels. In

addition, the depth of predicted shear wave velocities was only 20 m, while shear wave velocities were estimated to a depth of almost 40 m with the ASARS system.

The Old Farmer's Market site consisted of approximately 5 m of urban fill overlying saturated inorganic silt. The dispersion curve obtained with the ASARS systems suggested several modes, whereas the dispersion curve from the SASW system showed only one mode. The velocities for the SASW system were higher than those from the ASARS system and exhibited a sharp increase in velocity below 4 m. It is not clear if the data obtained with the SASW system at this site is reasonable, and there may have been issues during data collection (e.g. poor coupling between the ground and the geophones) that affected the results. There are published shear wave velocities for the silts at this site that were obtained using a seismic CPT (Bradshaw et al. 2012), however the SASW system did not produce usable results at these depths.

For the Middleton Building site, only the dispersion curves were compared between the SASW and ASARS systems (Greene 2011). There was reasonable agreement between the dispersion curves in terms of wavelength vs. phase velocity, however there was significant scatter in the frequency-phase velocity relationship obtained with the ASARS system; the cause of this scatter is unclear. The dispersion curve obtained from the SASW system was used to estimate the shear wave velocity profile, and the results suggest that a high velocity layer (possibly bedrock) may be present at a depth of 5 m. This could be verified by performing geotechnical borings at the site.

From a comparison of all the results at the Gainer Dam, Old Farmer's Market, and Middleton Building sites, it appears that the Olson Instruments, Inc. SASW

system was better able to estimate the shear wave velocity at depths less than 6 m than at deeper depths. There are two possibilities that might have influenced the results for deeper soil investigations in a negative manner. The first possibility is the use of different geophones for spacings larger than 6 m. The 2 Hz geophones, unlike the 4.5 Hz geophones, did not have spikes attached for better coupling with the ground. This may have affected the accurate measurement of surface waves, particularly for the Old Farmer's Market site that was covered with gravel and brush. The second possibility relates to the NDE 360 platform. The highest sampling rate that could be chosen was 500 μ s, which determines that the frequency span that is recorded is about 1 kHz. For larger geophone spacings, the frequency band of interest is significantly lower (for example up to 62.5 Hz for a spacing of 8 m). The data points that are saved per record are limited. If a frequency spectrum of 1 kHz is recorded for a large spacing, most of the acquired data points do not contain usable information and are masked out so that in total less data points can be utilized for the calculation of the individual dispersion curve for these spacings.

The second objective of this study was to collect shear wave velocity data at two different beach sites. This was done to begin collecting data at coastal sites in Rhode Island where erosion is significant and also at locations where there is a history of beach replenishment. Quonochontaug Beach was chosen as a natural site and SASW results were compared to those collected from Misquamicut Beach, which was replenished following Superstorm Sandy in 2013. The estimated shear wave velocity profiles for these sites showed only slight differences. At Misquamicut Beach, there

was a sharp increase at a depth of about 4 m, and it is possible that this could be the depth where the natural layers of soil at this certain site are located.

6.1 Recommendations for Future Research

There were clearly many challenges in obtaining reasonable data in this study using the Olson Instruments, Inc. SASW system. Future improvements should include better coupling of the 2 Hz geophones with the ground, and encouraging Olson Instruments, Inc. to remove the limitations on the sampling rate. If it is not possible to acquire more reliable data with the current SASW system, future tests should be performed with a MASW system. A MASW system potentially has several advantages because the setup does not need to be changed and more measurements for different spacings are obtained for the same impact, as more receivers are available.

The testing for the different beach sites has shown conspicuities in the shear wave velocity profiles that should be confirmed by other tests and if applicable investigated further to estimate if a relation between stiffness properties and erosion exists at susceptible sites.

100 WATER STREET EAST PROVIDENCE, R. I.
 et & Maloney Providence, R.I.

SHEET _____ OF _____
DATE _____
HOLE NO. 1 B-4
LINE & STA. _____
OFFSET _____
SURF. ELEV. 72.1'

GROUND WATER OBSERVATIONS				Rods-AW		CASING	SAMPLER	CORE BAR.	Date	Time	FORM NO.
At	10'4"	after 1/4	Hours	Type	NW	S/S	NXD3	START	11/25/75		
	20' of casing			Size I. D.	3"	1-3/8"		COMPLETE	11/26/75		
At	7'-5"	after 1/4	Hours	Hammer Wt.	300#	140#		TOTAL HRS.			FORM NO.
	no casing			Hammer Fall	24"	30"		BORING FOREMAN	T. Canning		
							BIT	INSPECTOR			FORM NO.
							Diamond	SOILS ENGR.			

[illegible]

GROUND SURFACE TO		20'		USED NW		"CASING: THEN		C TO 30'	
Sample Type		Proportions Used		140lb Wt x 30" fall on 2" O.D. Sampler		Cohesiveness		Density	
D=Dry	C=Cored	W=Washed	Trace	0 to 10%	0-10	Loose	0-4	Soft	30 + Hard
UP=Undisturbed	Piston		little	10 to 20%	10-30	Med. Dense	4-8	M/Stiff	
TP=Test Pit	A=Auger	V=Vane Test	some	20 to 35%	30-50	Dense	8-15	Stiff	
UT=Undisturbed	Thinwall		and	35 to 50%	50 +	Very Dense	15-30	V-Stiff	
TOWN PRESS - EAST PROV.									
								SUMMARY: Earth Boring 20' Rock Coring 10' Samples 4	
								HOLE NO. TB-4 Page 3	

100 WATER STREET EAST PROVIDENCE, R. I.

SHEET 1 OF 1
DATE _____
HOLE NO. TB-5
LINE & STA. _____
OFFSET _____
SURF. ELEV. 73.10

GROUND WATER OBSERVATIONS		Rods "Aw"	CASING	SAMPLER	CORE BAR.	Date	Time
At 9' 5" after 1/4 Hours	Type	S/S	NXD3	START	11/25/75	a.m.	
17' casing	Size I.D.	NW	1-3/8"	COMPLETE	"	p.m.	
At 9' 1" after 1/4 Hours	Hammer Wt.	300#	140#	TOTAL HRS.			
no casing	Hammer Fall	24"	30"	BORING FOREMAN	T. Canning		
			BIT	INSPECTOR			
			d.b.t	SOILS ENGR.			

[illegible]

TOWN PRESS - EAST PROV.

100 WATER STREET EAST PROVIDENCE, R. I.

SHEET 1 OF 1
DATE _____
HOLE NO. TB-6
LINE & STA. _____
OFFSET _____
SURF. ELEV. 75.85

LOCATION OF BORING:

GROUND SURFACE TO 10' USED BW "CASING: THEN S/S to 10' 2"

SUMMARY:
Earth Boring _____
Rock Coring _____
Samples _____

HOLE NO TB-6
Page 5

American Drilling & Boring Co., Inc.

100 WATER STREET EAST PROVIDENCE, R. I.

TO Gilbert & Maloney ADDRESS Providence, R.I.
PROJECT NAME Prop. Marine Sci. Bldg. & Eco. LOCATION Narragansett, R.I.
REPORT SENT TO above / Systems Lab PROJ. NO. 6-122
SAMPLES SENT TO " OUR JOB NO. 6-122

SHEET 1 OF 1
DATE 11/25/75
HOLE NO. TP-7
LINE & STA.
OFFSET
SURF. ELEV. 76.00

GROUND WATER OBSERVATIONS				Rods "AW"	CASING	SAMPLER	CORE BAR.	Date	Time
At <u>7'</u>	after <u>1/4</u> Hours	Type						START	<u>11/25/75</u>
At <u>11' casing</u>		Size I.D.	<u>NW</u>	<u>S/S</u>	<u>NXD3</u>			COMPLETE	<u>"</u>
At <u>6' 9"</u>	after <u>1/4</u> Hours	Hammer Wt.	<u>300#</u>	<u>1-3/8"</u>				TOTAL HRS.	<u></u>
no casing		Hammer Fall	<u>24"</u>	<u>30"</u>	<u>BIT</u>			BORING FOREMAN	<u>T. Cantrill</u>
								INSPECTOR	<u></u>
								SOILS ENGR.	<u></u>

LOCATION OF BORING:

DEPTH	Casing Blows per foot	Sample Depths From - To	Type of Sample	Blows per 6" on Sampler			Moisture Density or Consist.	Strata Change Elev.	SOIL IDENTIFICATION Remarks include color, gradation, Type of soil etc. Rock-color, type, condition, hard- ness, Drilling time, seams and etc.	SAMPLE		
				From 0-6"	6-12"	To 12-18"				No.	Pen	Rec.
		0'-1'6"	D	3	9	7	dry medium dense	3'4"	4"-Brown TOPSOIL-Brown fine to medium SAND, Ash, Gravel (FILL)	1	18	1'6"
		5'-6'6"	D	11	21	36	moist very dense		Gray fine SAND, some silt, some schist	2	18	1'5"
		10'-11'	D	29	94		"	10'6"	Top of Rock	3	12	1'6"
		11'-16'	C							C1	60	1'6"
		16'-21'	C									

GROUND SURFACE TO <u>11'</u>	USED <u>NW</u> CASING: THEN <u>Drilled to 21'</u>	140lb Wt. x 30" fall on 2" O.D. Sampler	SUMMARY:
Sample Type	Proportions Used	Cohesionless Density	Earth Boring <u>11'</u>
D=Dry C=Cored W=Washed	Trace 0 to 10%	0-10 Loose	Rock Coring <u>10'</u>
UP=Undisturbed Piston	little 10 to 20%	10-30 Med. Dense	Samples <u></u>
TP=Test Pit A=Auger V=Vane Test	some 20 to 35%	30-50 Dense	
UT=Undisturbed Thinwall	and 35 to 50%	50+ Very Dense	
		Cohesive Consistency	
		0-4 Soft 30+ Hard	
		4-8 M/Stiff	
		8-15 Stiff	
		15-30 V-Stiff	

TOWN PRESS - EAST PROV.

HOLE NO TP-7
Page 6

American Drilling & Boring Co., Inc.

100 WATER STREET EAST PROVIDENCE, R. I.

TO Gilbert & Maloney ADDRESS Providence, R.I.
PROJECT NAME Prop. Marine Sci. Bldg. & Eco. LOCATION Narragansett, R.I.
REPORT SENT TO above/ Systems Lab PROJ. NO. 6-122
SAMPLES SENT TO " OUR JOB NO. 6-122

SHEET 1 OF 1
DATE 11/26/75
HOLE NO. TB-8
LINE & STA.
OFFSET
SURF. ELEV. 75.95

GROUND WATER OBSERVATIONS		Rods "AW"	CASING	SAMPLER	CORE BAR.	Date	Time
At <u>6'5"</u>	after <u>1/4</u> Hours	Type <u>BW</u>	<u>S/S</u>			START <u>11/26/75</u>	<u>8.m.</u>
no casing		Size I.D. <u>2 1/2"</u>	<u>1-3/8"</u>			COMPLETE <u>11/26/75</u>	<u>8.m.</u>
At <u></u>	after <u></u> Hours	Hammer Wt. <u>300#</u>	<u>140#</u>			TOTAL HRS. <u></u>	
		Hammer Fall <u>24"</u>	<u>30"</u>			BORING FOREMAN <u>T. Cammarino</u>	
						INSPECTOR <u></u>	
						SOILS ENGR. <u></u>	

LOCATION OF BORING:

DEPTH	Casing Blows per foot	Sample Depths From - To	Type of Sample	Blows per 6" on Sampler			Moisture Density or Consist.	Strata Change Elev.	SOIL IDENTIFICATION Remarks include color, gradation, Type of soil etc. Rock-color, type, condition, hard- ness, Drilling time, seams and etc.	SAMPLE		
				From 0-6"	6-12"	To 12-18"				No	Pen	Rec.
5		0'-1'6"	D	1	5	7	dry		6"-Brown TOPSOIL-Gray fine SAND, some silt (FILL)	1	18"	10"
11							medium					
10							dense					
11								4'6"				
7							moist					
5		5'-6'6"	D	5	6	6	medium		Brown fine SAND, some silt	2	18"	10"
14							dense	7'	FILL?			
27												
39									Gray fine SAND, some silt, some schist			
35												
24		10'-11'6"	D	22	18	86	moist					
53							very					
76							dense					
120												
20												
		15'-16'6"	D	56	48	140	"	16'6"		4	18"	10"
									Bottom of Boring - 16'6"			
									REFUSAL			

GROUND SURFACE TO <u>15'</u>		USED <u>BW</u>	"CASING: THEN <u>S/S to 16'6"</u>
Sample Type	Proportions Used	140lb Wt. x 30" fall on 2" O.D. Sampler	SUMMARY:
D=Dry C=Cored W=Washed	trace 0 to 10%	Cohesionless Density	Earth Boring <u>16'6"</u>
UP=Undisturbed Piston	little 10 to 20%	0-10 Loose	Rock Coring
TP=Test Pit A=Auger V=Vane Test	some 20 to 35%	10-30 Med. Dense	Samples <u>4</u>
UT=Undisturbed Thinwall	and 35 to 50%	30-50 Dense	HOLE NO. <u>TB-8</u>
		50+ Very Dense	Page 7

TOWN PRESS - EAST PROV.

American Drilling & Boring Co., Inc.

100 WATER STREET EAST PROVIDENCE, R. I.
 TO Gilbert & Maloney
 Prop. Marine Sci. Bldg. & Eco. ADDRESS Providence, R. I.
 PROJECT NAME Narragansett, R. I.
 REPORT SENT TO above / Systems Lab LOCATION
 SAMPLES SENT TO " PROJ. NO. 6-122
 OUR JOB NO.

SHEET 1 OF 1
 DATE TB-0
 HOLE NO.
 LINE & STA.
 OFFSET
 SURF. ELEV. 75.55

GROUND WATER OBSERVATIONS				Rods "AW"	CASING	SAMPLER	CORE BAR.	Date	Time
At 2'8"	after 1/4	Hours		Type	BW	S/S		START 11/28/75	a.m.
	no casing			Size I.D.	2 1/2"	1-3/8"		COMPLETE	p.m.
At	after	Hours		Hammer Wt.	300#	140#	BIT	TOTAL HRS.	
				Hammer Fall	24"	3 0"		BORING FOREMAN T. Canning	
								INSPECTOR	
								SOILS ENGR.	

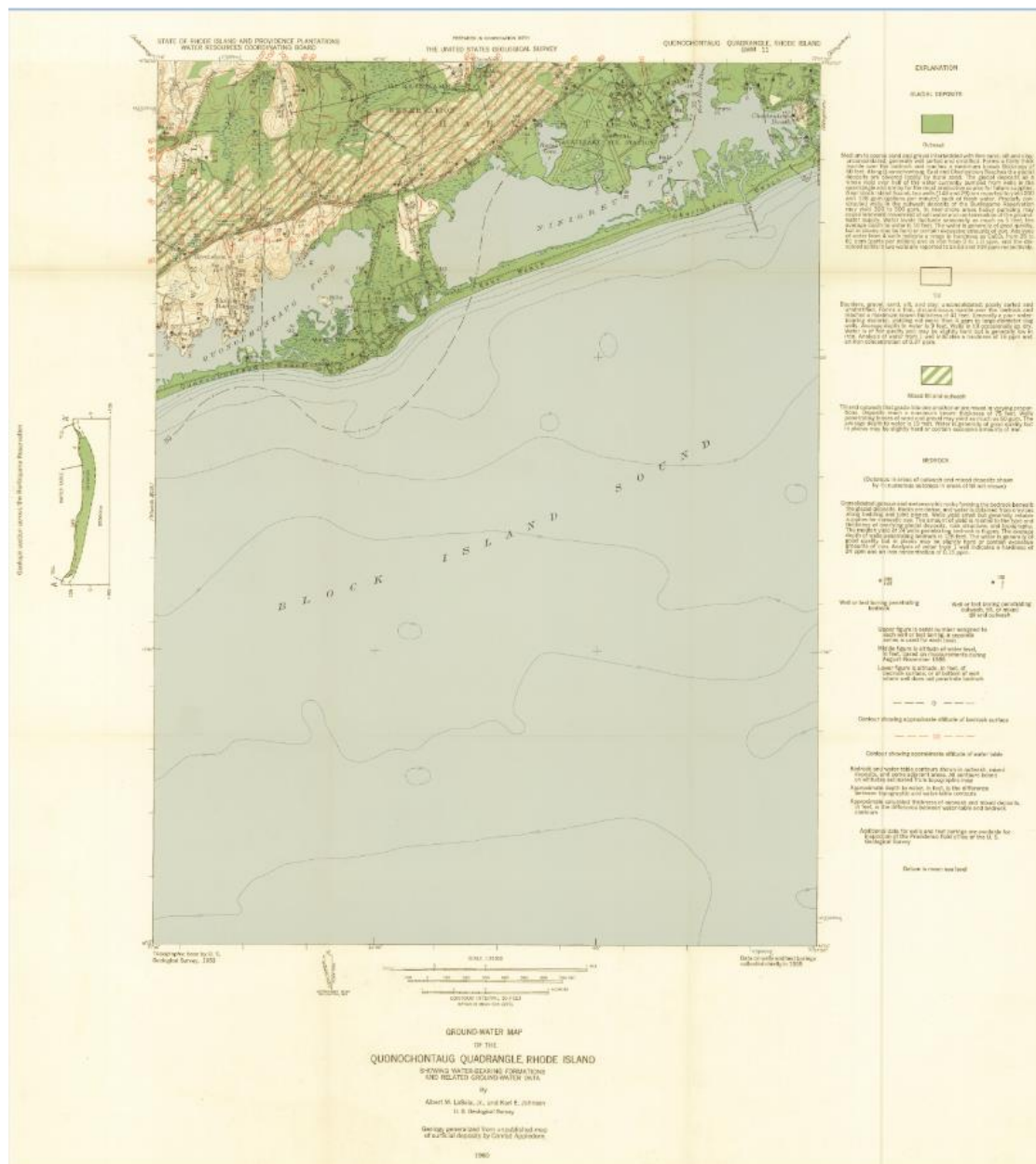
LOCATION OF BORING:

DEPTH	Casing Blows per foot	Sample Depths From - To	Type of Sample	Blows per 6" on Sampler			Moisture Density or Consist.	Strata Change Elev.	SOIL IDENTIFICATION Remarks include color, gradation, Type of soil etc. Rock-color, type, condition, hardness, Drilling time, seams and etc.	SAMPLE		
				From 0-6	6-12	12-18				No.	Pen	Rec.
5		0'-1'6"	D	3	7	7	dry		5"-Brown TOPSOIL-Gray fine to medium SAND, little fine gravel, some silt, Fill	1	18	1"
12							medium					
40							dense					
60												
59												
19		5'-6'6"	D	14	9	6	moist	7'		2	18	14"
13							med um					
38							dense					
38									Gray fine SAND, some silt, some schist			
42												
38		10'-11'6"	D	24	38	34	moist			3	18	14"
66							very					
93							dense					
84												
75												
		15'-16'5"	D	54	66	140	"			4	17	16"
		18'6"-18'7"	D	120			"	18'7"		0	1	0
									Bottom of Boring- 18'7"			
									REFUSAL			

GROUND SURFACE TO 15'		USED BW	CASING: THEN S/S W & D S/S to 18'7"
Sample Type	Proportions Used	140 lb Wt. x 30" fall on 2" O.D. Sampler	SUMMARY:
D=Dry C=Cored W=Washed	trace 0 to 10%	Cohesionless Density	Earth Boring 18'7"
UP=Undisturbed Piston	little 10 to 20%	0-10 Loose	Rock Coring
TP=Test Pit A=Auger V=Vane Test	some 20 to 35%	10-30 Med. Dense	Samples 4
UT=Undisturbed Thinwall	and 35 to 50%	30-50 Dense	
		50+ Very Dense	
		Cohesive Consistency	
		0-4 Soft 30+ Hard	
		4-8 M/Stiff	
		8-15 Stiff	
		15-30 V-Stiff	

TOWN PRESS - EAST PROV.

HOLE NO. TB-9
 Page 8



Bibliography

Bradshaw, A.S., Baxter, C.D.P., and Green, R.A., (2007). “A sitespecific comparison of simplified procedures for evaluating cyclic resistance of non-plastic silt”, Geotechnical Special Publication 160, ASCE, Geo-Denver, 2007.

Bradshaw, A.S., Morales-Velez, A.C., and Baxter, C.D.P. (2012), “Evaluation of Existing CPT Correlations in Silt,” Geotechnical Engineering Journal of the SEAGS & AGSSEA, Vol. 43, No.4, December 2012.

Bradshaw, A.S., and Reyes Mejía, B. (2015), “Using surface wave testing to screen for liquefaction potential of embankment dams: a case study at the Gainer Dam”. Presentation on RIWWA Meeting.

Department of Civil Engineering Chung-Ang University (2002), “WinSASW Version 2.0. Data Interpretation and Analysis for SASW Measurements”, AnSeong, Korea.

Foti, S., Lai, C.G., Rix, G.J., Strobbia, C. (2015), “Surface Wave Methods for Near-Surface Site Characterization,” CRC Press, Boca Raton.

Giard, J. (2013), “An Inversion Scheme for shear wave speed using Scholte waves dispersion”, M.S. Thesis, University of Rhode Island, Kingston.

Giard, J., Potty, G. R., Miller, J. H., and Baxter, C.D.P. (2013), “Validation of an Inversion Scheme for Shear Wave Speed using Scholte Wave Dispersion,” OCEANS 2013, September 23-26, San Diego, USA.

Greene, J. (2011). “Development of an amphibious seismo-acoustic recording system”, M.S. Thesis, University of Rhode Island, Kingston.

- Joh, S.-H. (1996), "Advances in the Data Interpretation Technique for Spectral-Analysis-of-Surface-Waves (SASW) Measurements," Ph.D. Dissertation, University of Texas at Austin.
- Joh, S.-H. (2010). WinSASW (Version 3.2.6). Soil Dynamics Lab Chung-Ang University.
- Kausel, E. and Peek, R. (1982). "Dynamic loads in the interior of a layered stratum: an explicit solution," Bulletin of the Seismological Society of America, 72, pp. 1459-1508.
- Kausel, E. and Roesset, J.M. (1981), "Stiffness Matrices for Layered Soils," Bulletin of the Seismological Society of America, 71, pp. 1743-1761.
- Kramer, S.L., (1996). "Geotechnical Earthquake Engineering," Prentice Hall, New Jersey.
- Lin, Y.-C., Joh, S.-H., and Stokoe, K.H. (2014), "Analysis of the UTexas 1 Surface Wave Dataset Using the SASW Methodology", Geo-Congress 2014 Technical Paper: pp. 830-839.
- Luke, B.A., and Stokoe, K.H. (1998). "Application of SASW Method Underwater." Journal of Geotechnical and Geoenvironmental Engineering, 124, pp. 523-531.
- McCaskill, A. (2014). "A Study on the benefits of including near-field effects in active-source surface wave data collection and interpretation", M.S. Thesis, University of Missouri, Columbia.

Olson Instruments Inc. (2013), “Spectral Analysis of Surface Waves (SASW-G). NDE-360 Platform with WinTFS Software Version 2.5.2”, Wheat Ridge, Colorado, Author.

Park, C. B., Miller, R. D. and Xia, J. (1997). “Multi-channel analysis of surface waves”, Kansas Geological Survey, Tech. Rep.

Potty, G., Miller, J., Lynch, J., and Smith, K. (2000), "Tomographic Inversion for sediment parameters in shallow water," J. Acoust. Soc. Am. 108(3), Pt.1, 973-986.

Potty, G.R., (2014) “Rayleigh Wave Dispersion modeling using Dynamic Stiffness Method.” Technical Report, University of Rhode Island.

Reyes Mejía, B., Bradshaw, A.S., Potty, G.R., and Norton, C.J. (2016),”Surface wave inversion as a screening tool for liquefaction potential: A case study at the Gainer Dam,” Association of Dam Safety Officials. **Manuscript Draft under Submission**

Stokoe, K.H., Wright, S.G., Bay, J.A., and Roesset, J.M., (1994). “Characterization of Geotechnical Sites by SASW Method.” Geophysical Characterization of sites, R.D. Woods, ed., IBH, New Delhi, India, 15-25.

Stokoe, K.H., Lin, Y.-C., Menq, F.-J. and Rosenblad, B. (2005),”SASW Measurements in Taiwan at 26 Strong-Motion Recording Stations: Summary Report of the Shear Wave Velocity Profiles”, Geotechnical Engineering Report GR05-2, University of Texas in Austin, Austin.

Pei, D., (2007). “Modeling and inversion of dispersion curves of surface waves in shallow site investigations,” Ph.D. dissertation, University of Nevada, Reno.

Wair, B.R., DeJong, J.T., and Shanty, T. (2012), "Guidelines for Estimation of Shear Wave Velocity Profiles," PEER Report 2012/8, Pacific Earthquake Engineering Research Center, Headquarters at the University of California.

WinTFS (Version 2.5.2). (2010).

Xia, J., (2014). "Estimation of near-surface shear-wave velocities and quality factors using multichannel analysis of surface-wave methods." Journal of Applied Geophysics, 103, pp. 140-151